A geophysical investigation of the south-east Greenland continental margin

P. S. Featherstone

'Twas whispered in heaven 'twas muttered in hell,
And echo caught faintly the sound as it fell;
On the confines of earth 'twas permitted to rest,
And the depths of the ocean its presence confessed.

Enigma, The Letter H - Catherine Marie Fanshawe

A GEOPHYSICAL INVESTIGATION OF THE SOUTH-EAST GREENLAND CONTINENTAL MARGIN

by

P.S. Featherstone

A thesis submitted for the degree of
Doctor of Philosophy at the University of Durham

Van Mildert College

September, 1976

ABSTRACT

During the summers of 1973 and 1974 geophysical observations were made, aboard R.R.S. Shackleton, across the south-east Greenland continental margin, between 58° and 65°N. The thesis describes the reduction and interpretation of the magnetic, bathymetric, gravimetric, and deep seismic reflection data and gives details of the digital deconvolution and C.D.P. stacking techniques developed for processing the reflection data.

The magnetic results indicate that, south of 63°N., anomaly 24 is the earliest recognisable oceanic magnetic anomaly. North of 63°N., anomalies 22-24 cut out against the margin, and a complementary widening of ocean floor of this age, on the opposite Rockall margin, north of Hatton Bank, indicates that a local westward migration of the spreading axis occurred, north of 63°N., shortly after the split. Igneous intrusives, outcropping on the rise, post-date the continental split by several million years, indicating that the volcanic activity of East Greenland may have occurred some time after continental separation started.

Airgun and sparker profiles show three major sediment groups. Two groups of Tertiary age are separated by an erosional unconformity, beneath the rise north of 62°N. The upper sediments are interpreted as contour current deposits of Miocene and later age, and the lower sediments as lithified oozes of about Eocene age. Below these Tertiary sediments, older, seaward dipping reflectors occur between anomaly 24 and the scarp. These are interpreted as Mesozoic sediments overlying subsided continental crust. The oceanic-continental crustal boundary, as recognised from magnetic anomalies, occurs to the east of this subsided region and lies up to 80 km seaward of the scarp, which is an erosional feature cut by contour currents.

Gravity profiles indicate that the main change in crustal thickness beneath the margin lies up to 80 km landward of the scarp north of 63.5°N., but corresponds more nearly with the scarp further south.

CONTENTS

LIST OF FIGURES

LIST OF TABLES

LIST OF ACCOMPANYING MAPS

ACKNOWLEDGEMENTS

Firstly, and above all, I would like to thank Professor Bott, without whose support, guidance and provision of departmental facilities this work would have been impossible. Valuable assistance and discussion were also provided by Mr. S. Armstrong, Dr. R.E. Long, and Mr. J.H. Peacock during the processing of the seismic records and the departmental technicians are praised for patching up the equipment nearly as fast as I could wreck it.

Thanks are due to the Captains, officers and crew of the R.R.S. Shackleton; to Mr. J.H. Peacock as senior scientist; to Mr. M. Beaney who kept the shipborne equipment, and himself, humming; to the shipborne computer development group at Cambridge whose data gave this thesis a flying start; to the shipborne computer group at Barry who helped with the rest of the data reduction.

Valuable discussions with members of staff, particularly Dr. G. Larwood, and Dr. C.H. Emeleus at Durham and Dr. D.H.Tarling at Newcastle helped keep my feet on fairly safe ground, while the sympathetic ear of fellow students helped direct the flights of fancy. Mr. A.R. Armour must be singled out if I could find him beneath the pile of paper I left behind, and if his wife ever wants good references.....

Thanks also go to Mr. D. West and Mr. P. Marren for pointing out that I can not spell, to Mrs. H. Winn for extremely efficient typing, and to the Lemmings and particularly Yvie for maintaining my morale.

The work for this thesis was carried out while in receipt of a Natural Environment Research Council Research Studentship and their sponsorship is gratefully acknowledged.

CHAPTER 1

INTRODUCTION

1.1 The survey area

During the summers of 1973 and 1974, the Department of Geological Sciences at the University of Durham carried out exploratory marine geophysical surveys of the south-east Greenland continental margin, aboard R.R.S. Shackleton. Gravity, magnetic, bathymetric and seismic reflection observations were made along a series of east-west profiles over the margin between Cape Farewell and Angmagssalik. The area of investigation, bounded by latitudes 58°N. and 65°N. and by longitudes 32°W. and 48°W., includes the Greenland continental shelf, the continental scarp and a portion of the west Reykjanes ocean basin. A track chart of the survey is given in Appendix map 1.

The south-east Greenland margin is a passive Atlantic type continental margin. Until recently it has been little studied, mainly because of (1) its location outside major shipping routes, (2) the danger of icebergs that prevent any work close to the coast, and (3) the hostile weather conditions which prevent geophysical study for most of the year. Thus the structure and history of the neighbouring

margins of the Atlantic, are considerably better understood than those of the Greenland margin; the aim of these geophysical surveys was to improve the knowledge of this area. A short account of the interpretation of the data on the south-east Greenland margin is given in Featherstone, Bott and Peacock (1976).

The Greenland margin must be considered in the wider context of its plate tectonic setting and the history of opening of the North Atlantic, as outlined in section 1.2. The limited previous geophysical work has shown that the marine geology differs markedly from the rocks outcropping on the adjacent Greenland coast, and this thesis attempts to tie together the recent marine studies and the geology on land.

1.2 The plate tectonic setting and opening history of the North Atlantic

The major structural elements of the North Atlantic are shown in simplified form in fig. 1.1. The term "North Atlantic", as used in this thesis, is restricted to the oceanic areas north of the Azores fracture zone and south of the Knipovitch ridge, and, although the spreading history of the adjoining South Atlantic and Arctic ocean basins is integrally linked with that of the North Atlantic to form one coherent phase of opening, these more distant

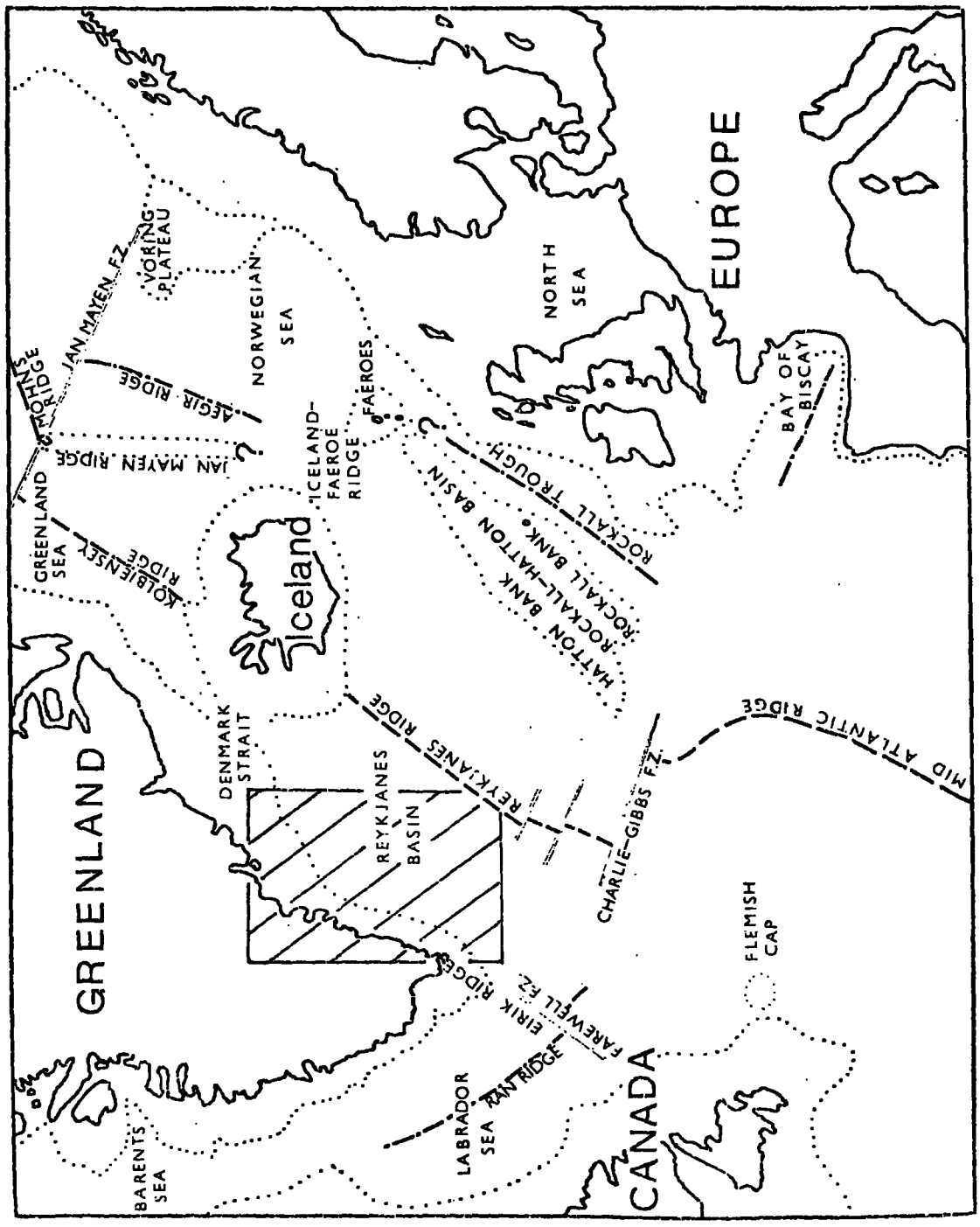

Fig. 1.1 Summary map of the main structural features of the North Atlantic, largely after a map of the "Atlantic ocean floor", National Geographic Society. Continental scarps are shown as dotted lines, active spreading ridges dashed lines, extinct ridges dot-dash lines, transform faults double lines and survey area is diagonally shaded.

oceanic areas are not discussed. Geophysical investigations in the North Atlantic have been carried out for about the last 15 years, and the area has proved to be one of the best examples of the break-up of a macro-continent, and the formation of new intervening oceanic crust. Details of the complex history of continental separation in this area have added much supporting evidence to the now widely accepted theory of plate tectonics. The summary that follows is an attempt to draw together the current ideas on the tectonic setting and opening history of the North Atlantic; in many cases the sources quoted are recent summary papers rather than the numerous original survey reports.

The major continental blocks in this area are north America, Greenland, and Europe and these, together with the minor micro-continental fragments of the Rockall plateau and the Jan Mayen ridge, were all part of one macro-continent that has gradually drifted apart in Mesozoic and Cenozoic times.

The intervening oceanic crust can be structurally divided into different regions, each with a distinct spreading history. These are described below, starting in the south and working northwards, and this is followed by a summary of the opening history. The dates given for the different phases of opening are largely dependent on the dating of oceanic

magnetic anomalies and are derived using the time-scale of Heirtzler et al. (1968).

The southernmost, and perhaps the simplest, area to be described lies immediately north of the Azores fracture zone. Spreading about the Mid-Atlantic ridge separating north America from southern Europe may have begun in this area during the Jurassic (180 my), but the major phase of rifting did not occur until the late Cretaceous (84 my) (Pitman and Talwani 1972). Spreading has continued to the present day with only minor changes in spreading rate. This area of simple spreading is terminated to the north by the Charlie-Gibbs fracture zone, a large transform fault with a sinistral offset of 320 km (Vogt and Avery 1974). The fault leaves a large gap in the otherwise nearly continuous Mid-Atlantic-Reykjanes ridge system, which has an important effect on the circulation of ocean currents (Worthington and Volkmann 1965).

To the east of the Charlie-Gibbs fracture zone is the much studied (but little understood) Bay of Biscay. The spreading axis, now extinct, has rotated the Iberian peninsula in an anti-clockwise direction (Williams 1975). Spreading was probably preceded by an intense phase of rifting during the Jurassic but started in the early Cretaceous (130 my) and continued to the end of the Cretaceous (73 my) (Williams 1973, 1975).

To the west of the Charlie-Gibbs fracture zone is the Labrador Sea, also an extinct spreading axis, which split Greenland from north America. The zone of oceanic crust in the Labrador Sea is bordered on both sides by wide belts of attenuated continental crust (van der Linden 1975b). Spreading began in the late Cretaceous (84 my) (Johnson et al. 1973, Laughton 1972, Le Pichon et al. 1971) and continued until the mid-Eocene (47 my), when it slowed down considerably, to finally stop in the late Oligocene (38 my) (Kristoffersen and Talwani 1974). The eastern end of the Labrador sea is marked by a large sinistral transform fault, the Farewell fracture zone (Johnson et al. 1967), and by a depositional ridge of sediments, the Eirik ridge, which projects from the southern tip of Greenland (Johnson and Schneider 1969). Immediately north of the Charlie-Gibbs fracture zone are two areas of oceanic crust. To the east, lying between the European continent and the Rockall micro-continent, is the Rockall trough, a presumed extinct spreading axis. The age of spreading in the Rockall trough is poorly dated, but the separation may have started in the early Cretaceous (130 my) and continued until the late Cretaceous (84 my) (Roberts 1975). To the west, between the Rockall micro-continent and Greenland, is the actively spreading Reykjanes Ridge. Separation began in the mid-Palaeocene (60 my) (Johnson et al. 1975a, Vogt and Avery 1974),

and has continued to the present day, with only minor changes in spreading rate.

The northern boundary of the Reykjanes ridge system is defined by the Iceland-Faeroe-Greenland aseismic ridge. This ridge, which runs through Iceland, and includes the shallow water areas of the Denmark Strait to the west and the Iceland-Faeroe ridge to the east, is an anomalous area in many ways (Bott and Browitt 1971). The presence of this ridge, which is attributed to the effects of a supposed hot-spot now thought to be centred beneath Iceland, and the history of subsidence of the ridge below sea-level, has affected the circulation of ocean currents, sediment history (Vogt 1972) and the tectonic and volcanic activity of the neighbouring margins. Geophysically the ridge is little understood, and the Denmark Strait, in particular, has not been geophysically surveyed. The history of formation of this transverse ridge is not well known, partly because consistent linear oceanic magnetic anomalies cannot be identified, but the onset of spreading is likely to have coincided with that of the adjoining basins in the mid-Palaeocene (60 my), and the formation of the Iceland plateau has been tentatively dated as late Oligocene (38 my) (Bott 1974).

North of the Iceland-Faeroe-Greenland ridge, there is an area of complex tectonics including the Norwegian and Greenland Seas. Spreading started in this area in the

mid-Palaeocene (60 my) about the Aegir ridge (Avery et al. 1968, Vogt et al. 1970) and the Mohns ridge (Johnson et al. 1974, Talwani and Eldholm 1974). The spreading rate changed, and the Aegir ridge migrated westward at a time variously estimated between mid-Eocene and mid-Oligocene (Vogt et al. 1970, Fleischer 1974). During the late Oligocene (38 my), spreading began about the Knipovitch ridge (Johnson et al. 1974, Talwani and Eldholm 1974) splitting Greenland from Spitzbergen. Up to this time, this margin had undergone shearing, while the Norwegian and Greenland seas to the south, and the Arctic seas to the north, opened. In the early Miocene (10 my), the axis of spreading in the Greenland sea jumped westward, splitting off a sliver of the Greenland continent, the Jan Mayen ridge, and spreading has continued about the newly-formed Kolbiensey ridge to the present day (Talwani and Eldholm 1974).

The study of individual areas, as outlined above, has shown that the complex spreading history can be considered as one continually developing phase of opening about varying ridge axes and that there are a number of important events, which have marked changes in the spreading regime in several areas. These are tabulated below:

(1) 180 my, mid-Jurassic. Spreading begins south of the Azores. Possible small scale spreading begins north of

the Azores accompanied by intense rifting in the Bay of Biscay.

(2) 130 my, early Cretaceous. The Bay of Biscay starts to open, possibly together with opening in the Rockall trough and continued small scale opening along the Mid-Atlantic ridge between the Azores and the Charlie-Gibbs fracture zone. These three areas of spreading may have formed a triple junction.

(3) 84 my, late Cretaceous, anomaly 34. Spreading in the Rockall trough has ceased, but spreading begins in the Labrador Sea, and the main phase of spreading starts about the Mid-Atlantic ridge between the Azores and the Charlie-Gibbs fracture zone. This is accompanied by continued spreading in the Bay of Biscay, again possibly forming a triple spreading junction.

(4) 73 my, end Cretaceous, anomaly 32. Spreading in the Bay of Biscay ends.

(5) 60 my, mid-Palaeocene, anomaly 24. Greenland splits from Rockall to form a triple junction south of Cape Farewell with spreading along the Ran ridge, the Reykjanes ridge and the Mid-Atlantic ridge. Greenland splits from Norway about the Aegir and Mohns ridges and transform movement along the Greenland Spitzbergen margin begins.

(6) 47 my, mid-Eocene, anomaly 19. Spreading slows down considerably in the Labrador Sea and spreading rates change on the Reykjanes ridge and the Aegir ridge. The axis of the Aegir ridge possibly migrates westward.

(7) 38 my, late Oligocene, anomaly 14. Spreading in the Labrador Sea ceases and spreading begins between Greenland and Spitzbergen about the Knipovitch ridge. Spreading now occurs about a single sinuous ridge from the south Atlantic through the Mid-Atlantic ridge, the Reykjanes ridge, the Aegir ridge, the Mohns ridge, the Knipovitch ridge and into the Arctic ocean basins.

(8) 10 my, early Miocene, anomaly 5. Spreading axis of the Greenland sea jumps to form the Kolbiensey ridge splitting off the Jan Mayen ridge, a thin sliver of the Greenland continent.

(9) Present day. Spreading continues about the Mid-Atlantic ridge, the Reykjanes ridge, the Kolbiensey ridge, the Mohns ridge and the Knipovitch ridge.

1.3 Previous surveys of the south-east Greenland margin

The most comprehensive bathymetric chart of the south-east Greenland margin is by Johnson et al. (1975a), and is based largely on work by Dietrich (1959, 1965) and Ulrich (1960) (fig. 5.1). The usual features of an Atlantic type

margin are present, namely a continental shelf, continental scarp, rise and ocean basin. The continental scarp is well defined by the 1000 m depth contour, and parallels the nearly north-south coastline from the southern tip of Greenland to latitude 63.5°N., the shelf being about 75 km wide (fig. 1.2). At 63.5°N., the scarp swings eastward, and the shelf widens to about 225 km, remaining at this width northwards into the shallow water of the Denmark Strait, to the north of the survey area.

Marine magnetic profiles have been collected and interpreted by Vogt (1970), Larsen (1974 and pers. comm.) and Johnson et al. (1975a), and the areas covered by these studies are shown in fig. 1.2, together with aeromagnetic measurements by Hood and Bower (1973) and Project Magnet. The previous magnetic work has defined the linear oceanic anomalies as shown in fig. 1.2. The earliest recognisable anomaly, identified as anomaly 24 (60 my, mid-Palaeocene) on the time scale of Heirtzler et al. (1968), runs in a NE-SW direction from the southern tip of Greenland to latitude 64°N. ; it does not parallel the coast and lies up to 80 km seaward of the scarp. Between anomaly 24 and the scarp, there is an elongate triangular-shaped area (diagonally shaded in fig. 1.2) which is of oceanic depth and magnetically quiet.

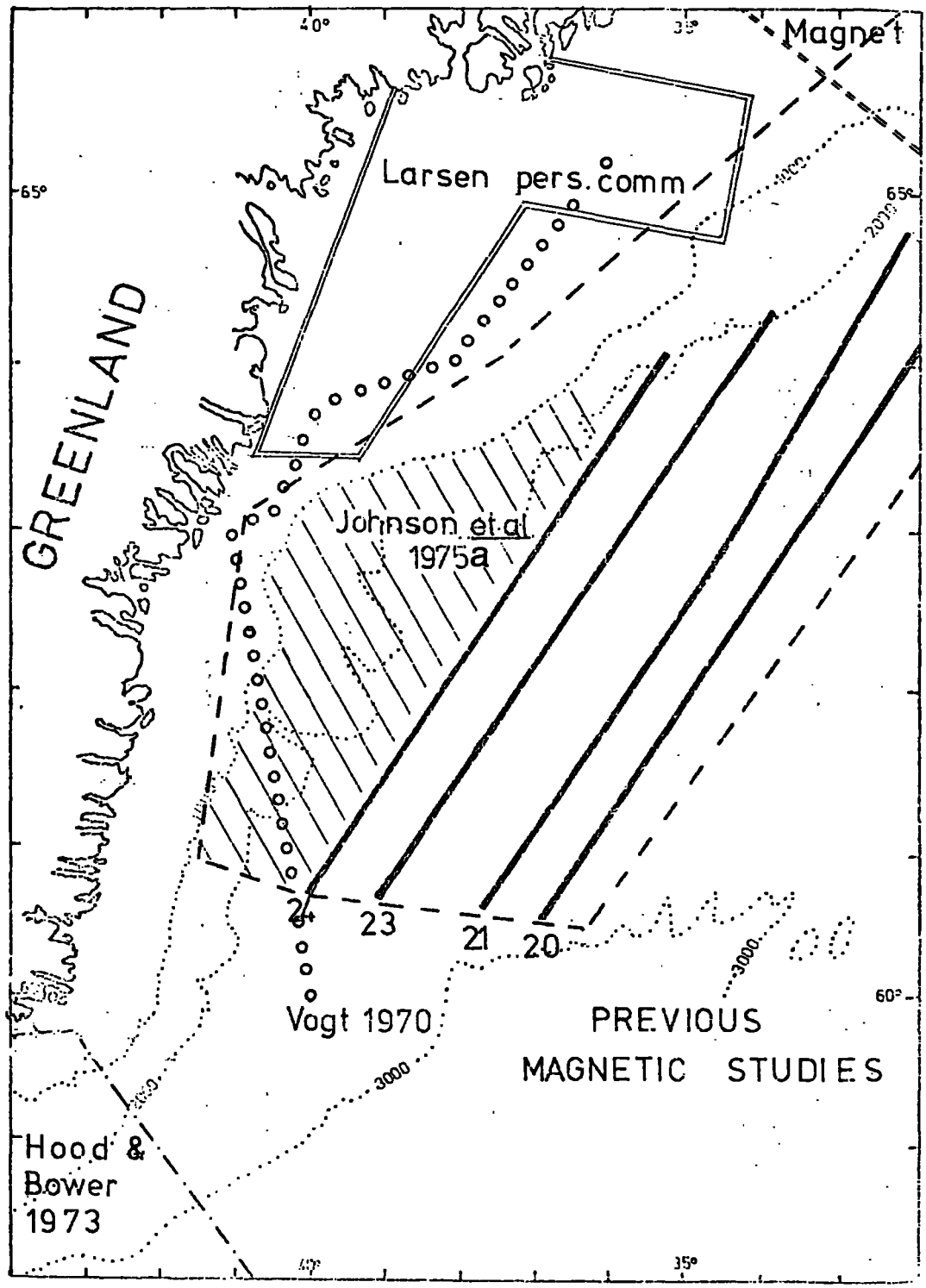

Fig. 1.2 Location of previous magnetic surveys on the Greenland margin. Numbered heavy lines are linear magnetic anomalies after Johnson et al. (1975a). Shaded area is magnetically quiet crust of oceanic depth lying between anomaly 24 and the scarp.

On reconstructed continental fits of the North Atlantic (fig. 5.11), this triangular-shaped area remains as a gap between Greenland and Rockall (Laughton 1972). The nature of this triangular-shaped area is unknown, but it has been attributed to either subsided continental crust or to magnetically quiet oceanic crust formed during a period of pre-anomaly 24 spreading (Johnson et al. 1975a) It has been noted (Johnson et al. 1975a) that anomalies 23 and 24 cannot be traced north of 64°N. and, if they were to continue northwards, along the same trend but with considerably reduced amplitude, they would run into the continental shelf.

The morphology of the margin has been intensively studied using shallow seismic methods and sediment coring by Avilov (1965) and Sommerhoff (1973). This has been supplemented by medium penetration seismic investigations by Vogt (1970), Larsen (1974), and Johnson et al. (1975a), and by dredge hauls up the scarp (Johnson et al. 1975b). The surface morphology of the shelf has been shown to be a result of glacial erosion and deposition (Sommerhoff 1973, reported in English by Johnson et al. 1975a). The unusually steep scarp has been suggested by Johnson et al. (1975a) to be a progradational feature; however, this view is not supported by the reflection results of Larsen (1974). The dredge hauls of Johnson et al. (1975b), which yielded

Devonian-Carboniferous, Permian, Oligocene and Miocene rocks from the scarp, would appear to contradict the suggestion that the scarp has prograded in recent times. The rise and ocean basin have been shown to be morphologically one unit (Johnson et al. 1975a), cut by a well developed system of submarine canyons. The deep sedimentary structure and pre-Pleistocene sediment history of the shelf, scarp and rise had been very little studied prior to this work, but the remarkable range of comparatively old rocks dredged from the scarp indicates that the sediment history may be complex.

The coastal geology immediately west of the survey area is a complex of little studied Precambrian metamorphic rocks (fig. 1.3). To the north, between latitudes 68°N. and 70°N. (fig. 1.3), there is one of the world's most impressive piles of Tertiary flood basalts, totalling some 9 km in thickness (Wager 1947). These basalts have been correlated as contemporaneous with the Faeroese and Hebridean basalts (Holmes 1918) and with the initiation of continental separation (Brooks 1973). These contemporaneous areas of igneous activity are known as the Brito-Arctic eruptive field, and their presence has been attributed to the supposed hot spot now beneath Iceland. Recent dating, however, (discussed in Chapter 4) indicates that the Greenland basalts are not contemporaneous with those to

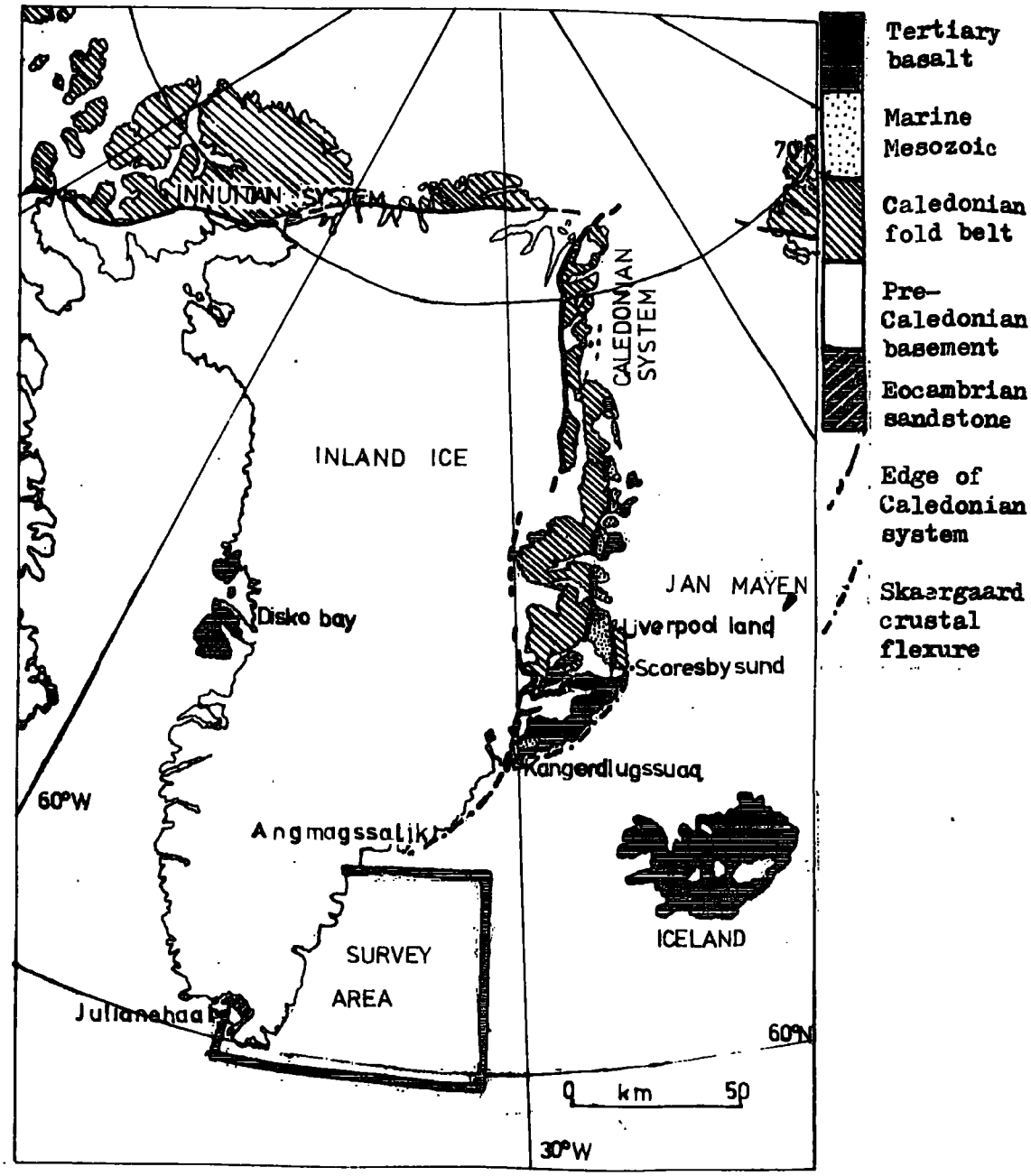

Fig. 1.3 Summary Geological map of Greenland redrawn from Haller (1970).

the east of the Atlantic, and their relationship with the initiation of spreading is uncertain. The coastline adjacent to the area of plateau basalts is defined by a massive crustal flexure and associated dyke swarm, with a total vertical movement of about 9 km (Wager 1947).

To the north of the basalts, there is a north-south trending Caledonian fold belt composed of tectonically highly disturbed Lower Palaeozoic rocks (fig. 1.3) (Haller 1970). Let into this fold belt, between 70°N. and 78°N., is a north-south trending graben-like basin, in which marine sedimentation began in the Upper Palaeozoic but reached its zenith during the Jurassic (Callomon 1972). This basin probably extends southwards beneath the basalts, and, if it extends offshore into the survey area, it may have potential as a hydrocarbon source rock.

There were, therefore, several unanswered questions about the Greenland margin:

(1) What factors govern the line of the original continental split and the shape of the present continental scarp?
(2) What type of crust lies between anomaly 24 and the scarp?
(3) What happens to anomalies 23 and 24 in the north of the survey area?
(4) What is the sediment history?
(5) To what extent has the scarp prograded and why have comparatively old rocks been dredged from the scarp?

(6) To what extent has the anomalous Iceland-Faeroe-Greenland ridge affected the tectonics and sediment history?

(7) How does the coastal geology extend offshore?

(8) How do the extrusives on land tie up with the continental split?

(9) Is there any economic potential for oil production?

1.4 The scope of the current survey

The deep penetration of the airgun seismic records of the 1973 and 1974 surveys, and the systematic coverage of the area with marine gravity measurements, has made a considerable contribution to the understanding of the area and has helped answer some of these questions.

This thesis is principally concerned with the interpretation of the data collected and with details of some of the techniques used in the data reduction and interpretation. The ship time, technical support and much of the scientific instrumentation, on which this work was dependent, was provided by the Natural Environment Research Council through the Research Vessels Base at Barry, Glamorgan. The reduction of the cruise data was performed on the IBM 1130 system at Cambridge and R.V.B. Barry (Chapter 2) and the seismic data was processed on the CTL Modular 1 computer in the Department of Geological Sciences at the University of Durham (Chapter 3). The manipulation and

interpretation of the data relied heavily upon the IBM 360/370 Northern Universities Multiple Access Computer (NUMAC). The computational and interpretational techniques used are generally well known and so they are only briefly described in the text.

CHAPTER 2

DATA ACQUISITION AND PROCESSING

2.1 Introduction

The data on which this thesis is based was collected during geophysical surveys carried out by the Department of Geological Sciences, University of Durham in the summers of 1973 and 1974. Navigational, gravity, magnetic, bathymetric and seismic reflection observations were made aboard R.R.S. Shackleton on a series of predominantly east-west lines across the S.E. Greenland margin. In addition disposable sonobuoy and coring experiments were carried out.

The navigational, gravity, magnetic and bathymetric data from both the 1973 and 1974 cruises was recorded on a modified Decca data logger and reduced, as described in Section 2.4, on the IBM 1130 computer system, developed by members of the NERC shipborne computer development group at the Department of Geodesy and Geophysics, Cambridge (Stacey et al. 1972). The reduced data is available as two separate cruise reports. The profiles and track charts given in Appendix 1 are an amalgamation of the data on the Greenland margin taken from both these reports. The reduced data is also recorded digitally on magnetic tape in the 'Formats for Marine Geophysical Data Exchange' (Anon. 1972);

Appendix 1 contains an index to these tapes.

The seismic data was produced on an independent system, which is described in Section 2.3. The original seismic records are unsuitable for inclusion in this thesis, but interpretations of these records along simplified ship's track are given in Appendix map 2. The digital processing of the seismic records is described in Chapter 3. The sonobuoy data collected over the Greenland margin has been analysed by Mr. C.D.T. Walker (thesis to be submitted). Details of the coring experiments are given in Appendix 1, and foraminifera extracted by the author from portions of these cores have been palaeontologically examined by Dr. G. Larwood.

2.2 Summary of the survey program

The Shackleton surveys in the summers of 1973 and 1974 were only partly located around the Greenland margin. The 1973 cruise left Barry (Glamorgan) on June 13 (Julian Day 164) with Mr. J.H. Peacock as senior scientist, and surveyed the Rockall area and Reykjanes ridge before entering the Greenland survey area on July 16 (Day 197). Surveying on the Greenland margin between latitudes 62^{o}N. and 65^{o}N. was hampered by icebergs, but continued until July 23 (Day 204) when the ship returned to dock in Aberdeen on July 30 (Day 211). The author had intended to join this cruise in early July,

but bad weather and logistic reasons prevented this.

The 1974 cruise was therefore planned to extend the previous year's survey on the south-east Greenland margin, both to the north and the south. The ship left Barry three days later than expected on August 7 (Day 219) with the author on board and Mr. J.H. Peacock as senior scientist. Because of equipment failure and a change of captain due to illness the Greenland survey area was not reached until August 18 (Day 230). The area between latitudes 58°N. and 61.5°N. was surveyed before refuelling at Juliannehaab on August 24 (Day 236). After surveying one further profile at about latitude 62.5°N. and carrying out the coring experiments, an attempt was made to extend the survey north of 65°N. into the Denmark Strait. This was abandoned because of extreme weather conditions and the threat of a hurricane, and on August 30 (Day 242) the ship returned to the Rockall area where it extended the previous year's survey before returning to Barry on September 11 (Day 254). The Greenland data was, therefore, collected over a total of 18 days, and includes over 4000 km of gravity, magnetic, bathymetric and seismic data.

2.3 Equipment

The equipment and technical support used during the surveys was largely provided by the Natural Environment

Research Council, through the Research Vessels Base at Barry, Glamorgan. The equipment used was:

Geophysical; La Coste and Romberg shipborne gravity meter, instrument no. S.40, (set with a 4 minute time constant)

Barringer proton magnetometer (set at a 6 second polarization period)

Navigation; Two component Electromagnetic log

Ship's gyrocompass: Microtechnica

Satellite navigation system Magnavox 702 receiver with Hewlett-Packard 2100 computer

Bathymetry; Precision depth recorder; M.S. 38

Logging; Modified Decca data-logger

2 RDL magnetic tape decks (series 10500) and controller (½ inch, 9-track, 800 B.P.I., NRZI, IBM-compatible tape)

Read-after-write output via Data Dynamics 390 teletype

Computer; IBM 1130 system:- (not on board ship in 1974)

1131 C.P.U. (8 k core) disc drive

2310 double disc drive (512 k-word discs)

1133 multiplexer

Data Dynamics fixed head disc

RDL magnetic tape deck (series 10500) plus interface

Facit paper-tape input-output

Calcomp 1627 drum plotter (0.01 cm increment)

Tektronix Visual Display Unit

Seismic source; Bolt airgun, 300 or 150 cubic inch interchangeable chambers

E.G. and G. Sparker 12 kJ, 3 candle

Seismic array; Geomechanique towed streamer 4 active sections 250 m offset, 150 m between sections, active sections 50 m, total length 750 m

Seismic recording; EMI 1" 8 track F.M. analogue tape recorder: 4 seismic array channels (1-4), sonobuoy channel (5), shot instant (6), digital clock (7), voice track for day and leg identification (8)

Seismic display; Geospace variable area monitor recorder, single channel, on ultra-violet sensitive paper

Geospace automatic gain control (AGC) and band pass filter, single channel

E.G. and G. sparker display equipment on heat sensitive paper

In general the equipment worked well; for a detailed account of the equipment performance reference should be made to the cruise reports.

2.4 Data acquisition and reduction

The raw gravity, magnetic and navigational data were sampled and digitally recorded, as they were measured, by a modified Decca data logger. The logger sampled the input at 1 second intervals and stored the data in 10 second blocks on magnetic tape. These tapes were then transferred

to an IBM 1130 computer for processing. In 1973 the computer was on board ship, and the data was reduced, while at sea, by members of the shipborne computer development group, who also prepared the data report. In 1974 the computer was not on board ship and so the data was reduced, and the report prepared, by the author at the Research Vessels Base, Barry with assistance from members of the shipborne computer group. A summary diagram of the data acquisition hardware is given in fig. 2.1.

On the computer the data was demultiplexed and all parameters were filtered, in 2 stages with 3 second and 4 minute cut-off frequencies, to remove spikes. The principal navigational aid for the survey was a Magnavox 702 satellite navigator. Satellite fixes were produced aboard ship by a Hewlett-Packard 2100 computer, and recorded on paper tape, which was read into the IBM 1130 computer. In the survey latitudes a high density of satellite fixes were recorded, but a large percentage of these were of doubtful accuracy due to their angle of elevation, thus only those fixes that passed a series of tests were used to define the position of the ship. The satellite navigator worked well apart from a 9 hour breakdown in 1974 (covering days 239-240). The ship's position between satellite fixes was calculated by dead reckoning, the survey being outside Decca range and the Loran 'C' receiver being inoperative. Dead reckoning fixes

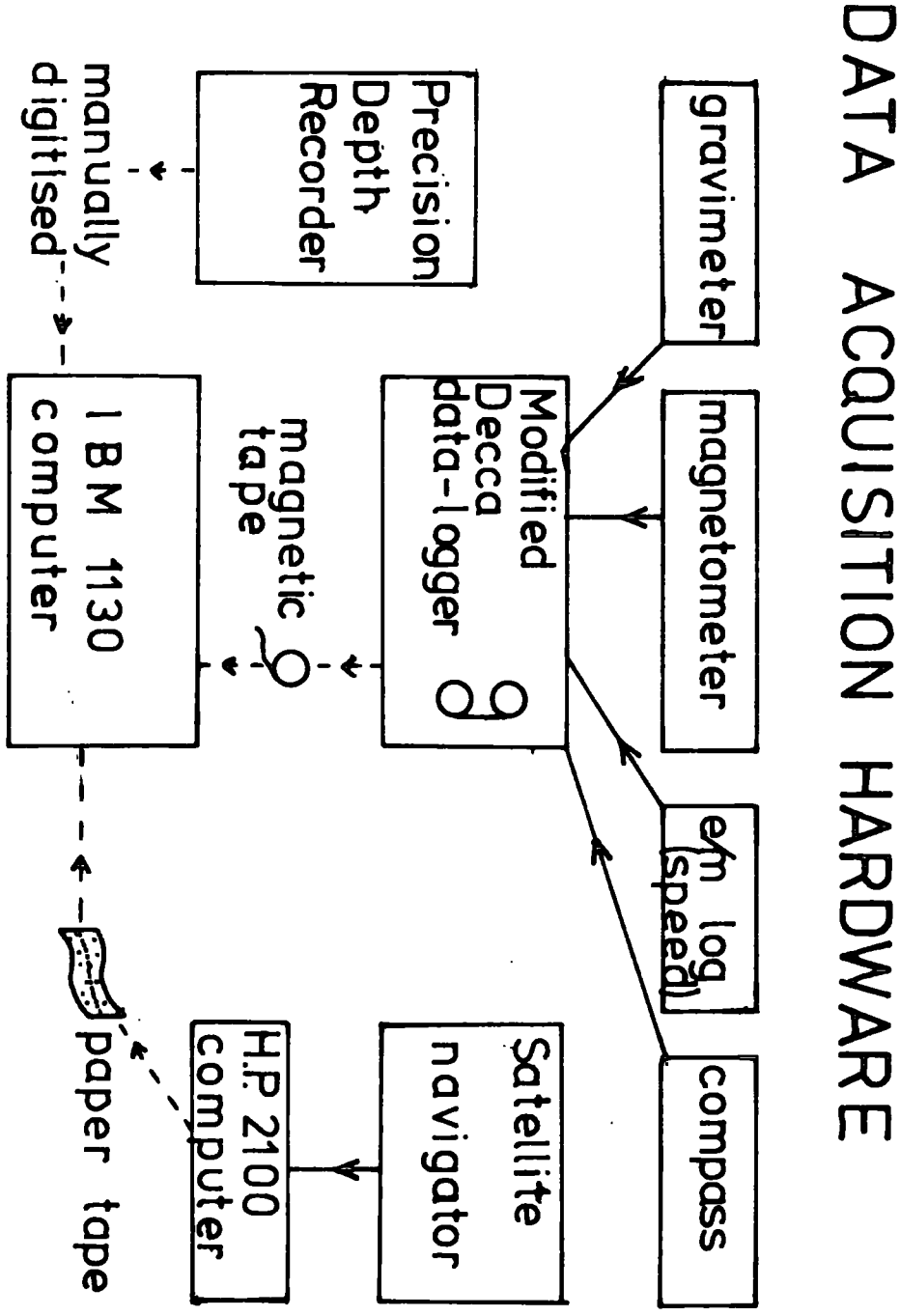

Fig. 2.1 Schematic diagram of the hardware used to collect and reduce the navigational, gravity, magnetic and bathymetric data. Solid arrowed lines indicate electrical wiring, dashed lines indicate manual transfer of data.

were calculated from the logged course and speed (Tucker et al. 1970) at 2 minute intervals, and directly updated to the satellite fixes. Having obtained a series of 2 minute navigation fixes, together with true course and speed, the gravity and magnetic anomalies were calculated. A summary of the data processing software is given in fig. 2.2.

The free air gravity anomaly was derived using the international gravity formula (1967), referred to the International Gravity Standardised Net 1971 (IGSN'71, Coron 1972). The shipborne meter was tied in to base stations at Barry, the Faeroes and Aberdeen in 1973, and Barry, Juliannehaab and back at Barry in 1974, a Worden Master gravimeter being used for this. The station ties at the start and end of the 1973 cruise show that the drift was less than 0.1 mgal (J.E. Lewis thesis to be submitted). The base ties at Barry at the start and end of the 1974 cruise show a drift of 0.11 mgal (fig. 2.3); no drift corrections have been applied to the data.

The gravity base used at Juliannehaab (Juliannehaab 'I') was established in 1950 and refers to Buddinge (Copenhagen 'K') as a base. Copenhagen 'K' has been tied into IGSN'71 as shown in fig. 2.3, and allowing for this the 1950 survey and the 1974 Durham survey differ by 0.44 mgal. This discrepancy is possibly explained by some confusion over the exact position of the base station at Buddinge (E. Kejlso 1958).

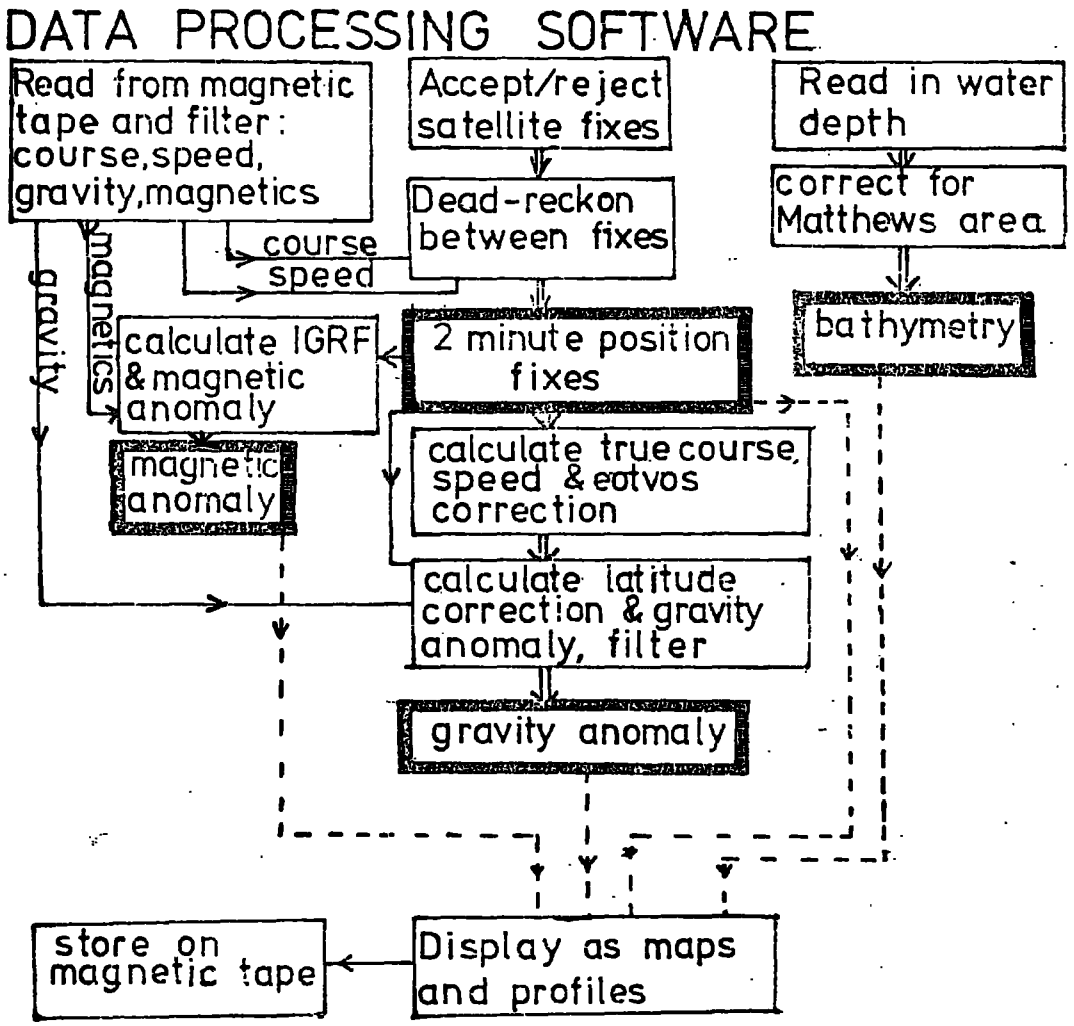

Fig. 2.2 Schematic diagram of the various steps involved in the reduction and display of the navigational, gravity, magnetic and bathymetric data.

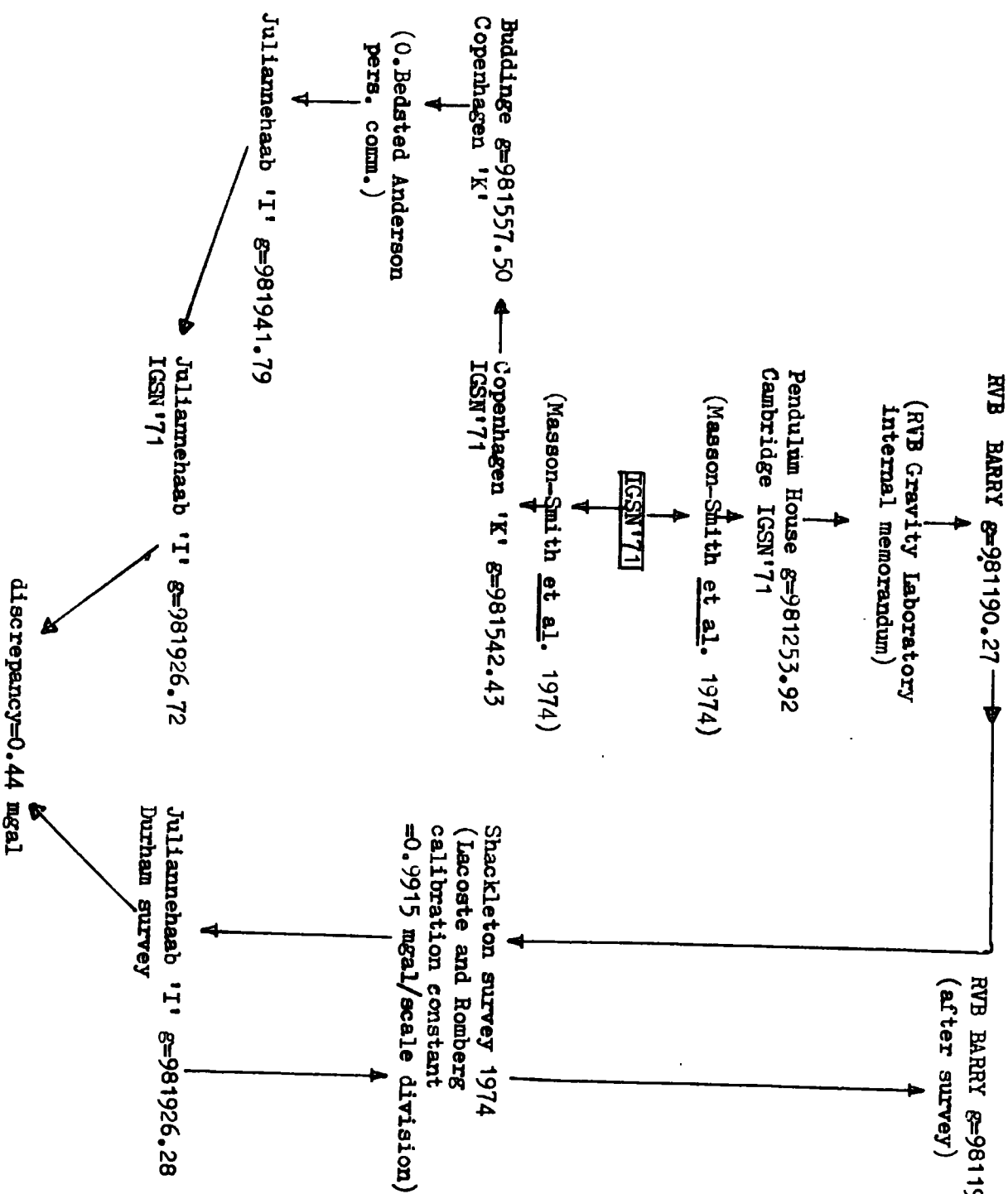

Fig. 2.3 Gravimeter ties for the 1974 cruise and their relationship to previous gravity surveys.

The calculated free air anomaly profiles show a high frequency component with a period of 6 to 9 minutes and amplitudes of 2 to 3 mgal. In very heavy seas, notably days 234, 235 and 243, the corrections applied within the gravimeter exceeded 50 mgal and very noisy records result. All the gravity readings were therefore filtered with a 12 minute sliding average. Estimates at crossover points indicate an accuracy of at least $\pm$ 1 mgal, both during each survey and between the 1973 and 1974 surveys.

The magnetic anomaly was calculated using the International Geomagnetic Reference Field (Mead 1970). No corrections were applied for daily variations. Examination of observatory magnetometer charts from Lerwick and Eskdalemuir (provided by the Geomagnetism unit, IGS, Edinburgh) show that a large magnetic storm has affected the records during days 231 to 234 (1974), and these records are of doubtful accuracy; evidence is given in section 4.4 for an additional minor short lived magnetic storm on day 202. The effect of the ship on the magnetometer was minimised by towing the magnetometer fish at greater than 3 times the ship's length (at 700 feet).

The bathymetric data was digitised manually onto paper tape, as automatic digitising equipment was not available. Values were recorded in fathoms every 10 minutes by inspection of the P.D.R. output charts, a velocity of sound in water of

800 fms sec^{-1} being assumed. In the computer these depths were corrected by the Matthews corrections for the relevant area (Matthews 1939).

During the several stages of the reduction process the data was displayed, either as profiles and maps on the automatic plotter or as listings, and data spikes that had escaped the automatic edit traps were removed. The ship's radio transmissions severely affected the majority of the survey equipment in 1973 and caused numerous small data breaks; in 1974 these breaks were greatly reduced by re-location of the gravimeter and cooperation from the radio officer, but the discharge of the sparker banks frequently stopped the logger causing data breaks. Further breaks occur in the data when instruments were switched off. A full account of the programs used in the reduction and display of the data is given in the Institute of Oceanographic Sciences Manuals (1974).

2.5 Seismic reflection data

The seismic reflection data was collected using one of two differing systems. A 12 kJ E.G. and G. sparker recording on heat sensitive paper, produced high resolution shallow penetration records, defining the near surface sediment characteristics of the shelf. In deeper water, and for greater penetration a higher energy Bolt airgun, with varying

gun volumes (150 and 300 cubic inch) was used as a seismic source and a Geomechanique towed array of hydrophones as receivers. This gave good sediment penetration, in places exceeding 3 seconds (2 way time) below the sea bed. The resolution however was poor and in shallow water the sediment structure was lost in the multiples. The airgun records were displayed on a Geospace variable area monitor recorder with automatic gain control (AGC) and band pass filtering; the signals were also recorded (together with the sparker records in 1974) on an EMI analogue tape deck. The shot firing rate was one shot every 22 seconds in 1973 and every 11 seconds in 1974; these rates were chosen to allow common depth point (CDP) stacking. Some of the seismic recordings have been subsequently digitally processed as described in Chapter 3, but with over 4000 km of seismic records most of the interpretation was of necessity performed on the original records produced aboard ship. This is single fold data recorded from the second section of the array (the section with the highest signal to noise ratio). This large quantity of original seismic data is unsuitable for reproduction in this thesis. However, the data has been interpreted and plotted as line drawings along track and is presented in this form in Appendix map 2.

The original seismic data is a time section; the vertical scale is 2 way travel time and the horizontal scale is time

dependent (.05 inches per shot ie. per 11 or 22 seconds). To produce a map of seismic profiles along track the data must be transformed and plotted as 2 way travel time against distance. Some of the line drawings in Appendix map 2 were produced by digitising interpretations of the seismic data and scaling and plotting the profiles by computer. However, it was found more convenient to plot the interpretations manually (the computer was unavailable for a large part of the time in which the profiles were prepared). To do this a best fit straight line was drawn for each track across the margin on a 1 to 1,000,000 track chart. The position along this line of the hourly navigation fixes was then transferred at a scale of 1 to 4,000,000 to graph paper. The seismic interpretations were then plotted at ten minute intervals, or less for complex structures, with detail inserted between ten minute fixes, the ship's speed being assumed constant over any hour.

A series of 1 to 4,000,000 profiles of 2 way time against distance was produced by this means and photographically reduced to 1 to 1,000,000 for incorporation in the chart. As the profiles are taken from a Mercator chart the horizontal scale varies slightly between profiles by up to $\pm$ 10%. The vertical exaggeration is approximately 7 to 1 at water velocities. The profiles are so positioned on the chart that the best fit straight line through each track

over the margin coincides with the top of the respective profile, the regular line distribution of the survey allows this without too much overlap between profiles.

CHAPTER 3

DIGITAL PROCESSING OF SEISMIC RECORDS

3.1 Introduction

The digital processing of seismic reflection records is now very widely used in the search for hydrocarbons, and an entire industry has evolved based on such processing. The industrial practice and its accompanying research programmes are far ahead of the capabilities within the University sphere. The digital processing techniques described here are therefore of necessity not original. The constraints of working with existing low-cost equipment (fig. 3.1) and in part existing computer software, have meant that in some ways the implementation of these techniques is unusual and may be of interest. The methods used for acquiring the seismic data, recording it onto analogue magnetic tape and displaying it as an original paper record are described in Chapter 2. It was hoped that by using digital processing techniques, the following problems inherent in the original data would be reduced:

(1) The presence of random noise. In part this could be removed by band-pass filtering on display, as the noise frequencies differ from the signal frequencies (fig.3.2B,C). The low frequency noise component, presumably due to surges

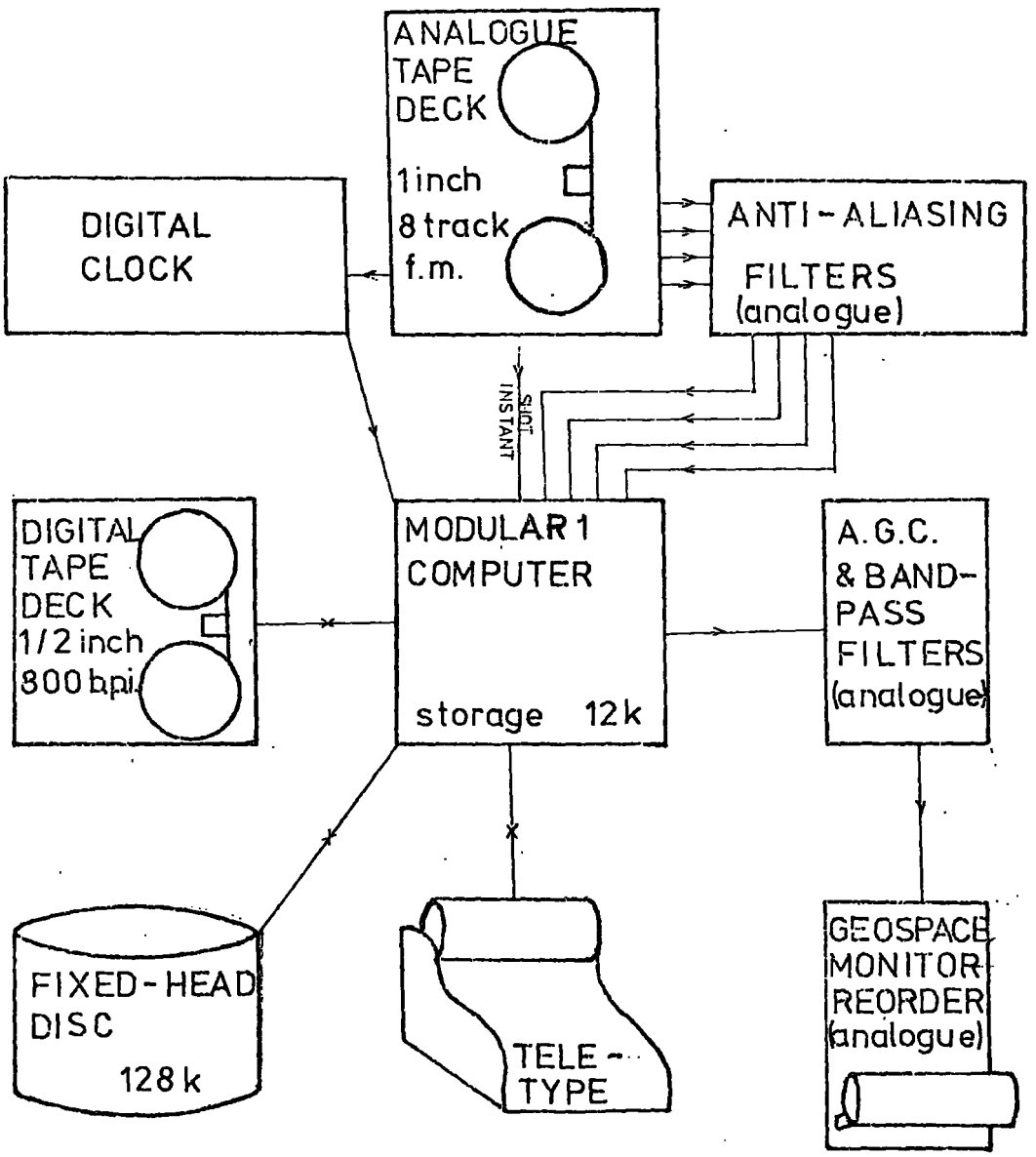

Fig. 3.1 Diagrammatic representation of the seismic processing hardware configuration.

on the end of the array, frequently saturated the recordings of the last active section of the array during the 1973 cruise making them unusable.

(2) The ringing of the airgun source. This produced a wavelet of several cycles (fig. 3.2A,E) which gave rise to a series of traces on the seismic record from a single reflector. By digital convolution of the seismic records, using specially designed spiking filters, the airgun wavelet can be compressed into a single spike. This treatment considerably improved the resolution of the records.

(3) The presence of signal induced noise, principally the air-surface sea-bed multiple. In deep water, in the ocean basins, this multiple occurs below the depth of penetration of the seismic source and is of little problem. In shallow water, however, the multiples obscure most of the sediment structure. This problem is particularly evident with the airgun seismic source. The sparker, having a shorter pulse length and lower energy, defines the shallow water near surface sediments well, but with little penetration. In an attempt to attenuate the multiples (and also the random noise) the technique of common depth point stacking was performed on some of the records.

(4) During replay of the analogue recordings variation in tape speed caused misalignment of reflections from successive

shots. The effect of this was variable but at its worst meant that replayed records were practically uninterpretable. By using the varying 1 khz time signal recorded on the analogue tapes to govern the digitising rate and then replaying the digital tapes at a constant sampling rate this problem was eliminated.

(5) The original seismic records are practically photographically unreproduceable. Replay of the records through the Geospace display onto photographic paper (Kodak Linagraph 1801)that can be chemically developed (using Permatex 517) to produce black and white prints has enabled the seismic profiles in this thesis to be reproduced.

The digital processing of the seismic records was performed largely on the CTL Modular 1 computer in the Department of Geological Sciences at the University of Durham. Analogue equipment was used for both replay and display, the same EMI tape deck and Geospace display being used as on board ship (Chapter 2). This equipment was interfaced to the computer by Mr. J.H. Peacock, who also wrote the initial test software to digitise and replay reflection records. A diagrammatic representation of the hardware configuration is given in fig. 3.1. The software of the Modular 1 has been specifically written for handling of time series data by Dr. R.E. Long, and consists of a set of

about 40 instructions, each programmed in assembler that can be combined to produce a program. One of these instructions to remove normal moveout (RNSO), has been added to the set by the author with the invaluable help of Mr. Simon Armstrong. The Modular 1 programs written by the author and given in Appendix 2 consist of combinations of these instructions; they are therefore dependent on the machine software.

3.2 Digitising

The analogue seismic tapes must first be digitised by the computer and stored either on digital tape or disc. A digitising rate of 250 samples s^{-1} was found convenient, the rate being divided down from the 1 khz clock signal on the analogue tapes. This gives a maximum sampled frequency of 125 hz (Robinson 1967a); On display, frequencies above this are normally filtered out. To prevent aliasing (Robinson 1967a), frequencies above 125 hz are removed prior to digitising. This is done with a set of analogue variable gain anti-aliasing filters, the gain being adjusted to give near full dynamic range within the computer (0-10.24 volts) without overloading. The program DELSTORE (Appendix 2.3) can be used to digitise 4 seismic channels onto magnetic tape.

The data in the computer and on digital tape and disc is in multiplexed form and all processing is performed on multiplexed data. This departs from normal procedure in processing seismic data, the data normally being demultiplexed prior to processing and each channel processed separately. The need for both input and output to be performed at constant speed (analogue devices being all that was available) and the presence of only one digital tape deck means that multiplexed data handling, although more difficult to program, is in this case more practical. Once the data has been digitised a variety of processing techniques can be employed as described in the following sections.

3.3 Deconvolution

The principal seismic source for the reflection work was a single large volume airgun (150 or 300 cubic inch). This gave good sediment penetration but the long pulse length, consisting of a wavelet of several cycles, gave poor definition and produced several traces on the seismic record from a single reflector. Deconvolution is an attempt to compress this wavelet into a single spike. The theory of the design of a spiking filter from a knowledge of the original source wavelet is well known (Robinson 1967b) and

will not be repeated here; rather this account deals with implementation of that theory on the seismic records of the survey.

The computing involved in the design of a spiking filter is not currently within the capabilities of the Modular 1, and therefore samples of the seismic data were transferred to the NUMAC IBM 360/370 computer either by paper tape or magnetic tape and used on this bigger machine to design the filters. Program FOAM1 (Appendix 2.2) enables Modular 1 magnetic data tapes to be read into the IBM 360/370.

The principal problem in the design of a spiking filter is that nowhere on the original seismic record (fig. 3.2A) is there a single discrete original source wavelet as is needed to produce the filter. The direct wave, which might at first appear to be this, is in fact a complex of original pulse, reflections off the sea-surface and random noise.

A program (FILPAC provided by Mr. J.H. Peacock) which produces a standard airgun pulse from airgun pressure, volume, depth and array depth considerations and calculates the best spiking filter was therefore used. However, the airgun depth and array depth were not measured during the cruise (the airgun volume is also only spasmodically recorded). Therefore, a small section of the original seismic record (a section for ½ a second after the sea

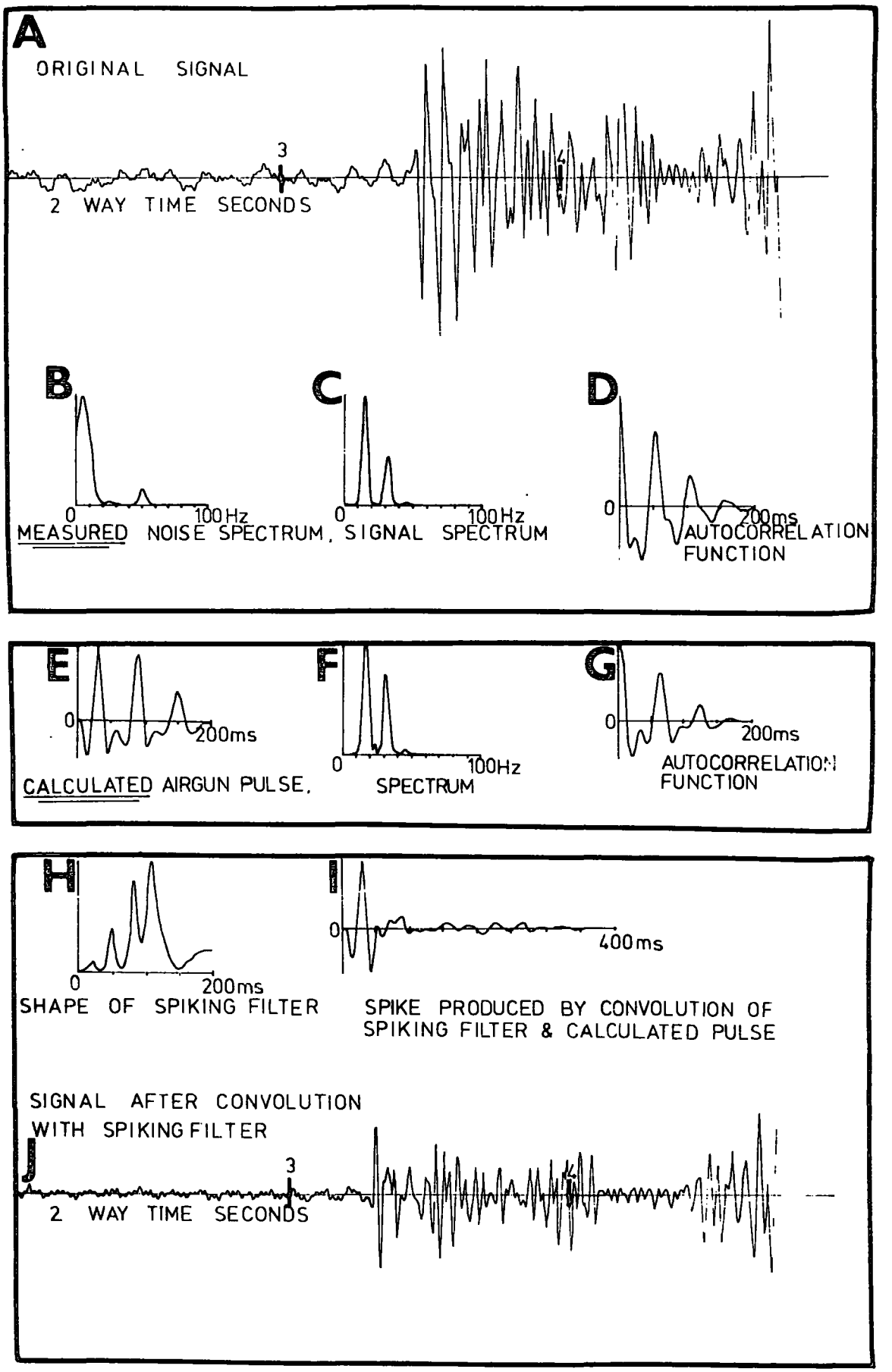

Fig. 3.2 Diagram showing the stages involved in the design of a spiking filter, for a detailed description see text.

bottom reflection where the signal to noise ratio is highest) was taken and the power spectrum (fig. 3.2C) and auto-correlation function of this section calculated (fig. 3.2D). The unknown depth parameters were then adjusted until the power spectrum (fig. 3.2F) and auto-correlation function (fig. 3.2G) of the calculated pulse (fig. 3.2E) gave a good fit to the measured results. This calculated pulse was then used to design the spiking filter (fig.3.2H). This is not predictive deconvolution (the type most commonly used in industry) which makes assumptions about the original wavelet (that it is minimum delay) to find that original wavelet from measurements on the recorded signal. The source wavelet is rather calculated by means independent of the seismic signal, which is used merely as an external control on this calculation.

There is a unique solution of depth of airgun and array that gives the best fit to the measured data. Changing the depth of the airgun varies the fundamental frequency of the signal, which is the most important factor when designing the spiking filter. Changing the depth of the array has no effect on the airgun frequency, but changes the relative intensities of the fundamental frequency and its harmonics by adding in a pulse (delayed in time) that has been reflected off the sea surface. For certain con-

figurations (particularly in the 1974 data) the first harmonic has in fact a greater amplitude than the fundamental frequency and it is important when modelling the airgun pulse that this is recognised.

The filter that produces the best spike from any given airgun pulse, may not be the best for any set of data as it may also considerably amplify the noise on the record. Thus a sample of the noise characteristics fig. 3.2B is also input, and the effect of the spiking filter on this noise is taken into account during filter design. The spiking filter in fig. 3.2H is shown as a continuous waveform although it is of course used as a set of discrete samples. A filter length of 0.2 s, or 50 samples at 250 samples s^{-1}, is normally found sufficient. Although for optimum results a spiking filter should be designed for each shot, in practice the variation in the airgun pulse is small over the length of section that it is convenient to process at one time (about 800 shots), and this refinement was unnecessary.

The convolution of seismic records with the spiking filter can be performed on the IBM 360/370 to produce spiked tapes, but it is normally more convenient to perform this on the Modular 1. To spike records on the Modular 1 the program FILIP is used (Appendix 2.4). Fig. 3.3 shows a seismic section both before and after spiking. The filters

DECONVOLUTION

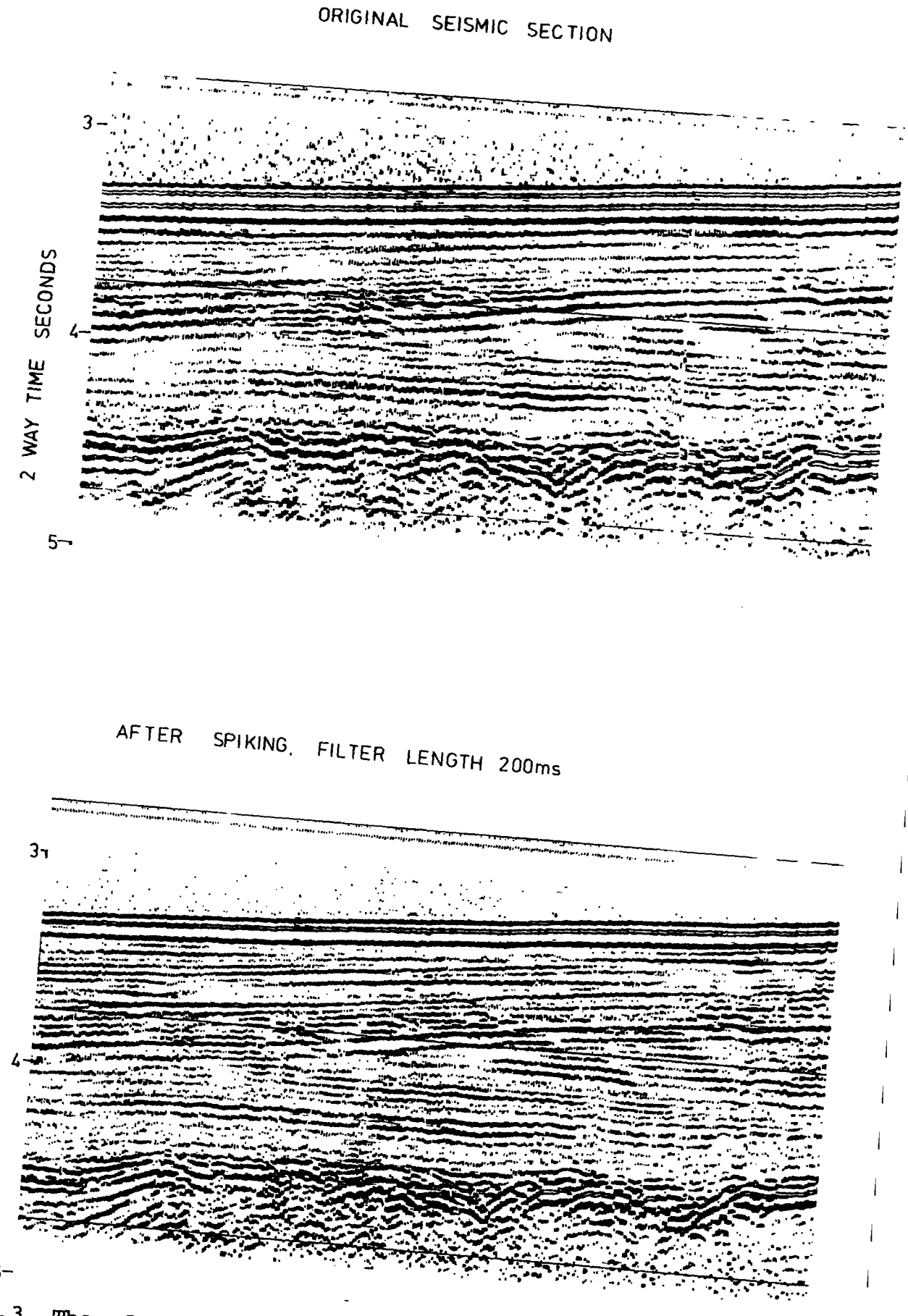

Fig. 3.3 The effect of deconvolution on a seismic record, before and after; all display parameters are constant, the spiking filter used is given in Appendix 2.4 and fig. 3.2.

designed by FILPAC are unit energy spiking filters, i.e. a signal will have the same power both before and after convolution with the spiking filter. However, the Modular 1 has a very limited dynamic range and therefore the filter values are multiplied by ten before being input into the computer. The instruction FIL in the Modular 1 software performs the convolution and the necessary complementary division by ten.

The process of convolution requires that, for each channel to be spiked, there is at least the same number of samples of seismic data in the computer as there are samples of the filter. This means that all channels to be spiked must be time series channels, and that no system delay is needed as convolution is performed on past samples.

The Modular 1 does not have a fast array processor and the act of convolution is slow, requiring for example 50 multiplications and 50 additions per sample (per 4 ms). When convolving single channel data the Modular 1 is sufficiently fast for the program FILIP to work in real time provided the spiking filter is of fewer than 120 samples. However, when spiking multi-channel data, for instance prior to stacking, the computer cannot perform the convolution in real time. Thus when spiking and stacking multi-channel data the two processes must be performed separately, the spiking being performed first, and the spiked records stored on disc file.

The stacking is then performed in real time and output to the analogue display. Programs SPIFIL and STAFIL (Appendix 2.5, 2.6) perform these two operations.

3.4 Common depth point stacking

The technique of common depth point (CDP) stacking to attenuate multiples is widely used in industry. To enable this to be done on the Modular 1 software has been written by the author, with the help of Mr. Simon Armstrong. The concept of CDP stacking is to add together the reflections from several shots that arise from a common point. In fig. 3.4 a shot at 'b' recorded at the start of the geophone streamer 'p' reflects off the same series of points at depth (dotted line) as a later shot at 'a' recorded at the end of the streamer 'q'. Thus if these two shots are added together (after a correction for the geometry of the situation) the reflections from the depth points should sum coherently and any other reflections, multiples, or noise will add incoherently.

It is important that the distance p-q' (fig. 3.4), which is the distance between recording sections of the array, is twice a-b (which is the distance between successive shots). Taking the case of active recording sections every 150 m and a ship steaming at 3.09 m s^{-1} (6 knots), which was the situation in both the 1973 and 1974 cruises, a shot

Fig. 3.4 Reflection paths for common depth point stacking; ship fires a shot at 'b' (light lines) and then later at 'a' (heavy lines). 'h' is the depth of the reflection point below the source, 'v' the mean velocity to that point and 'x' the shot-receiver separation.

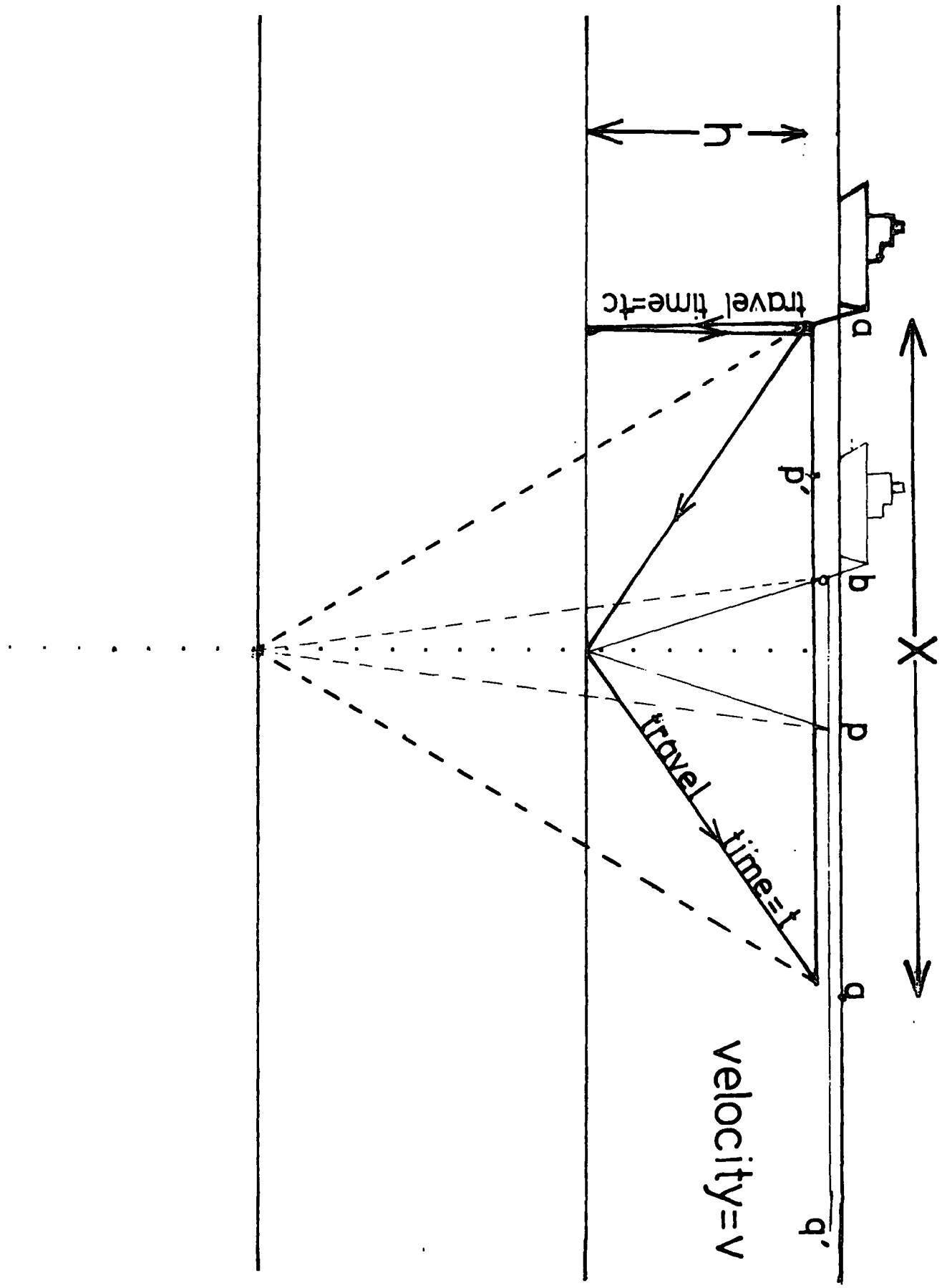

is required every 24 seconds. This was approximately the firing rate in 1973, whereas in 1974 twice this rate was used. Thus for 1973 seismic data each depth point can be considered as the sum, over 4 successive shots, of each of the 4 seismic channels, as in fig. 3.5. For the 1974 data, either every other shot must be CDP stacked or two adjacent shots must be summed (vertically stacked) and then treated as for the 1973 data.

As the processing is performed on multiplexed data the 4 channels of each shot can be handled at the same time and a running total of partially stacked records kept on disc until 4 shots have been added when the sum is output (as in fig. 3.5). Thus the data is streamed through the computer and CDP stacked without the tape skipping backwards and forwards between shots.

3.5 Moveout correction

From fig. 3.4 it can be seen that the path distance for a reflected ray from 'b' to 'p' is smaller than that from 'a' to 'q', because of a greater shot-receiver separation. This will result in different arrival times (after the shot instant) on reflection traces measured at 'p' and 'q'. For these reflections to add coherently when stacked the arrival times must first be lined up. To do this each record is distorted in time so that the arrival times are

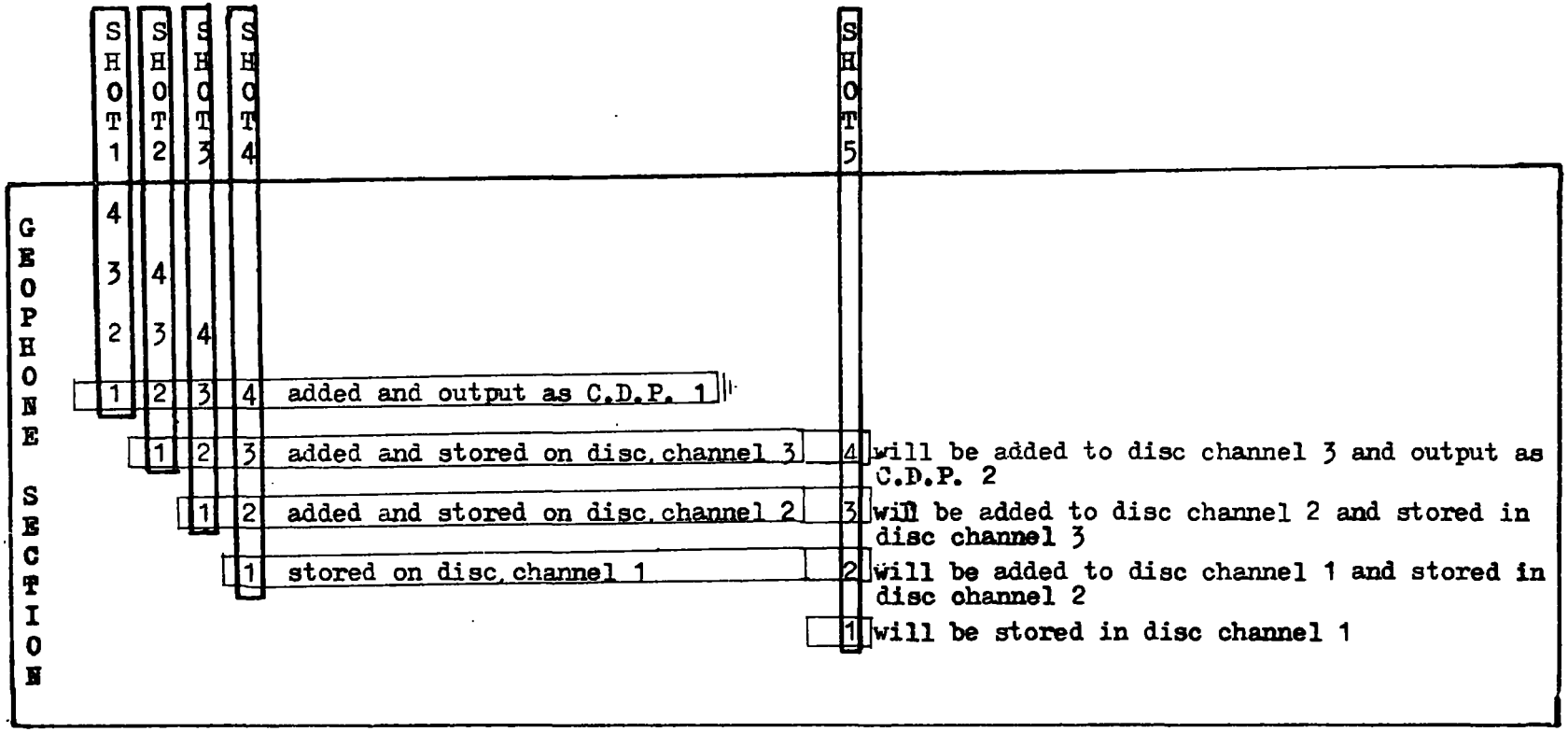

Fig. 3.5 Position after common depth point stacking of 4 shots and how the 5th shot will be stacked.

those expected for a coincident shot and receiver. This distortion is termed normal moveout correction.

Using the nomenclature of fig. 3.4. For a coincident shot-receiver;

$$t_c = 2h/V \quad \text{or} \quad h = V\, t_c/2$$

For a shot-receiver separation 'x';

$$t = \frac{2}{V}\left(\sqrt{h^2 + x^2/4}\right)$$

Therefore time difference;

$$\Delta t = t - t_c = \frac{2}{V}\left(\sqrt{\frac{V^2\, t_c^{\,2}}{4} + \frac{x^2}{4}}\right) - t_c \quad \text{or} \quad \Delta t = \sqrt{t_c^{\,2} + x^2/V^2} - t_c$$

From this equation at any time t_c (for a coincident shot-receiver) a time shift Δt can be calculated, and is the amount of time that one must look into the future to find the same arrival on a shot and receiver of separation 'x'.

The expression is plotted for several values of 'x' in fig. 3.6. It can be seen that for large values of t_c (for example reflections in deep water) the time shift Δt is small and approximately constant for increasing values of t_c. Use of a 'static' time correction for each channel on such records is suitable and program DEEPSTACK (Appendix 2.7) performs such a static common depth point stack, the static time delays being inserted when declaring the

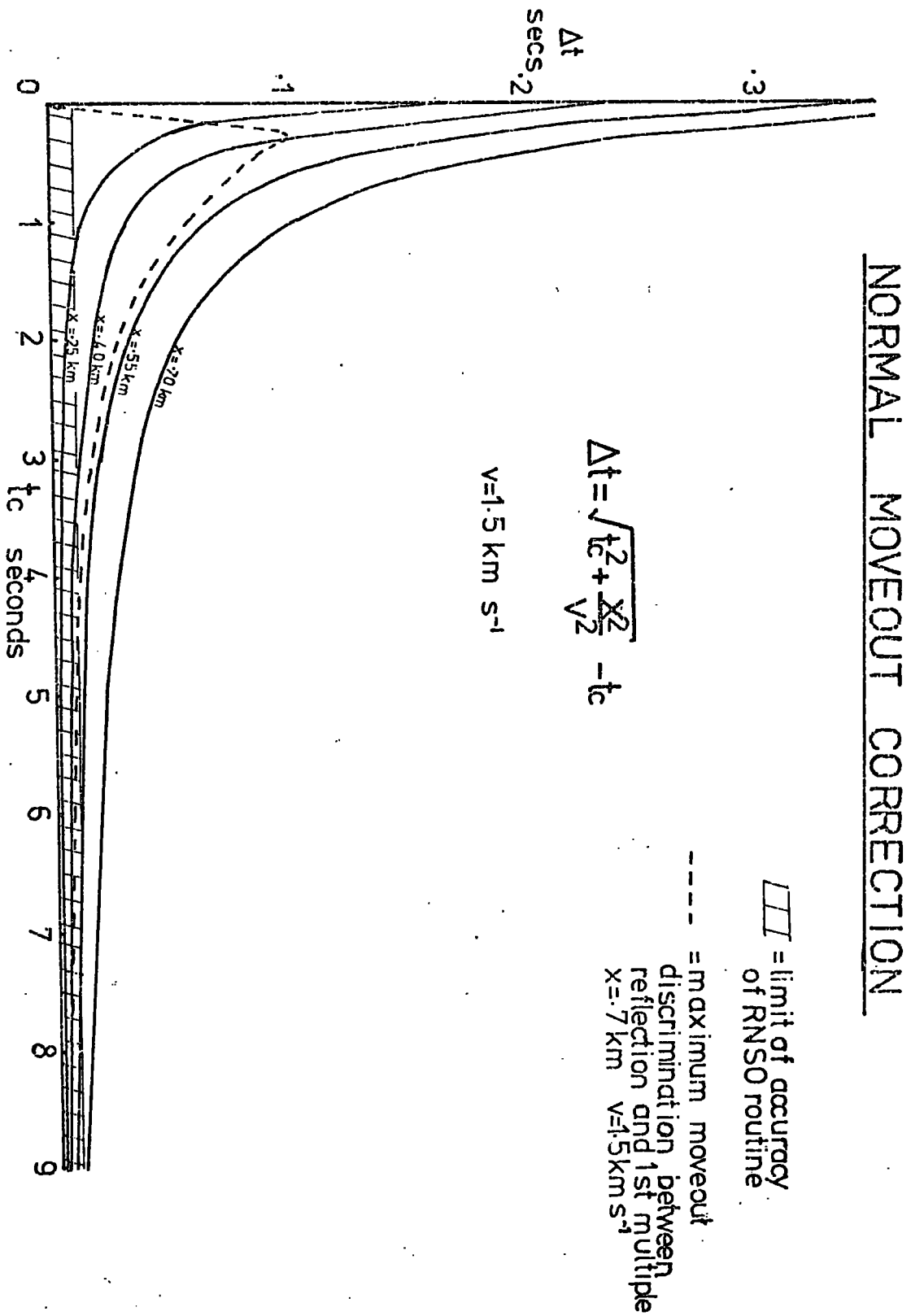

Fig.3.6 Plot of the moveout correction Δt against time down record t_c, for different values of shot-receiver separation 'x' used in the 1973 and 1974 surveys. Dotted line is the difference in moveout for a reflection and the first order multiple that arrives at time t_c for the last section of the array. Shaded area is the limit of accuracy of the RNSO routine.

parameters of the geophone array (opn. 12, fig. 3.7). This sort of stacking will improve the signal to noise ratio of the records (by up to the square root of the number of channels stacked) but will have no effect on the attenuation of multiples.

For shallow reflections, however, the time shift required to convert the records to a simulated coincident shot-receiver condition is not linear but varies along the length of each record (fig. 3.6). Thus for each sample that is to be stacked a time shift must be calculated and applied. This is done in the Modular 1 by the RNSO (remove normal step out) instruction written by the author, with the help of Mr. Simon Armstrong, in assembler and listed in Appendix 2.1. There are two ways in which the calculated time shift could be applied; the first is to input each sample and transfer it to an output queue with the requisite time delay, the second is to have an input queue and select from this each sample to be output. The former scheme is undesirable because, as the records are stretched on output, transferring input samples to their place in an output queue would leave unfilled holes in the output queue. Thus the latter scheme has been used in the RNSO instruction.

Fig. 3.7 shows an example of the use of the RNSO statement, both as a set of computer instructions and also the seismic output generated by the program. Four reflection

```
OPN?12;
APPAY?PSF;X,Y,C,(30.00)?
.25,,,
.40,,,
.55,,,
.70,,;
SAMPLING RATE?250;N TIME SERIES CHS?4;DELAY+-10.00S?1;
OPN?4;FILTER ?0;
FILTER      0
N. STATEMENTS?4;DIMENSION<10.00 ?0;

      1 ?INPUT;FILEN?.01;DELAY+-10.00S?0;I/P CHN?1,2,3,4;O/P  CHNS?
1,2,3,4;

      2 ?RNSO;  CHNS?1,2,3,4;X,Y?0,0;VELOCITY<30.00KMS?1.5
;DELAY+-10.00S?0;O/P  CHNS?5,6,7,8;

      3 ?OUTPUT;FILEN?0;DELAY+-10.00S?0;I/P CHN?1,2,3,4,5,6,7,8
;O/P  CHNS?1,2,3,4,5,6,7,8;

      4
END
N TIME SERIES CHS?      4@    2295    1000       4
FILE      0       1       0       0
OPN?0;FILTER ?0;STATMT ?0;
```

X,y coordinates & static time correction for recording array (x,y km, c seconds)

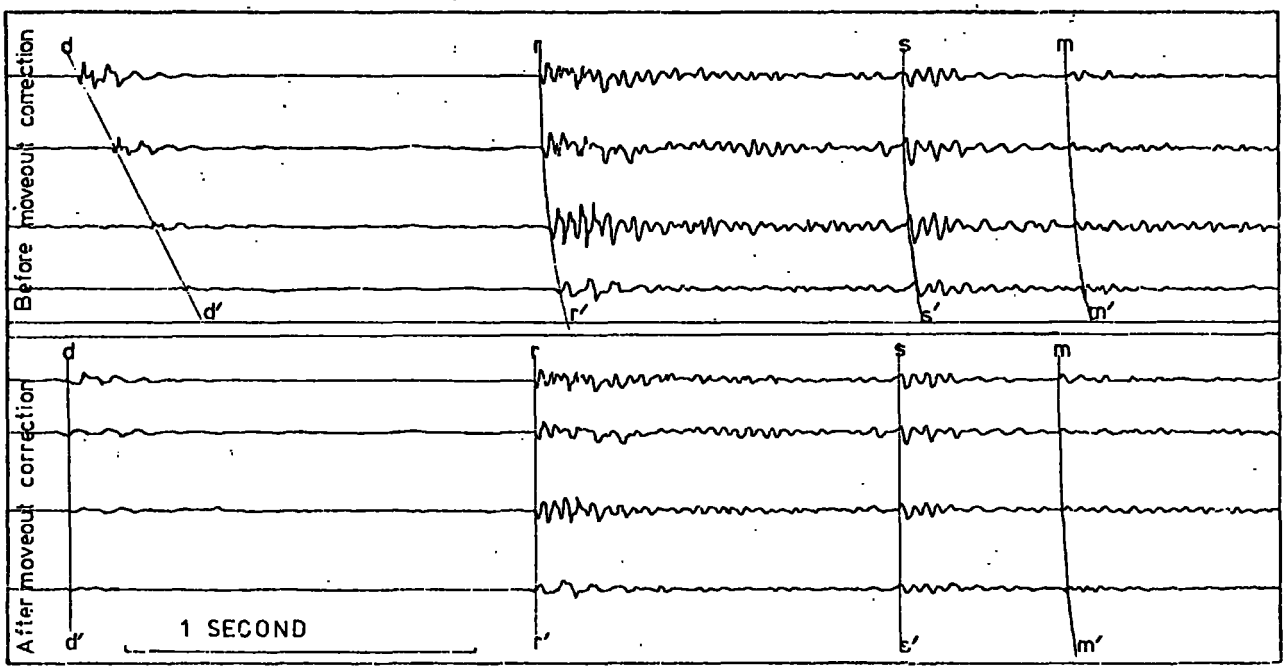

Fig. 3.7 The use of the RNSO instruction both as a teletype listing (instructions typed in are underlined) and a jet pen play-out. d-d' is the direct wave, r-r' the reflection of the sea bottom, s-s' a deeper reflection m-m' the first order multiple.

traces are shown both before and after normal moveout correction. The direct wave d-d' and reflections r-r' and s-s' have been accurately lined up. The multiple m-m' is not perfectly lined up, although the discrepancy is small, and will be attenuated when stacked. As can be seen from fig. 3.7 any given reflector occurs earlier on the record after moveout correction than before. The process of moveout correction requires access to the data ahead of the output time; therefore an input queue (time series channel) of sufficient length (the system delay) must be in the computer, ahead of the output time pointer, to allow such access. The greatest time shift needed is at $t_c = 0$ when $\Delta t = x/V$. Now x/V is the direct wave arrival time and has physical meaning as, for a coincident shot-receiver, the direct wave will occur at $t_c = 0$. Thus all channels requiring moveout correction must be time series channels with a system delay greater than the largest direct wave arrival time for the velocity and array configuration (opn. 12, fig. 3.7) that will be used by the RNSO instruction. It should be emphasised that at no time during this process is the entire waveform in the computer. The machine storage of the Modular 1 is too small for this to happen. The signals are processed sample by sample and in every 250th of a second one sample of each channel is added to the input queue, one sample lost from the front of

the input queue and one sample transferred from within the input queue to the output location and output.

The time t_c is calculated from a sample counter (TBP). The point $t_c = 0$ is the point where the record, after removal of moveout, begins. Prior to this, however, for the time of the system delay, samples have been input. Therefore if TBP is to be zero at time $t_c = 0$ it must start negative (minus the system delay). This situation with TBP negative is the part of the waveform prior to the direct wave arrival and so normal moveout correction is inapplicable. For a typical record of 1250 samples (5 seconds at 250 samples s^{-1}) the expression $t_c^2 + x^2/V^2$ under the square root becomes very large (1.6×10^6) if calculated in samples, and special square root software would be needed to evaluate this. Instead the calculations are performed in seconds (and hundredths of a second) and provided no records of more than 15 seconds in length are processed (never needed for standard reflection work) the existing software is adequate. This however does mean that in the worst case, an error of up to a hundredth of a second is possible in the calculation of Δt (as shown in fig. 3.7).

The calculation of moveout is dependent on velocity. For any reflector, the velocity required for correct removal of moveout is the root mean square velocity down to that layer. The moveout velocity should thus be a function of

time down section. However, with only 4 seismic channels and an 800 m array, the data does not warrant this refinement, and a mean velocity throughout the section has been used. Fig. 3.8 shows the effect of velocity on moveout. It was produced using program VELVET (Appendix 2.8). This technique of displaying sequential channels from the same shot or series of shots can be used on better seismic data to define the velocity distribution with time down section.

3.6 Common depth point stacking on the cruise data

The data from the cruises in 1973 and 1974 show some improvement when common depth point stacked. The multiples in this area are very strong, presumably because the surface sediments are highly reflective, eroded and compacted by ice. The attenuation of multiples in both deep and shallow water is shown in fig. 3.9. There is very little attenuation in deep water, but attenuation becomes noticeable in about the top two seconds of record. Fig. 3.6 shows (dotted line) the maximum difference in moveout (i.e. for the last section of the array) between a reflection, with a velocity of 1.5 km s^{-1}, and the first order multiple arriving at the same time. This time difference, termed moveout discrimination, is always small (less than 0.1 seconds) but becomes insignificant below about 2 seconds down the record, and

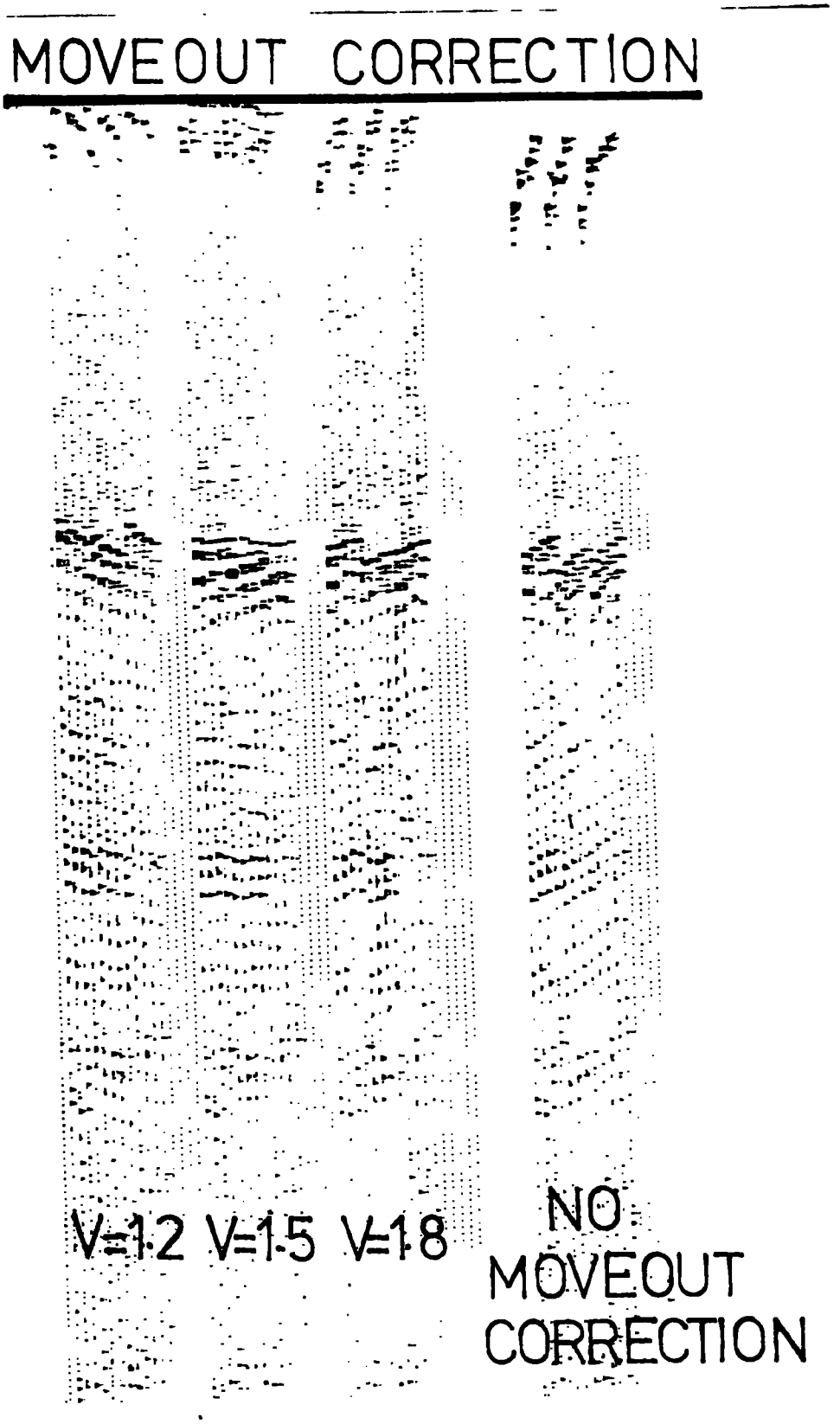

Fig. 3.8 The effect of velocity on moveout correction; the 4 seismic channels are displayed sequentially for each of 3 shots, each shot is half the array length from the previous shot to give single-fold cover. The best stack velocity in this case is 1.5 km s^{-1}. V is the velocity used to calculate moveout in km s^{-1}.

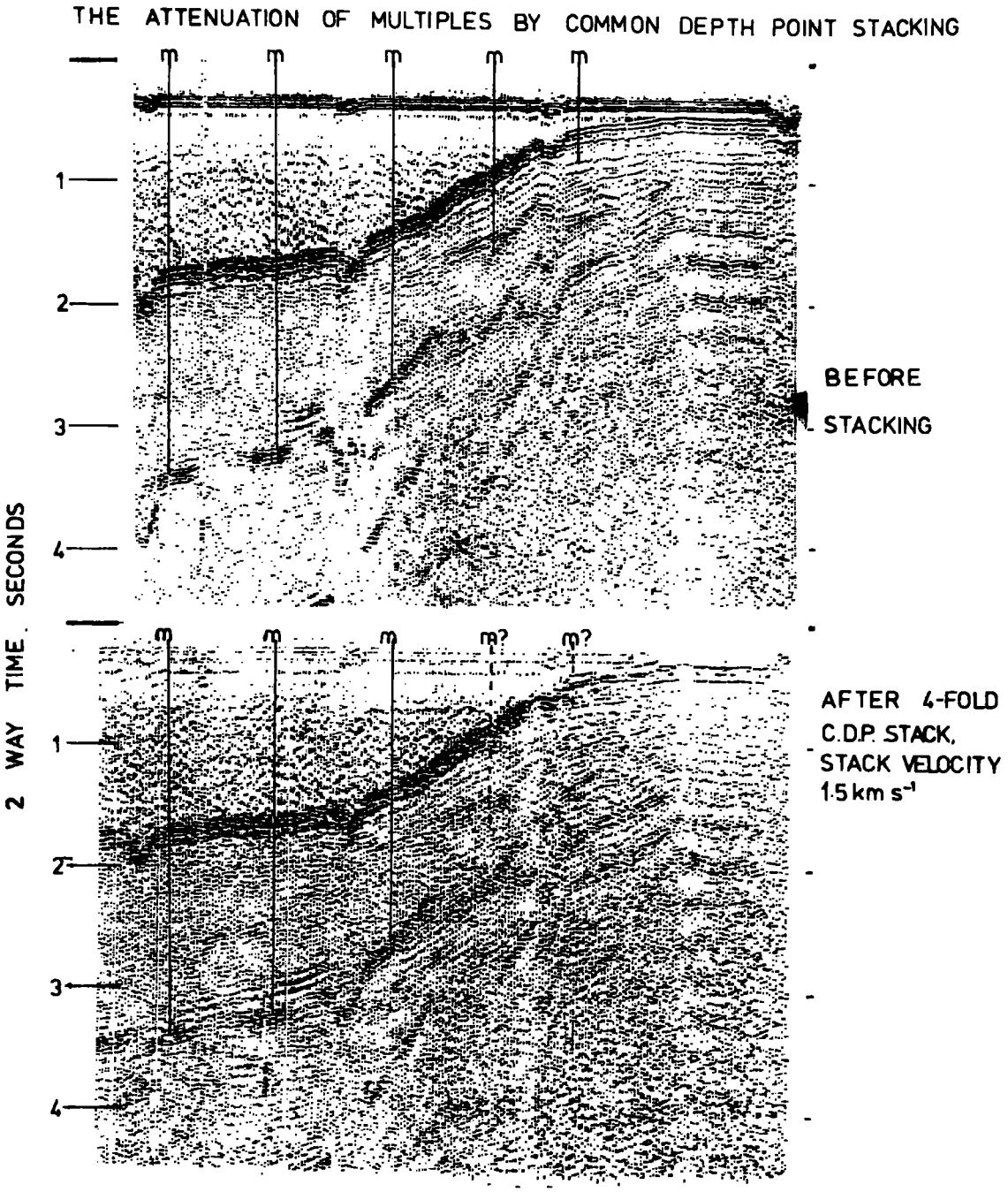

Fig. 3.9 The effect of common depth point stacking on the cruise data. The attenuation of multiples (labelled m) is apparent in shallow water, but not in deep water.

as moveout discrimination is the reason behind multiple attenuation, the lack of attenuation in deeper water is to be expected. A greater seismic streamer length would considerably improve the discrimination and hence multiple attenuation; this must however be accompanied by improved control of the depth of the seismic streamer. For example, an error in the streamer depth of 30 m (and there is evidence for such errors in the cruise data) will mean a mismatch of the stacked channels of 0.2 seconds, and lead to a considerable deterioration in data quality. Such errors can be removed as static corrections, as described earlier, with the existing software provided they are known and remain constant through any one profile. With a seismic array of greater length containing an increased number of seismic channels, the software given in Appendix 2, will need to be slightly altered. However, the principles do not change, and in particular the RNSO statement can handle up to 24 seismic channels. There are, however, limitations on its use introduced by the available machine storage and the speed of calculations. The RNSO routine can handle up to 12 time series channels in a 250th of a second; above this limitation the stacked data must be buffered onto disc if analogue display is still required. However, the current available machine storage means that the 4 seismic channels of the data from the 1973 and 1974 cruises are

about the limit of the current system. With the advent of a new disc based system now being developed on the Modular 1, 12 fold C.D.P. stacking in real time should be possible if there is the available data.

3.7 Data streaming

The preceding sections have described the process of preparing a digital tape of an entire seismic section and then subsequently replaying and processing the digital tape. This is a time consuming procedure and the length of section that can be processed is limited to about 1000 shots by the length of available digital tapes. However, as has previously been stated, the shot firing rate was every 12 or 24 seconds, and the maximum amount of useful seismic data that can be displayed per shot is only 4.25 seconds. Therefore by digitising to disc for 4.25 seconds, and then processing and replaying during the remaining time between shots, it is possible to produce processed sections without going through the intermediate stage of a digital tape. To do this, however, the computer must be able to switch between the irregular timing signal being read off analogue tape for digitising, and a regular generated signal for replay. To allow this, a hardware switching circuit was built that interchanges the incoming time signal, depending on which of two computer analogue

outputs is of a higher voltage. The program JUSTINTIME (Appendix 2.9) will perform this operation, and, once the software has been loaded, any section of analogue tape can be played out through the computer, which convolves the section with a predesigned spiking filter and outputs the section to the display. Each shot is input, processed and output before the next shot occurs on analogue tape. The data is thus streamed through the computer and displayed at the speed it was recorded; Fig. 5.9 is an example of a seismic section produced in this way.

CHAPTER 4

MAGNETIC INTERPRETATION

4.1 Introduction

The magnetic anomalies observed during the 1973 and 1974 cruises are plotted as profiles along simplified ship's track in fig. 4.1. The magnetic anomalies divide the area into three zones: To the east in the deep water of the ocean basin there are the characteristic long wavelength linear oceanic magnetic anomalies numbered in fig. 4.1. Further west beneath the land-ward part of the continental rise, and beneath the scarp and outer shelf, there extends a magnetic quiet zone, with low amplitude anomalies, usually less than 200 gamma. There are a few larger anomalies within this region but these cannot be traced laterally between profiles. Inland from this quiet zone, at the eastern end of the profiles beneath the inner shelf, there is an area of very short wavelength and high amplitude anomalies of up to 1500 gamma peak to peak amplitude. Individual anomalies are not traceable between profiles, but the abrupt change from quiet zone to high amplitude anomalies is a noticeable nearly north-south trending feature of the shelf (fig. 4.1). These three distinct zones are shown in profile form in fig. 4.2.

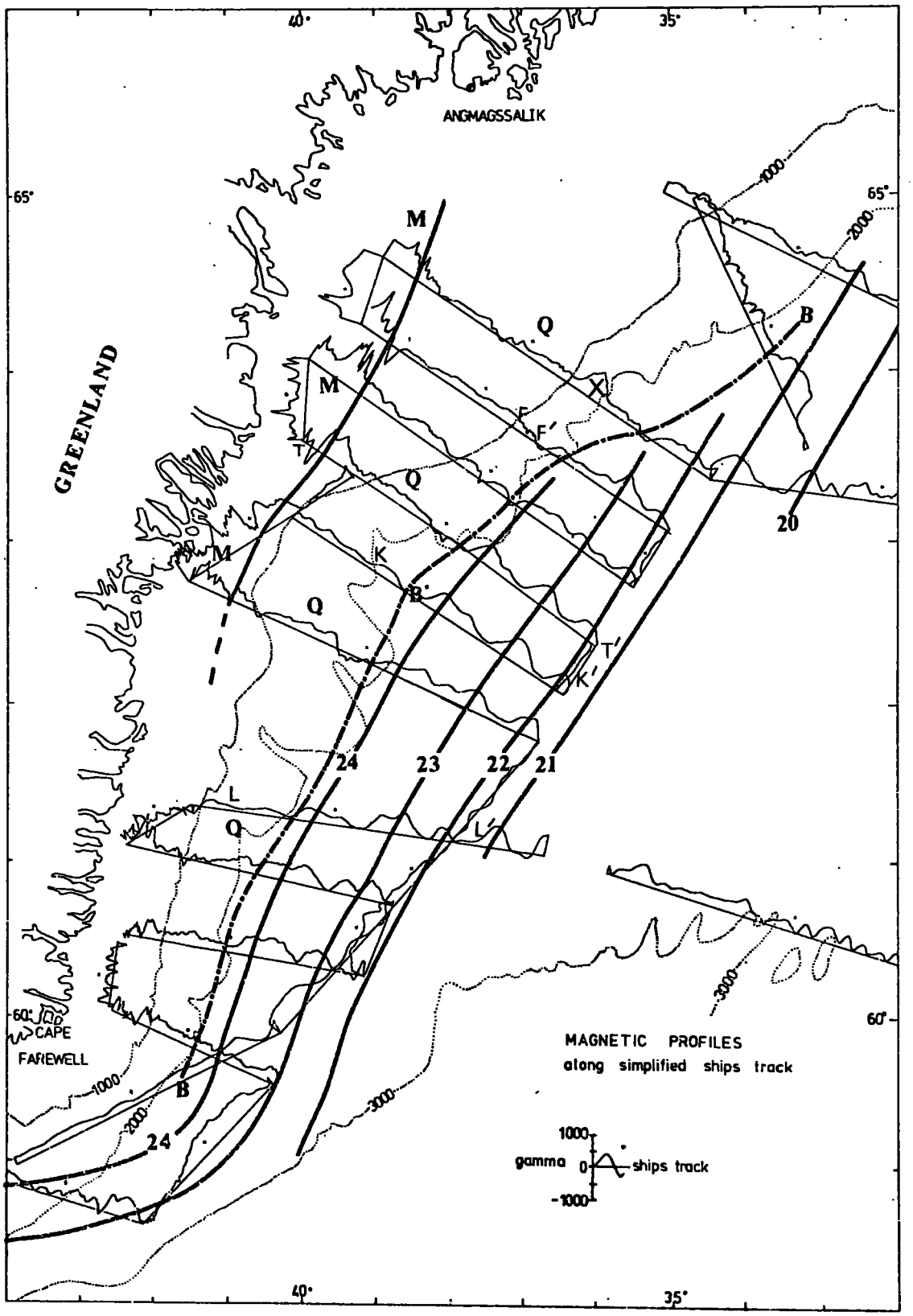

Fig. 4.1 Magnetic anomalies along simplified ship's track, bathymetry (dotted lines) after Johnson et al. (1975a); numbered solid lines are linear oceanic magnetic anomalies in part after Hood and Bower (1973) and Johnson et al. (1975a); line B-B is the magnetic low interpreted as marking the continent-ocean boundary; area Q is the magnetic quiet zone; area M contains the high amplitude, short wavelength anomalies.

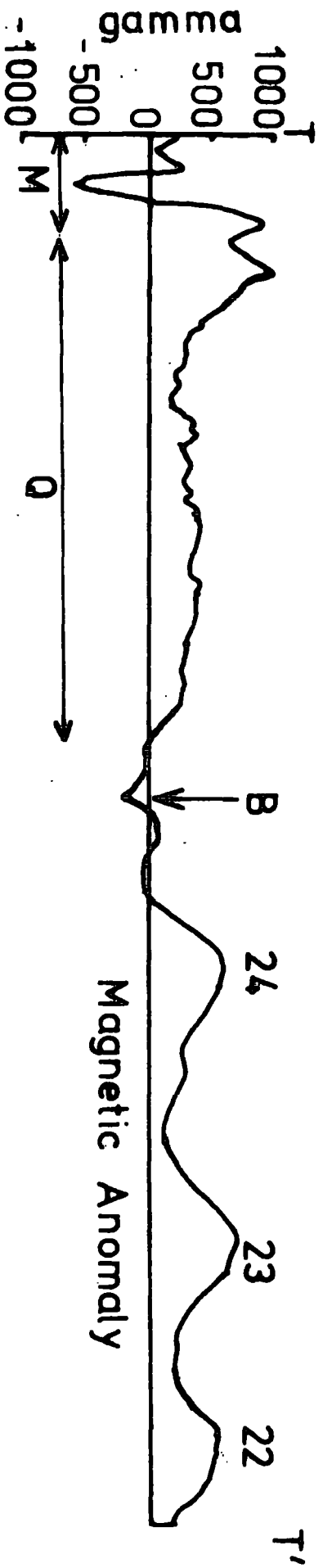

Fig. 4.2 Magnetic profile showing the differing types of magnetic anomaly, along T-T' located on fig. 4.1, labelling as in fig. 4.1.

4.2 Oceanic magnetic anomalies

Fig. 4.1 shows an identification of the oceanic magnetic anomalies, using the anomaly numbering system of Heirtzler et al. (1968). The identification of the anomalies in the Reykjanes basin largely follows that of Johnson et al. (1975a) and those around Cape Farewell follow Hood and Bower (1973). The data provided by these authors has been included in the identification of the anomalies but for clarity is not presented in fig. 4.1. Additional checks on anomaly identification were performed by 'counting out' the anomalies from the axis of symmetry over the Reykjanes ridge, which is crossed by four of the survey profiles, and correlation of anomaly shape with computed profiles derived from a standard magnetic polarity time scale (Heirtzler et al. 1968)

South of 63.5°N. anomaly 24 is the earliest recognizable oceanic magnetic anomaly. Thus the anomalies of the Greenland margin south of 63.5°N. are symmetrical about the Reykjanes ridge with those of the Rockall margin (Vogt and Avery 1974). The split of Greenland from Europe is therefore dated at 60 my (end Palaeocene) by the Heirtzler polarity time scale, although this date has been challenged by recent work discussed in section 4.4.

At about 63.5°N. anomalies 23 and 24 appear to terminate as was tentatively suggested by Johnson et al. (1975) who

note that if they do continue northwards, with considerably reduced amplitude, they would run beneath the continental scarp, which swings eastward across the anomalies. Between 64°N. and 65°N. anomaly 21 (and possibly part of 22) is the earliest recognisable anomaly.

The missing ocean floor between anomalies 21 and 24 can be recognised on the complementary margin of Rockall Plateau. Here the strip of ocean floor older than anomaly 21 approximately doubles its width just north of Hatton Bank (Roberts 1975). Reconstructed continental fits (eg. Laughton 1972) place these two areas against each other prior to continental separation (fig. 5.11). This doubling in width on the Rockall margin is attributed to a westward movement of the spreading axis prior to the time of anomaly 21, as shown diagramatically in fig. 4.3. The initial split and early spreading in this region appears to have been sinuous; the profiles are not closely enough spaced to decide whether this was as a result of sinuous spreading as shown in fig. 4.3 or straight spreading offset by one or more transform faults. The local migration prior to the time of anomaly 21 had the effect of straightening up the spreading axis. This migration may have occurred either as a single jump as shown in fig. 4.3, or as a series of jumps, or as apparently asymmetric spreading about a repeatedly moving ridge axis. The data to decide between these

Fig. 4.3 Strip cartoon showing how a jump in spreading axis can explain the apparent disappearance of anomalies 22, 23 and 24 on the Greenland margin.

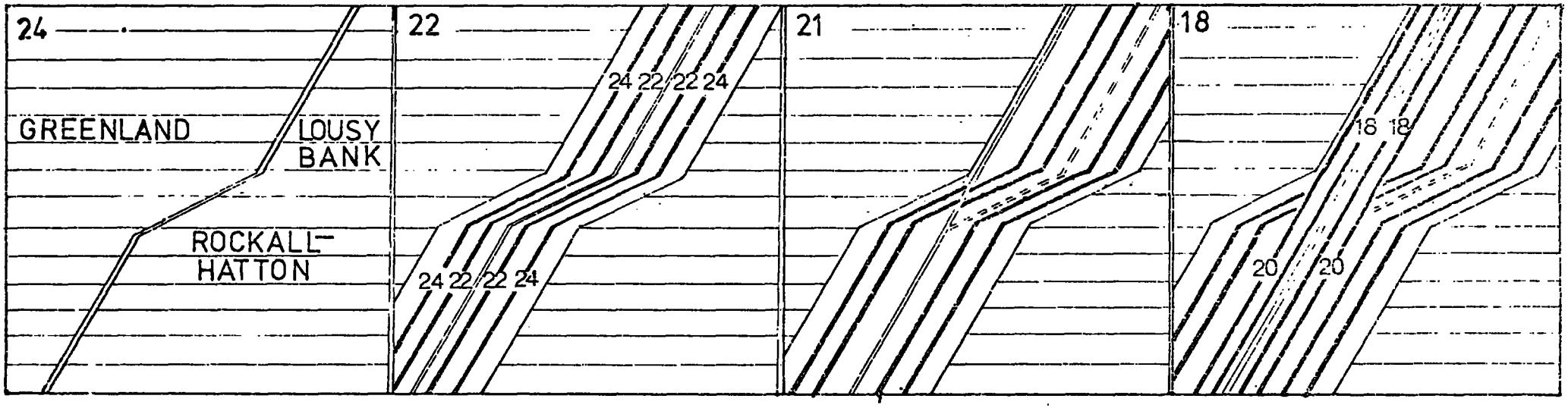

(1) initial sinuous split

(2) sinuous spreading about ridge (double line) producing anomalies 24, 23 and 22 (heavy lines)

(3) Jump in spreading axis to leave extinct ridge (dashed double line). New spreading axis now linear

(4) Spreading about new straight ridge continuing to present day

alternatives is sparse, and must be found on the opposite side of the Atlantic outside the Greenland survey area.

4.3 The quiet zone

Between anomaly 24 and the continental scarp there is an extensive magnetic "quiet zone", with dominantly low amplitude poorly defined anomalies that cannot be correlated with any oceanic anomaly sequence. Within the quiet zone there are a few large magnetic anomalies of several hundred gamma, peak to peak amplitude. These anomalies however cannot be correlated between profiles, and appear to reflect local variations in the underlying crust. Some of these anomalies are analysed in the next section and interpreted as being caused by dyke intrusions and other igneous bodies. The marginal magnetic quiet zone lies to the east of the scarp and is up to 100 km wide, but in the northern part of the survey area it also extends west of the scarp beneath the outer shelf, and achieves a total width of some 250 km at latitude 64.5^{o}N.

Marginal quiet zones have been described from many of the world's Atlantic-type continental margins (Vogt et al. 1970), and the common term "quiet zone" has been used for areas with differing features formed by a variety of mechanisms. Thus no single theory for the formation of quiet zones will apply in all cases and many differing

theories have been proposed, including: (1) formation during a period of constant magnetic polarity (Heirtzler and Hayes 1967), (2) formation at low magnetic latitudes (Vogt et al. 1970), (3) erasure of the original magnetic signature by heating (Vogt et al. 1970), (4) rapid sedimentation inhibiting pillow lava formation (Vogt and Avery 1974), (5) the presence of subsided continental crust (Vogt and Avery 1974, Johnson et al. 1975a). Some of these theories are inapplicable in the case of the south-east Greenland quiet zone, as it is unlikely that the crust was formed at low magnetic latitudes, and abnormal sediment thicknesses are not observed. From consideration of other evidence discussed in later chapters, it is suggested that the south-east Greenland quiet zone is underlain by continental crust downwarped during the initial stages of rifting. This interpretation is also suggested as a possibility by Johnson et al. (1975a).

Subsided continental crust seaward of the scarp has been recognised from the nearby margins of the Labrador Sea (Hood and Bower 1973, van der Linden 1975b) and the Blake-Bahama area (Rabinowitz 1974). In both these areas the line of the continent-ocean boundary is inferred from the presence of a characteristic magnetic anomaly signature, thought to be caused by the juxtaposition of a highly magnetic oceanic crust against more weakly magnetised

continental crust. Fig. 4.4 shows a simple model of the anomaly produced by such a termination of oceanic crust; a small magnetic low can be seen to occur approximately 5 km landward of the termination. On many of the profiles such an anomaly is visible at the end of the oceanic sequence (marked B on figs. 4.1 and 4.4). There is not, however, always a simple low, and the vertical termination of a horizontal magnetic slab may in these cases be an oversimplification. The model given in fig. 4.4 is not an unique interpretation of the observed anomalies, and on its own the presence of such a magnetic low is not conclusive evidence for a continent-ocean boundary. However, the magnetic evidence is in general agreement with the hypothesis that the quiet zone is underlain by subsided continental crust.

4.4 Magnetic anomalies within the quiet zone and the age of anomaly 24

The dating of the onset of continental separation of Rockall and Greenland is dependent on the age of anomaly 24. Heirtzler et al. (1968) dated this anomaly at 60 my from data in the south Atlantic, and this date has been supported by Joides drilling. Recently Soper et al. (1976) and Tarling and Mitchell (1976) have suggested revising this date to 54 or 50 my, based mainly on age determinations

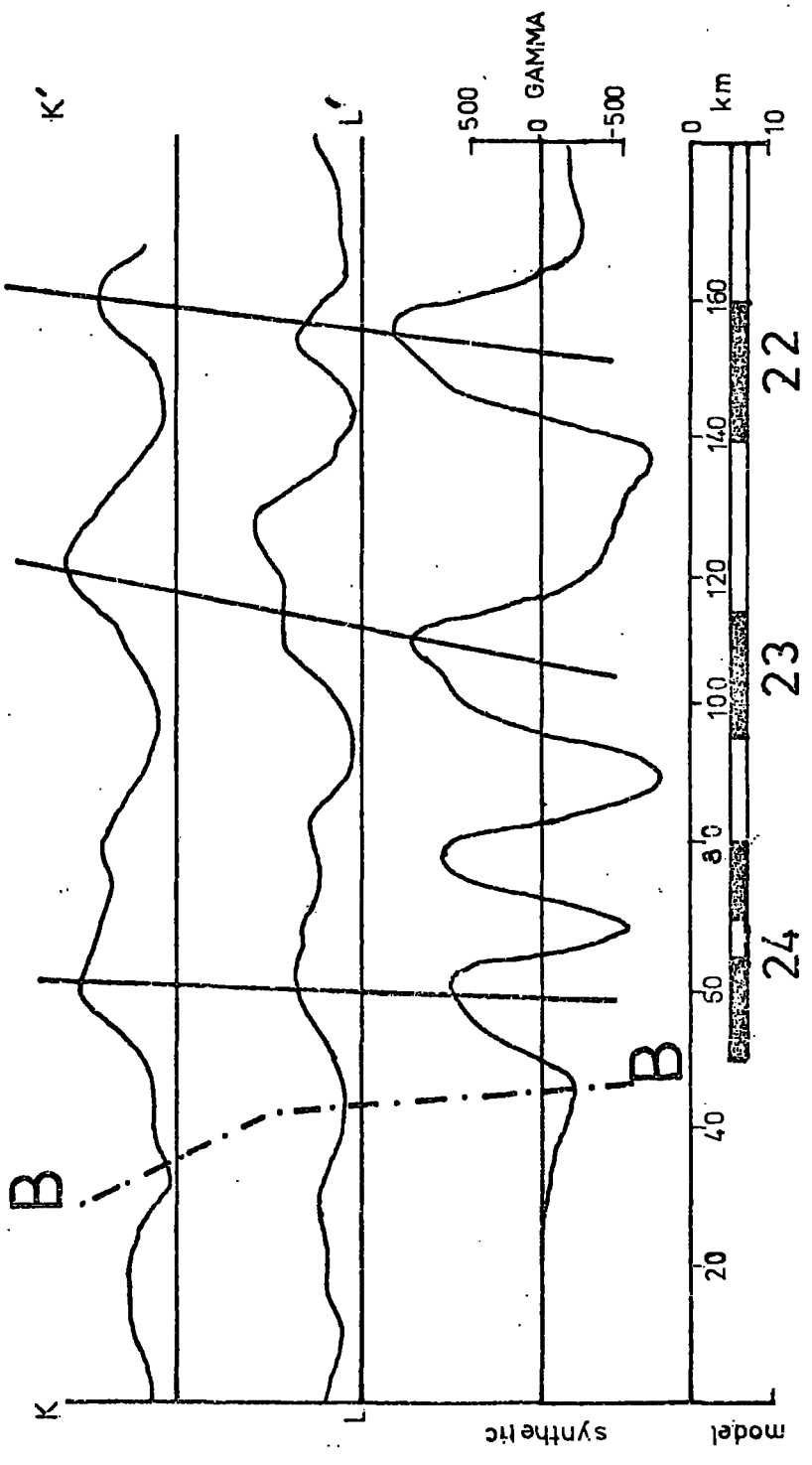

Fig. 4.4 Interpretation of magnetic low B-B as caused by the termination of highly magnetic oceanic material, relative intensities J = ± 16 amps m^{-1}, against non magnetic continental material. Polarity scale after Hiertzler et al. (1968); black blocks are normally magnetised, lines K-K' and L-L' located on fig. 4.1.

from the extrusives of East Greenland which they correlate as coinciding with the initiation of continental separation.

These extrusives outcrop on land to the north of the survey area (fig. 4.5) as a massive volume of Tertiary flood basalts, locally exceeding 9 km in thickness (Brooks 1973, Haller 1970, Noe-Nygaard 1974, Soper et al. 1976, Wager 1934). These basalts have been palaeontologically dated by interbedded marine sediments and found to be Lower Sparnacian (end Palaeocene) to Lower Eocene in age (Soper et al. 1976). Correlation of these stratigraphic ages with the rather poorly dated European sequence (Berggren 1972) gives the age of the basalts as 52-56 my.

Isotopic dating of the basalts (Beckinsale et al. 1970) gives ages between 43 and 59 my, but concordant ages of 48.4 $\pm$ 1.2 my on very fresh basalts (Hailwood et al. 1973) may represent the true cooling age. The extrusive basalts are closely followed in time by acidic plutonic intrusives which are dated as ranging between 36 and 51 my, but concordant ages of 49.4 $\pm$ 1.4 my are thought reasonable (Tarling pers. comm.).

Thus the extrusives, and intrusives, on land would appear to be 52-56 my old from palaeontological evidence, and about 50 my old from isotopic evidence. If these rocks were erupted at the time of, or shortly before, continental split (Brooks 1973, Soper et al. 1976) then it would

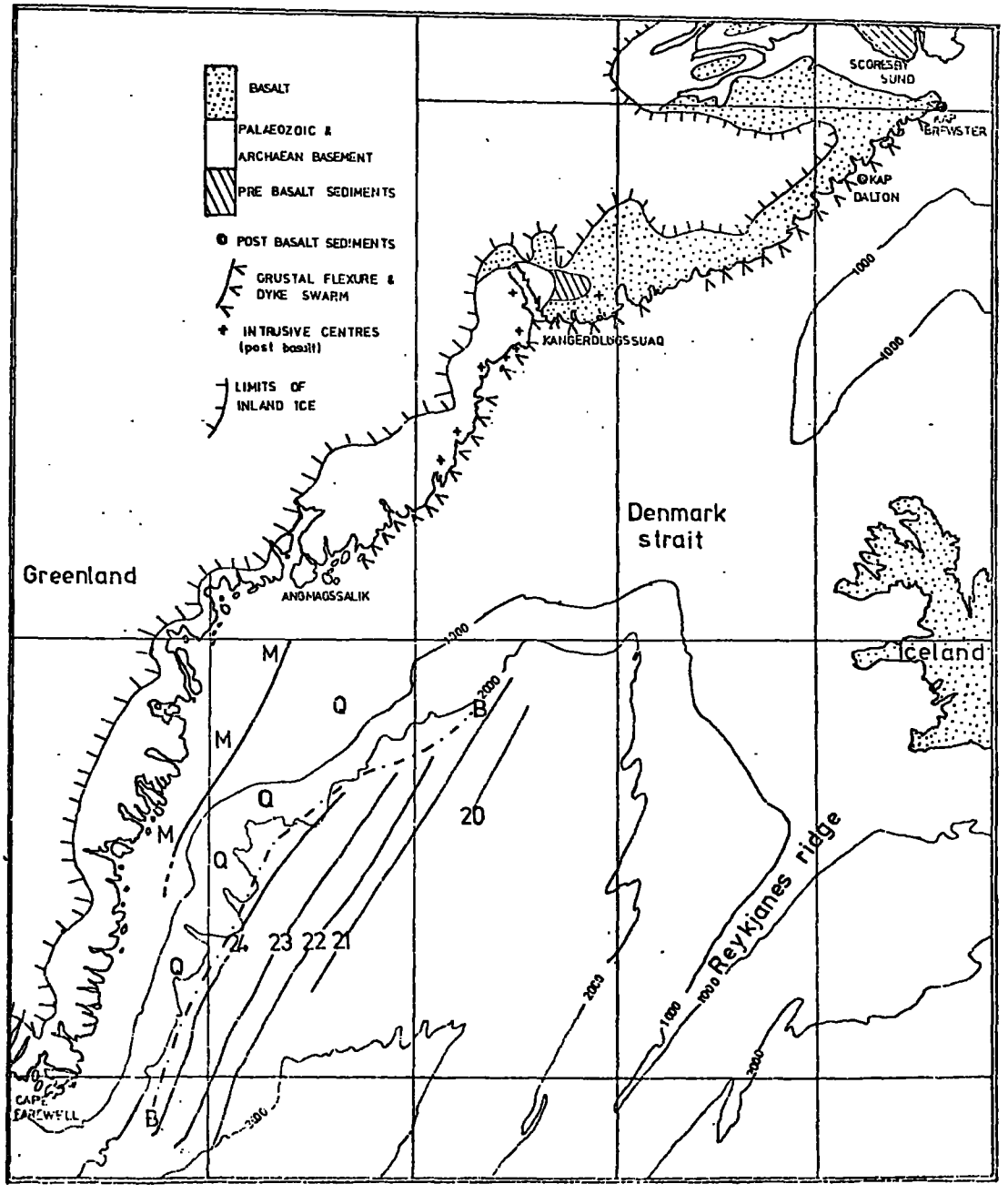

Fig. 4.5 Sketch map showing the relationship of the magnetic anomalies with the extrusives on land, anomalies as in fig. 4.1, geology after Wager (1934) and Escher et al. (1970).

indicate that the dating of anomaly 24 as 60 my is erroneous.

The Faeroese and Hebridean basalts on the east of the Atlantic, however, have a similar claim to being erupted at the time of continental split. These basalts show a wide scatter of ages (Evans et al. 1973, Macintyre et al. 1975, Musset et al. 1973, Tarling and Gale 1968), but in general appear to be in agreement with an age of 60 my (Tarling pers. comm).

Thus it would appear that there is a 10 my age difference between the basalts on land to the west and east of the split, and thus to correlate the Greenland basalts with the split, implies that the Faeroese and Hebridean sequences were erupted up to 10 my before the split. It is possible, however, that the Hebridean and Faeroese basalts formed at the time of split and that the Greenland sequence was erupted approximately 10 my later (at anomaly 21 times), perhaps as a result of the westward jump in the spreading axis at this time. It should also be emphasised that the northernmost occurrence of anomaly 24 in the Reykjanes basin is some 500 km from the basalt outcrop on land, although anomaly 24 is again the earliest anomaly even further north in the Greenland sea (Talwani and Eldholm 1974). The magnetic anomalies adjacent to the basalts in the intervening Denmark Strait are not identified (Johnson et al. 1975b), but it is doubtful that

anomaly 24 now abutts the continent, although it probably once did. Thus the correlation between the extrusives of East Greenland and the onset of spreading at anomaly 24 times is tenuous.

There is evidence from within the magnetic quiet zone for a significant time interval between the initiation of spreading and a period of volcanic activity. The seismic records show the existence of two piercement structures within the sediments of the rise that now outcrop on the sea floor. Similar bodies were noted from slightly further south by Johnson et al. (1975a) who described them as diapiric structures and suggested that they lie on subsided continental crust. The associated magnetic and gravity anomalies are included in fig. 4.6; the structures have no gravity signature, but have associated magnetic anomalies of over 100 gamma. The magnetic anomalies have been taken from the original magnetometer charts rather than the reduced data profiles, which have too coarse a sampling rate to accurately define the anomaly shape. The observed magnetic anomalies have a short wavelength component that cannot be a result of the underlying geology, as the water depth is too great to allow such short wavelengths even from a point dipole at the sea-bed. The short wavelength component with amplitudes of up to 30 gamma and periods of about 3 minutes is thought to be the result of a magnetic

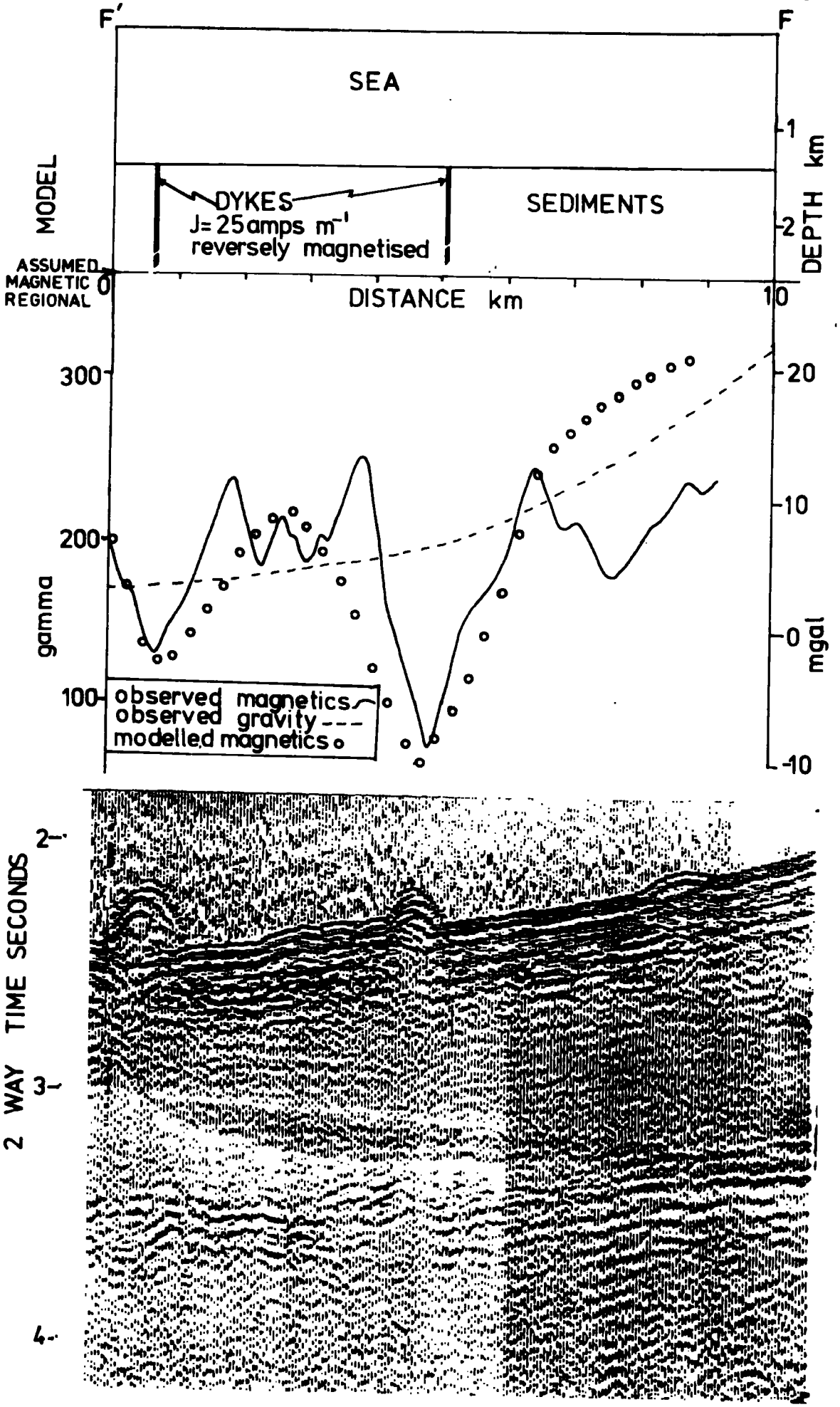

Fig. 4.6 Section showing piercement structure interpreted as intrusives within the Tertiary sediments of the rise, along line F-F'(located on fig. 4.1).

storm; observatory magnetometer charts from Lerwick show a short lived high frequency storm, with amplitudes of approximately 10 gamma, at this time and the difference in amplitude between Lerwick and the survey area may be explained by the higher magnetic latitudes of the survey area. The storm is, however, probably not large enough to completely explain the anomaly of fig. 4.6.

The structures are thought to be igneous intrusives rather than salt diapirs because of their magnetic signature. They cut, approximately 1.5 km of sediments tentatively dated as Palaeocene-Eocene in age (section 5.5). These sediments can be traced laterally and lie on oceanic crust of anomaly 23 age. There must thus be a time gap between anomaly 23 and the emplacement of these igneous intrusives to allow 1.5 km of sediment deposition.

The extrusives on land were all formed within a few million years, and palaeomagnetic studies indicate that the whole sequence is reversely magnetised (Tarling 1970, Hailwood et al. 1973, Faller 1975). Modelling of the magnetic anomalies over the intrusions (fig. 4.6) shows that they also are reversely magnetised. Thus the intrusions of fig. 4.6 may have been emplaced at the same time as the extrusives on land, although Nielsen (1975) has shown that there may be more than one phase of intrusion on land. The correlation of the two areas of volcanic activity is

tentative, but so is any attempt to correlate the extrusives of East Greenland with those of the Hebrides or with anomaly 24. Thus the case for revising the dating of anomaly 24 as 60 my is not considered proven, and the original time scale of Heirtzler et al. (1968) has been used in this thesis. This time scale dates anomaly 23 as 58 my; the intrusions are tentatively correlated with those on land at 50 my, leaving at the most 8 my for the deposition of 1.5 km of marine sediment. This is a fairly high sedimentation rate when compared with similar areas in the N. Atlantic (Davies and Laughton 1972).

There is one very conspicuous anomaly within the quiet zone with a total peak to peak amplitude of 700 gamma (labelled X in fig. 4.1); it is a solitary isolated anomaly within the area of inferred subsided continental crust, and no expression of the structure causing the anomaly is seen in the seismic reflection profiles. Depth estimates (using Peter's length) place the structure below the level of penetration of the airgun at 5 km. The anomaly is interpreted as being caused by an intrusive centre below the Tertiary sediments of the margin; similar centres are seen in the Hatton-Rockall area, on the Greenland coast (fig.4.5) and in the Hebrides. The centre is normally magnetised unlike most of the intrusive centres of the Brito-Arctic igneous province; only one other intrusive centre in the

Rockall area described from gravity evidence by Scrutton (1972) has been found to be normally magnetised (J.E. Lewis pers. comm). The age of the igneous centre on the south-east Greenland margin is unknown although the fact that it does not pierce the Tertiary sediments may indicate that it is earlier than the intrusives of fig. 4.6. The volcanic activity may thus have extended over a longer time span than at first thought, reaching its zenith with the eruption of the lavas, sometime after the onset of volcanic activity.

4.5 The area of short wavelength anomalies

At the western (landward) end of the profiles there is an abrupt change from the magnetic quiet zone to an area of large amplitude (up to 1500 gamma) short wavelength anomalies (M in figs 4.1, 4.2). The change can be seen from the seismic reflection records to correspond to the rapid emergence of a magnetic basement from below a thick sediment cover. The magnetic quiet zone corresponds to the area of basement buried by sediments, and the large amplitude anomalies correspond to the area of basement outcrop. Vogt (1970) and Johnson et al. (1975a) note the parallel fluctuations of the magnetic anomalies and bathymetric profiles, and suggest that basement structures containing basaltic intrusions outcrop on the sea-floor

and are differentially eroded by glaciers.

Vogt (1970) and Larsen (pers. comm.) suggest that these basaltic intrusions may be a continuation of a coastal dyke swarm seen on land further north (fig. 4.5). This dyke swarm is intruded along the axis of a large-scale crustal flexure (Wager 1947) which defines the coast from Kap Brewster southwards to run out to sea at Angmagssalik. The line of the dyke swarm on land is shown in fig. 4.5 and it can be seen that the boundary of the high frequency magnetic anomalies (M) appears to be a continuation of this line. Additional magnetic data around Angmagssalik (Johnson et al. 1975b, Larsen pers. comm.) strengthens this interpretation. The crustal flexure on land is a giant downwarp of the plateau basalts with a total vertical movement of some 8 km (Haller 1970, Wager 1947), the dykes being intruded along the axis of maximum flexure. The gravity and seismic evidence indicates that the postulated southward continuation of the dyke swarm, along the line of high frequency magnetic anomalies, is accompanied by a southward continuation of the crustal flexure.

CHAPTER 5

BATHYMETRIC AND SEISMIC INVESTIGATIONS

5.1 Introduction

The character of the magnetic basement, as indicated by the magnetic anomalies, has been discussed in chapter 4. On top of this basement there are thick accumulations of sediment which have been studied by seismic reflection methods. Previous seismic investigations carried out by Johnson et al.(1975a,b), Avilov (1965), Sommerhoff (1973) and Vogt (1970) have defined the near surface sediments and morphology of the south-east Greenland continental margin in detail. However, the deep penetration achieved by the large volume airgun used in the Durham surveys (Chapter 2) and improvement in resolution that has been possible by digital processing of the seismic records (Chapter 3) have enabled the deep sediment structure of the margin to be studied. The study falls naturally into three sections; bathymetry and surface morphology, Tertiary sediments, which were deposited after the continental split that formed the margin, and sub-Tertiary structure. The map in Appendix 1 gives line drawings of seismic reflection interpretations along ship's track for the Shackleton cruises in 1973 and 1974.

5.2 Bathymetry and surface morphology

Fig. 5.1 shows a bathymetric map of the margin from Johnson et al. (1975a), based largely on German work (Dietrich 1959, 1965, Ulrich 1960). The area exhibits the usual features of an Atlantic-type continental margin, namely the shelf, scarp, rise and ocean basin. These are shown in profile form in fig. 5.2a.

The shelf south of 63.5°N. is narrow (about 75 km) and has a sharp shelf break running parallel to the nearly north-south coastline. To the north of 63.5°N. the shelf break swings eastward and the shelf widens to 225 km at 65°N. Even further north in the Denmark Strait the continental slope is poorly developed and the transition from shelf to basin is gradual.

The shelf bathymetry and surface morphology, particularly south of 63.5°N. have been studied in detail by Sommerhoff (1973), and this work has been reported in English by Johnson et al. (1975a). The shelf is divided by Johnson et al. into an inner ice-scoured plateau, with an irregular topography cut by U-shaped valleys, and an outer shelf of shallower depth with glacially accumulated banks and saddles. North of 63.5°N., where the shelf widens considerably, this division still apparently holds. The ice-scoured topography of the inner shelf with minor sedimentary infillings continues

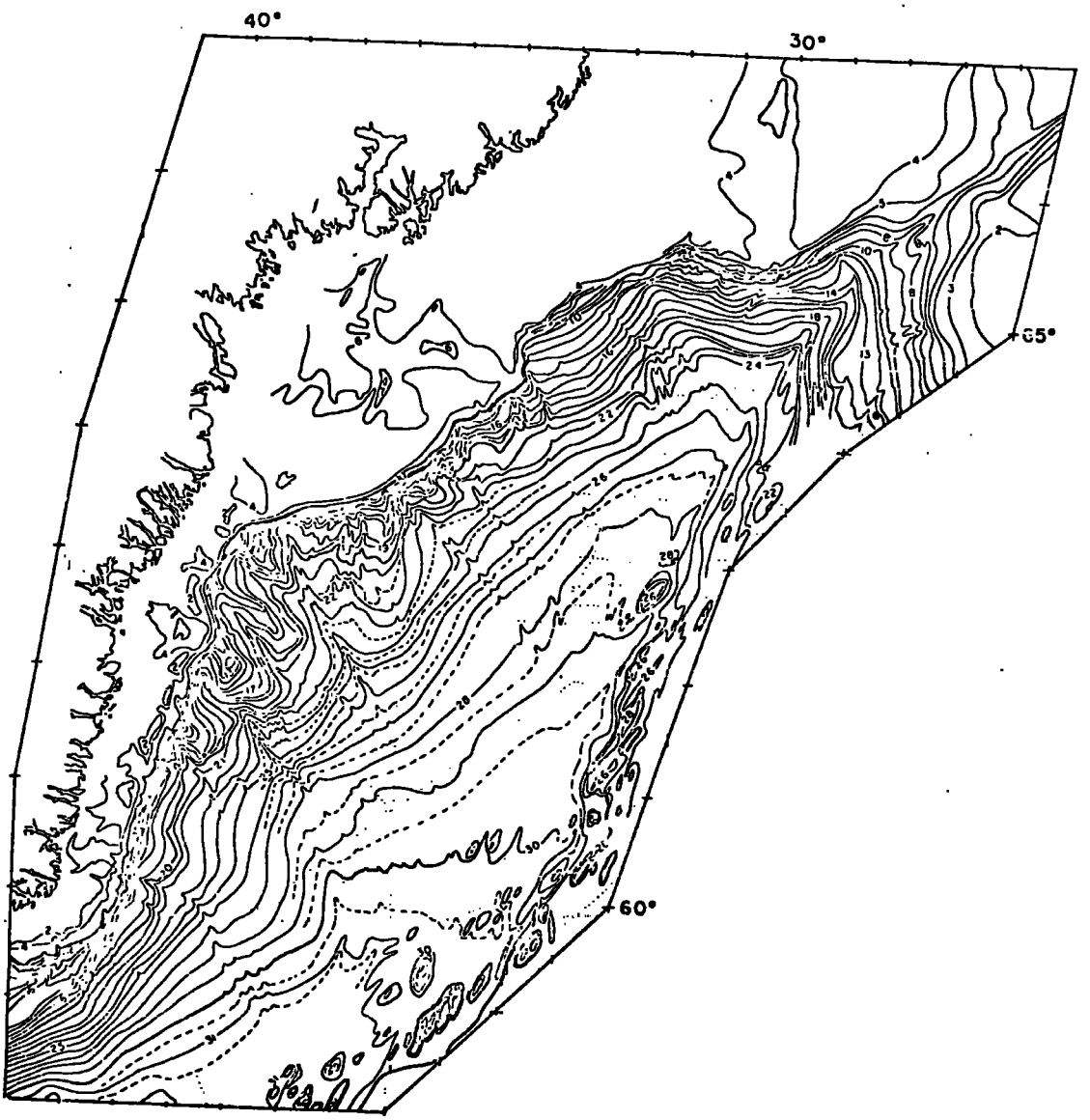

Fig. 5.1 Bathymetric map of south-east Greenland continental margin, after Johnson et al. (1975a) contoured at hundred meter intervals.

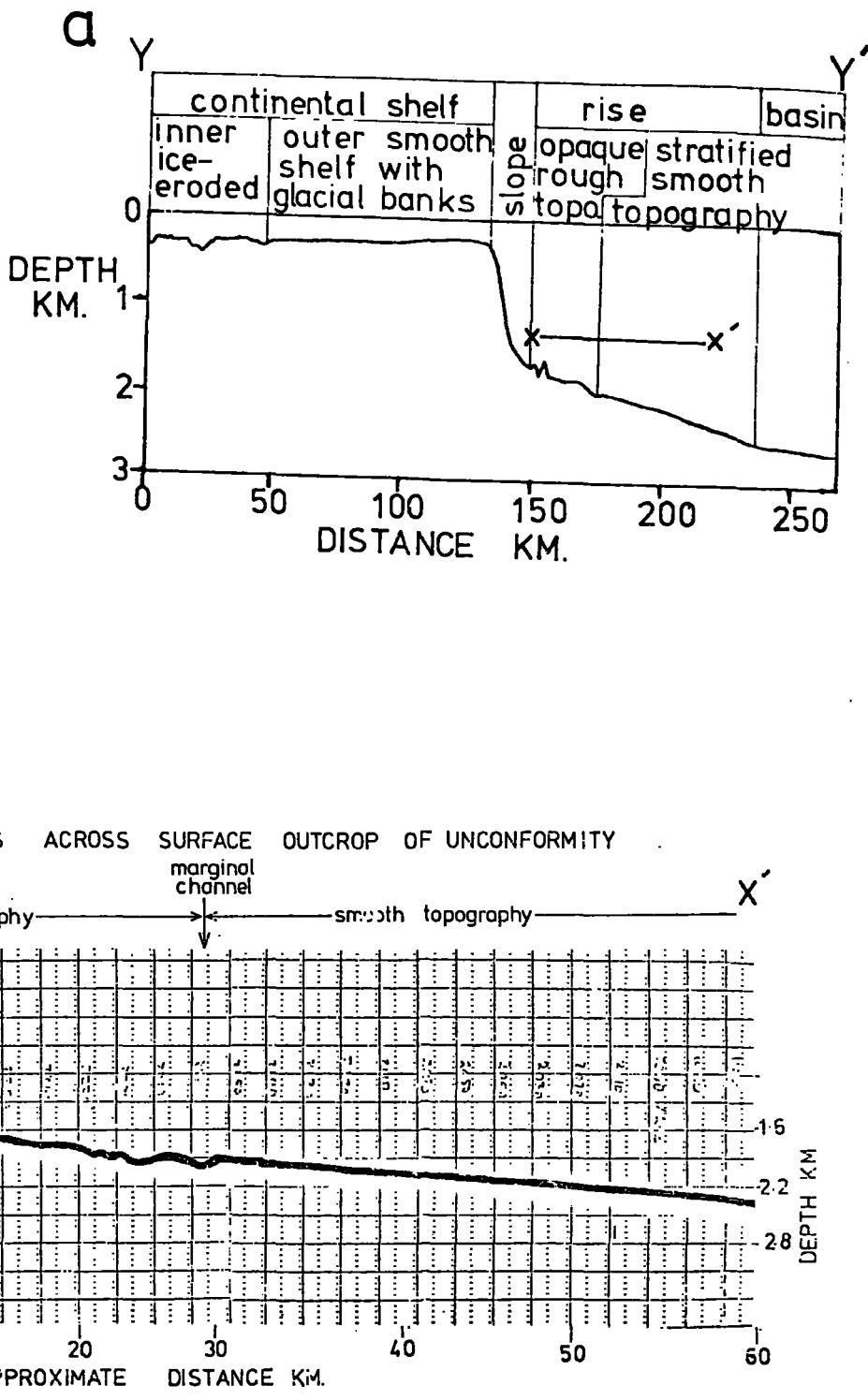

Fig. 5.2 Bathymetric profiles, (a) profile across Y-Y' located on fig. 5.3 showing morphological divisions used in the text; depths are corrected for Matthews area. (b) precision depth recorder chart along X-X' located on fig. 5.2a, showing detail of the rough and smooth rise topography caused by the outcrop of two differing Tertiary sediment types. Depths in fathoms assume a water velocity of 800 fathoms^{-1}, depth in kilometres are corrected for Matthews area.

northwards; the area of smoother topography on the outer shelf however widens to as much as 150 km (fig. 5.3). Seismic reflection, magnetic and gravity studies show that this change from rough to smooth topography on the shelf is not merely a result of glacial action but that it represents an important structural line in this region.

Attempts at coring on the outer shelf (core C1 - see Appendix 1 for details) yielded a small quantity of coarse sub-angular rock fragments with a little adhering fine clay. The fragments are mainly dioritic and granitic in composition (70%), some showing metamorphic textures (such rocks outcrop on the nearby coast), with some basalt fragments (20%). One large (2 cm) well-rounded basalt fragment shows clear parallel scratches on its surface, thought to be ice striations, indicating that this is glacially derived material. Similar material is reported from further south by Johnson et al. (1975a) who point out that basalt is not known to outcrop on the nearby coast (although it does outcrop north of 66°N.). Johnson et al. suggest that the high percentage of basalt fragments results from glacial scour of basalt outcrops on the shelf itself as indicated by the presence of high frequency magnetic anomalies (Vogt 1970).

South of 63.5°N., the continental scarp extends from an unusually sharp shelf break at a depth of 315 m to its base

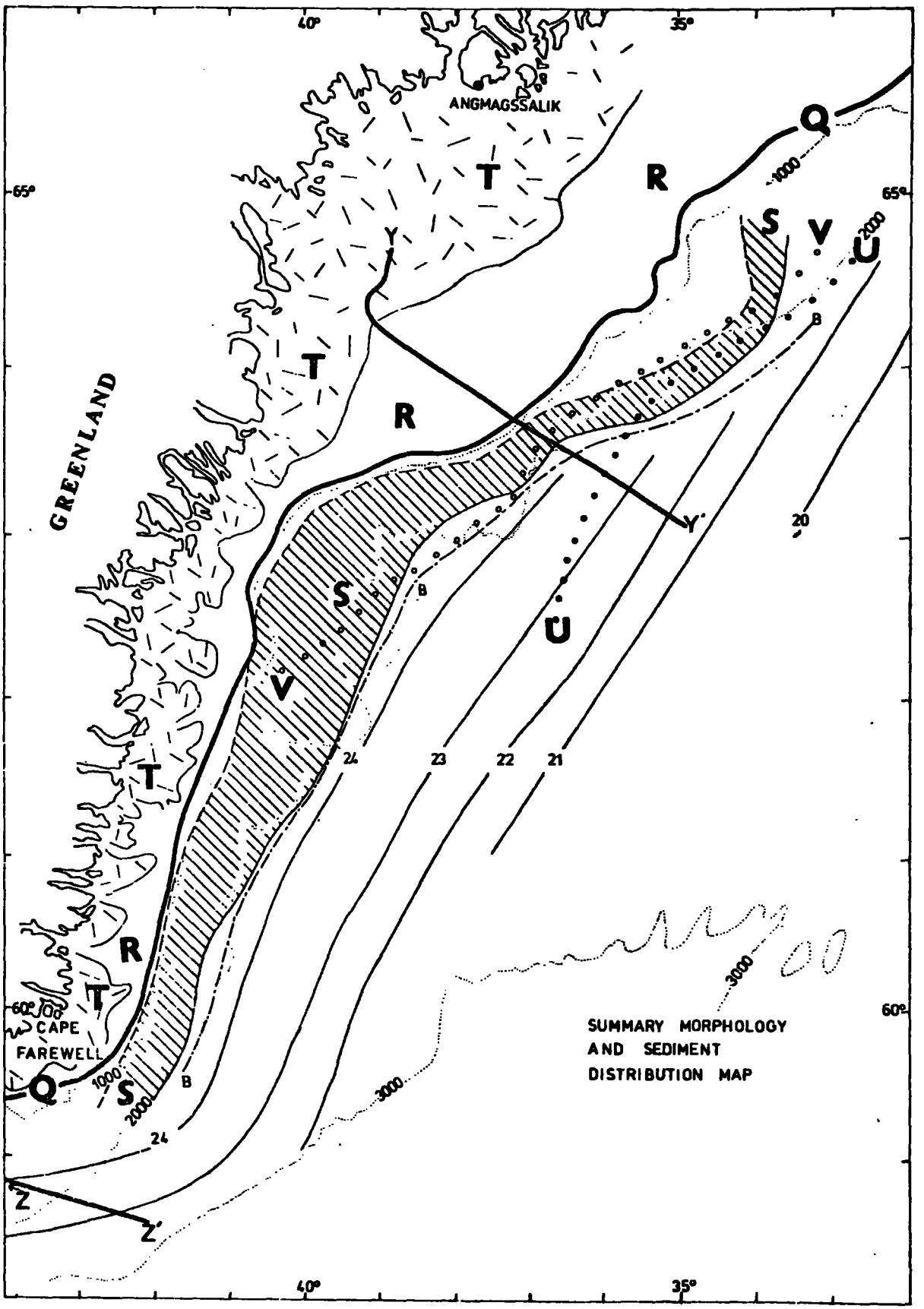

Fig. 5.3 Summary morphology and sediment distribution map, showing shelf break Q, outer shelf R, area of observable sub-Tertiary reflectors S, inner ice eroded shelf T - south of 63.5°N after Sommerhoff (1973), north of 63.5°N after this survey and Larsen (pers. comm.), unconformity basement contact U, surface outcrop of unconformity V, magnetic anomalies as in fig. 4.1, bathymetry after Johnson et al. 1975a.

at 1300 m with a slope gradient of between 1/4 and 1/7 (Johnson et al. 1975a). These gradients are unusually steep, those normally expected for an Atlantic-type margin being 1/5 to 1/25 (Heezen 1974). The slope gradient decreases northwards towards the Denmark Strait. Johnson et al. (1975a) note hills and ridges within the continental slope which they attribute to bedrock outcrops projecting through the sediment cover. Dredges from the scarp, discussed later, (Johnson et al. 1975b) have yielded Devonian-Carboniferous, Eocene and Miocene rocks. Thus, the suggestion by Johnson et al. (1975a) that the scarp has prograded eastward at least 10 km and is formed of glacio-marine sediment fans can not be true for the whole scarp. On all seismic reflection profiles gathered in 1973 and 1974 the scarp appears to be an erosional feature with no indication of recent progradation.

In deeper water, the division, on angle of slope between continental rise and ocean basin is not a useful one in this area. Rather, a twofold division based on surface morphology, as first suggested by Johnson et al. (1975a), is used (fig. 5.2). From the bottom of the continental scarp eastwards, for up to 70 km, there is an area of unusually shallow ocean floor, with a rough bottom topography (fig. 5.2b). This area is intensely cut by canyons and is swept clean of recent sediments. It is

bounded on its eastern edge by the 2000 m depth contour (fig. 5.3). East of this, the sea bottom gradient gradually decreases, levelling out into the ocean basin; the bottom topography here is remarkably smooth. The change between the two types of sea floor is frequently marked by a narrow marginal channel (fig. 5.2b).

South of about 62°N., this division of the rise into areas of rough and smooth bottom topography is not apparent. The smooth bottom topography covers the entire rise and ocean basin. Johnson et al. (1975a) note a similar subdivision of bottom morphology on the basis of echo-sounder reflection characteristics. The area of rough topography they describe as opaque, and the smoother topography as stratified. Johnson et al. however, did not recognise that the rough and smooth topography reflect the contrasting surface outcrops of two differing Tertiary sediment types as described in the next section.

5.3 Tertiary sediment structure

It is convenient to discuss the Tertiary sediment structure of the margin in two regions, starting with that north of about 62°N. Fig. 5.4a shows a typical line drawing seismic profile over the margin in this area. At the western end of the profile, acoustic basement outcrops on the shelf as an ice scoured platform. Towards the east the basement

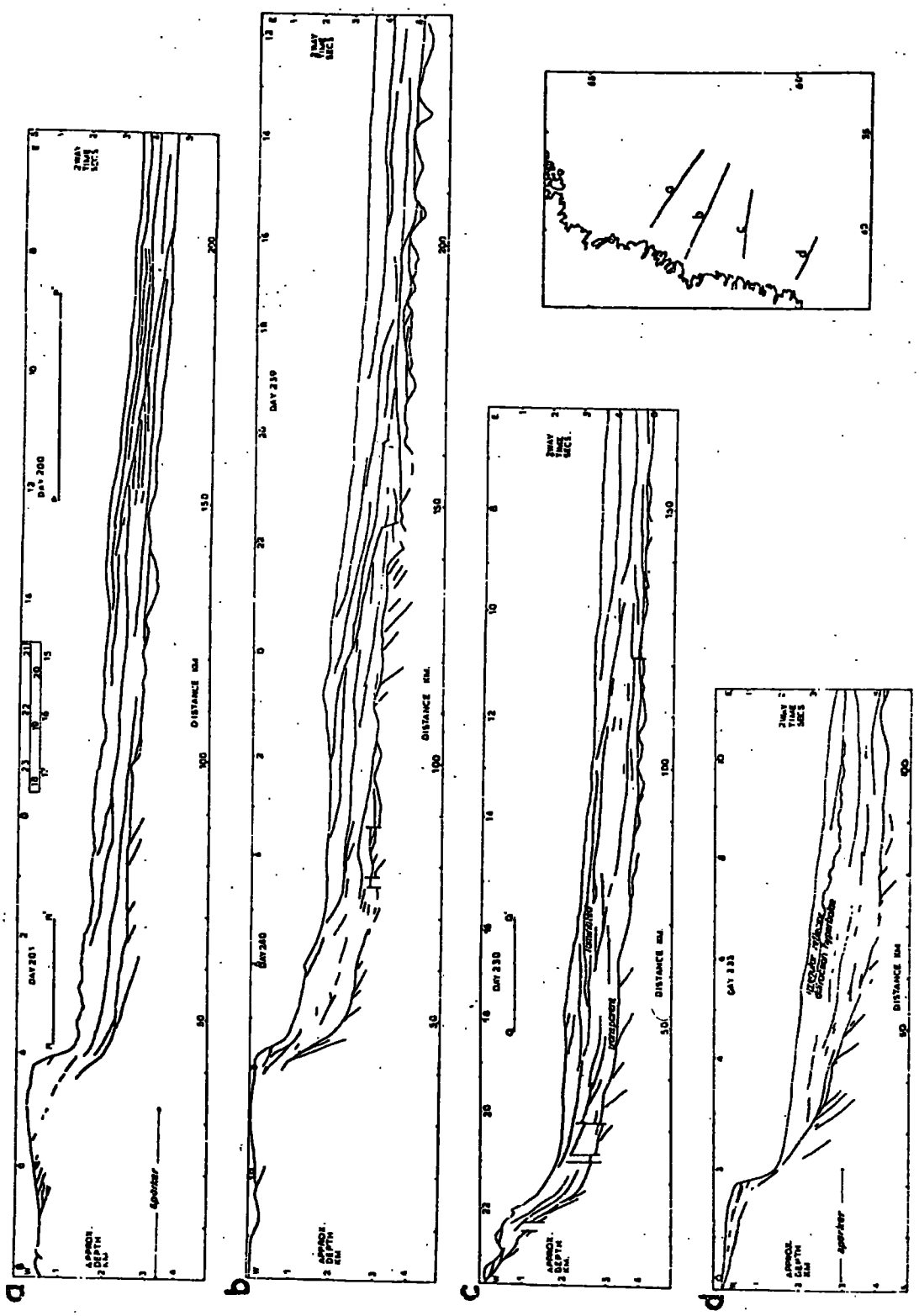

Fig. 5.4 Seismic profile line drawings across the margin showing the sediment structure.

disappears beneath a pile of 1 to 2 km of nearly flat-lying sediments with weak reflecting horizons. As the basement becomes buried there is an associated change from rough to smooth topography on the shelf as previously noted in section 5.2, and also a change in the character of the magnetic field, with high amplitude short wavelength anomalies over the basement outcrop, and a magnetic quiet zone over the thick sediment pile (section 4.5, fig. 5.8). This thick pile of sediments, which will be termed marginal sediments, is of early Tertiary age (see section 5.5), and is possibly covered by a thin veneer of glacial deposits (Larsen 1974). The sediments extend eastward beneath the continental slope and rise with a slight seaward dip possibly due to progressive subsidence towards the east. The scarp itself, as has been noted in section 5.2, is a steep erosional feature (Larsen 1974), although progradation may occur in places (Johnson et al. 1975a).

These marginal sediments outcrop north of 62°N. on the western part of the continental rise and produce the rough topography and opaque bottom morphology previously noted in section 5.2. The sediments are acoustically transparent, with a few reflecting horizons which appear to drape irregularities in the basement. The marginal sediments are overlain by a highly stratified (1.5 km thick) oceanic

sequence giving rise to the smoother lower lying topography and stratified bottom morphology of the ocean basin. The contact between these two sediment types can readily be seen in the more northern profiles to be a plane of unconformity, with the younger oceanic sediments onlapping the truncated older marginal sediments (fig. 5.4a,b; fig.5.6). The angle of unconformity shallows southwards and becomes too deeply buried to be recognised south of 62°N. (fig. 5.4). The seabed contact between these two sediment groups is marked by the change in character of the bottom topography at about the 2000 m depth contour (fig. 5.3). The contact between the plane of unconformity and the basement (U in fig. 5.3) transgresses the oceanic magnetic anomalies, crossing anomaly 23 (late Palaeocene) near its southernmost recognisable position. All the sediments described above must thus be of Palaeocene or later age.

To the south of 62°N., shelf sediments are absent or thin (fig. 5.4c, d) and those present may be entirely of glacial origin. The sediments of the rise, however, are up to 2.5 km thick. The lower group of marginal sediments may outcrop locally on the slope but does not appear to outcrop on the rise where it is buried beneath the later oceanic sediments; the angular unconformity between the groups is not visible on the reflection records. However, the top part of the sediment sequence is well laminated and

the lower portion is acoustically transparent, so that the two groups are probably present. South of 60°N. (fig. 5.4d) one or more irregular reflectors giving rise to overlapping diffraction hyperbolae occur at the base of the upper well laminated sequence.

The southernmost profile of the survey runs across the Eirik ridge (fig. 5.5). This sediment ridge extends from the southern tip of Greenland into the Labrador Sea (Johnson et al. 1969). The sediment sequence of this profile appears to be consistent with that observed to the north. A lower acoustically transparent sequence is overlain by an irregular reflector with diffraction hyperbolae followed by a well laminated sequence. There is no indication in the lower two sediment groups of the existence of a sedimentary ridge at the time of their deposition. The sediment ridge thus appears to be formed entirely of the upper well laminated sequence.

5.4 The unconformity

The unconformity observable north of 62°N. can be clearly seen as an airgun profile in fig. 5.6; analysis of multiples etc. shows that the unconformity is not an artifact of the records. The pre-unconformity marginal sediments are horizontally bedded, and are truncated by a cross-cutting erosional plane of unconformity, which dips to the east at

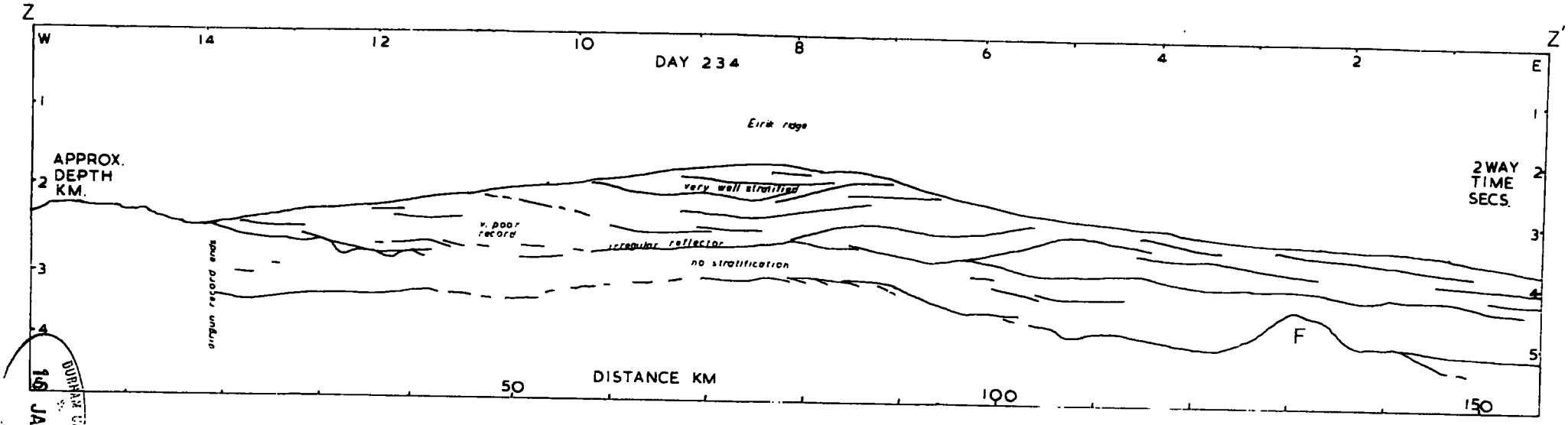

Fig. 5.5 Airgun profile line drawing interpretation across the Eirik ridge, Z-Z' located on fig. 5.3 showing sediment structure. Basement high F is interpreted as a continuation of the Farewell fracture zone.

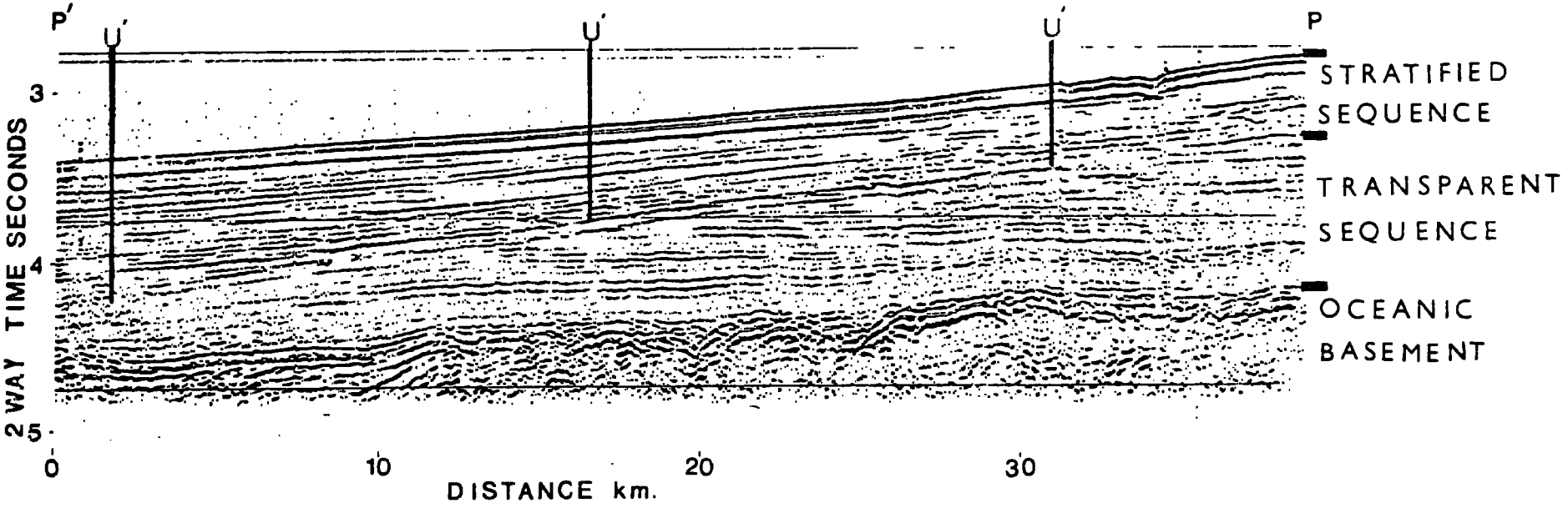

Fig. 5.6 Airgun reflection profile showing mid-Tertiary unconformity, labelled U' along line P-P' (fig. 5.4a). The record has been deconvolved to improve definition; note the profile is reversed relative to fig. 5.4.

about 2 degrees (assuming a sediment velocity of 1.9 km s^{-1}). The post-unconformity sediments were deposited onto this plane and have a slight easterly dip of about 1 degree, onlapping towards the west. If the unconformity was formed subareally deposition, tilting, uplift and erosion of the marginal sediments would be required in post-Palaeocene times before the oceanic sequence was deposited. The uplift would need to be greater in the east, on the ocean side, than in the west; this is considered unlikely as the oceanic crust beneath the unconformity, particularly that to the east, had been recently formed at the time the plane of unconformity was cut, and is therefore likely to have been subsiding. Also, after erosion of the marginal sediments, there would need to be approximately 3 km of subsidence, with reversal of the tilt formed during uplift, to bring the marginal sediments back to their present horizontal position before the oceanic sequence was deposited. Vertical movements of this magnitude are considered unlikely during the Tertiary on the Greenland margin.

The erosion is rather thought to have been caused by oceanic contour currents, which eroded the sediments while they were still at oceanic depths. Cold Norwegian Sea overflow water is known to spill over the Denmark Strait with a velocity locally exceeding 1 m s^{-1} (Jones et al. 1970) and to flow southward parallel to the margin and into the

Labrador Sea (Harvey 1961, Worthington and Volkmann 1965). This strong bottom current probably started when the Denmark Strait first sank below sea level, at about the time when subsidence of the Icelandic transverse ridge caused a radical change to the ocean circulation and thus to sedimentation in the North Atlantic (Vogt 1972). The onset of the new current system has been variously dated as late Eocene and Miocene (Vogt 1972, Roberts 1975). The marginal sediments of East Greenland predate this event and the oceanic group to the east postdates it. The East Greenland current not only prevented sediments forming along the margin (Jones et al. 1970) and shelf (Johnson et al. 1975a) but caused active erosion. At first it cut the plane of unconformity and subsequently it continued to cut back the continental scarp to its present configuration. This is a striking example of the erosional effects of a contour current, reported elsewhere on a smaller scale from the Blake-Bahama Ridge (Schneider et al. 1967) and the Rockall area (Roberts 1975). Further east, where the current was less strong, the oceanic sediments were deposited as contourites. The marginal channel at the junction of the two sediment types is a common feature of sediment deposits formed under the influence of bottom currents (Davies and Laughton 1972).

Recent turbidite deposits along the continental rise were suggested by Davies and Laughton (1972) to be responsible for the opaque morphology of the marginal sediments. Johnson et al. (1975a) correctly noted that this was not so, and stated that the velocity of the Greenland current along the margin precluded deposition until reaching the latitude of Cape Farewell, where the bottom currents reverse direction and flow round the southern tip of Greenland, dropping their sediment load to form the Eirik Ridge. This ridge, and therefore the contour currents that formed it, does not appear to have existed at the time of deposition of the sequence of irregular reflectors or the marginal sequence. The sediment sequence containing the irregular reflectors is interpreted, by analogy to similar reflectors in the Rockall area, as a chert sequence. The marginal sequence is thought to be a result of pelagic sedimentation; the transparent character of these sediments with weak reflectors draping the basement topography is indicative of this type of sedimentation (Davies and Laughton 1972). Inclusions of early Tertiary turbidites is, however, likely and may explain the apparent high sedimentation rate of this sequence (see next section).

5.5 Ages of the Tertiary sediments

The ages of the unconformity and the sediment groups

on either side are not known directly. Attempts at coring the older marginal sediments, cores C3 and C4 (Appendix 1 for details) yielded only recent deposits as identified from palaeontological evidence (Dr. G. Larwood pers. comm.). Johnson et al. (1975b) reported the results of dredges up the continental scarp in the positions shown in fig. 5.13. Greywackes and fine argillaceous sandstones of Upper Eocene and Oligocene age were found about halfway up the scarp in dredges 73-46 and 73-48. Johnson et al. draw attention to the similarity of these sediments with the post extrusive Kap Dalton sequence exposed on land (fig. 4.5). From the reflection profiles the continental scarp would appear to be cut into the upper portion of the marginal sequence thus dating the top part of this sequence as Oligocene in age. What appears to be very nearly the base of the marginal sequence rests on oceanic basement which can be identified from oceanic magnetic anomaly 23 as late Palaeocene age. The marginal sequence may well extend onto later anomalies further south but in the absence of an observable unconformity, distinction between the marginal and oceanic sequences is difficult. Thus the marginal sequence appears to be of late Palaeocene, Eocene and possibly Oligocene age. The presence of apparent intrusives cutting these marginal sediments (discussed in section 4.4) which might be correlated with intrusives on land of mid-Eocene age would imply that at

least the basal 1.5 km, which is the thickness of sediment that can be seen to be intruded, must have been deposited between late Palaeocene and mid-Eocene times (see table 5.1), which is a period of 8 million years at the most. This gives a sedimentation rate of 19 cm per thousand years, which is very rapid for Atlantic deep water marine sedimentation (Davies and Laughton 1972). Minor faulting that affects the marginal sequence but does not pass upward into the later oceanic sediments might be correlated with the tectonic flexuring and normal faulting during the Eocene and Oligocene on land. These correlations are summarised in table 5.1.

The age of the base of the overlying oceanic sequence is therefore late Oligocene or even younger. It is suggested that sedimentation of this sequence is still continuing. Fig. 5.7 shows the location of D.S.D.P. holes in this part of the North Atlantic (Laughton et al. 1972). The holes in the Hatton-Rockall basin (116 and 117) show a very similar sequence to that observed on the Greenland margin. The sediment regime of Rockall as described by Roberts (1975) is divided into two sequences separated by a reflector, R4. The older, pre-R4 sequence resembles the acoustically transparent marginal sequence of Greenland. The seismic profiles of Roberts show that these sediments have few reflectors, draping the basement topography and giving rise

AGE M.y.	Magnet Anom. No.	Epoch	East Greenland	Survey Area	Rockall	North Atlantic
		Plio				
10	5	Mio-cene	Kap Brewster Series	Contourites	Sediment drift deposits	
20	6					submergence of
			normal faults			Iceland-Faeroe-Greenland ridge
30	10	Oligo-cene	tectonic flexuring	Cherts in the South	Cherts	
40	15		Kap Dalton formation		R4	
		Eocene			Limestone oozes	Labrador Sea opening slows
50	20		Intrusions	Intrusions		
	21		Blosseville extrusives	Marginal sequence		Local jump in spreading axis
60	24	Palaeo-cene	Kangerdlug-ssuaq formation	Crustal thinning and Subsidence		Separation of Greenland and Rockall
70	30	C R E T A C E O U S				
	33					
80						Onset of Labra-dor Sea opening
90					?Formation of oceanic crust Rockall and Bay of Biscay	
100			Albian marine transgression			
110						
120						
130						
140		J U R A S S I C	Uplift & Block Faulting			
150						Sedimentary Basin Formation
160			Marine Sediments in coastal graben	Sediments forming sub-Tertiary reflectors		

Table 5.1 Correlation of the stratigraphy of the Greenland margin with neighbouring areas, partly adapted from Roberts (1975) Berggren (1972), Haller (1970), Heirtzler et al. (1968), Soper et al. (1976), and references cited in Chapter 1.

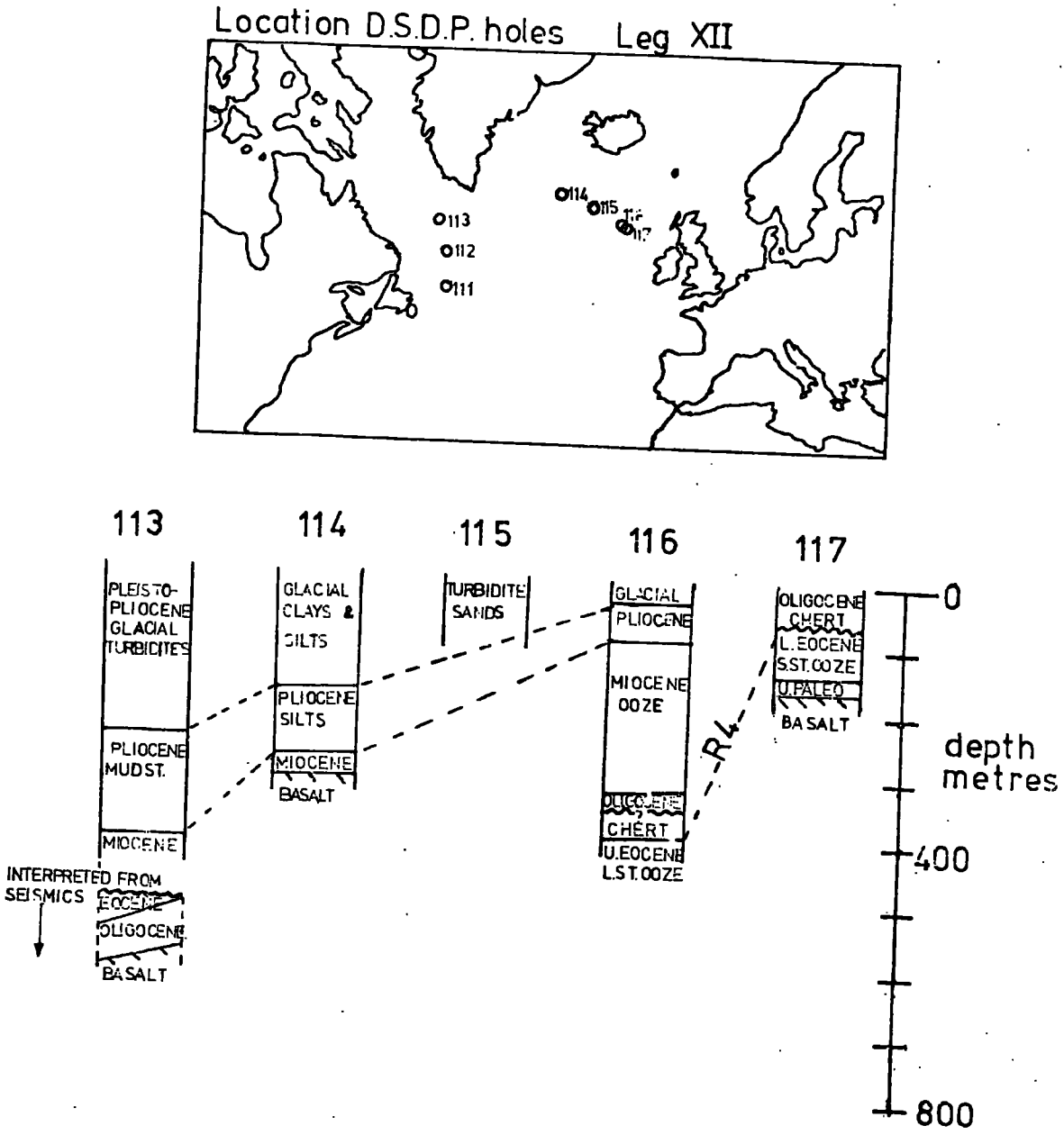

Fig. 5.7 Summary of Deep Sea Drilling Project holes from Leg XII (Laughton et al. 1972).

to a rough bottom topography where they outcrop on the sea-bed. The bottom parts of D.S.D.P. holes 116 and 117 penetrated the pre-R4 sediments which were found to be lithified limestone oozes of Eocene and Palaeocene age (Laughton et al. 1972). The reflector R4 represents a change in depositional regime and is locally a non-sequence; the overlying sediments show an onlap relationship although no distinct unconformity such as that of East Greenland can be recognised. R4 is overlain by a thin sequence of cherty beds of Oligocene age which give rise to conspicuous diffraction hyperbolae, similar to those seen south of 60°N. on the Greenland margin. Above the cherty beds, Miocene and Pliocene oozes occur in D.S.D.P. hole 116, and a differentially deposited sediment drift sequence correlatable with these oozes occurs widely throughout the Rockall region indicating bottom current activity (Roberts 1975).

Extrapolation of the lithologies and dates of the Rockall region to the Greenland margin as in Table 5.1 must be tentative. In the Rockall area, the change from chert beds to sediment drift deposits in the late Miocene (10 my) is correlated by Roberts (1975) with subsidence of the Iceland transverse ridge below sea-level, which allowed cold Norwegian Sea water to overflow into the north Atlantic and initiated the present regime of oceanic bottom currents and the deposition of sediment drift deposits. In the

southern profiles of the East Greenland margin, which lack the observable unconformity but have the chert-like reflectors, sedimentation may have been continuous and the sequence may be correlatable with the sediments of the Rockall region. Further north, where contour currents were presumably faster, and the water depths shallower, the Oligocene cherts were either not deposited or were subsequently eroded when the contour currents started in the late Miocene. Since that time, as the water depth of the Denmark Strait (Vogt 1972) and presumably also of the neighbouring basin has increased, sediment drift deposits of Miocene to recent age have been deposited over the eastern portion of the older eroded sediments.

5.6 Pre-Tertiary sediment and basement

The nature of the surface on which the Tertiary sediments rest exhibits two distinct styles. At the eastern end of the profiles, in the deep water of the ocean basin, the pre-Tertiary basement has a rough surface as shown by irregular diffraction hyperbolae (fig. 5.6), and it lacks visible internal structure. This is typical of the igneous basement which is oceanic layer 2. The magnetic profiles over this region show characteristic long wavelength oceanic magnetic anomalies (fig. 5.8). There are occasional pronounced basement highs; the largest of these on the

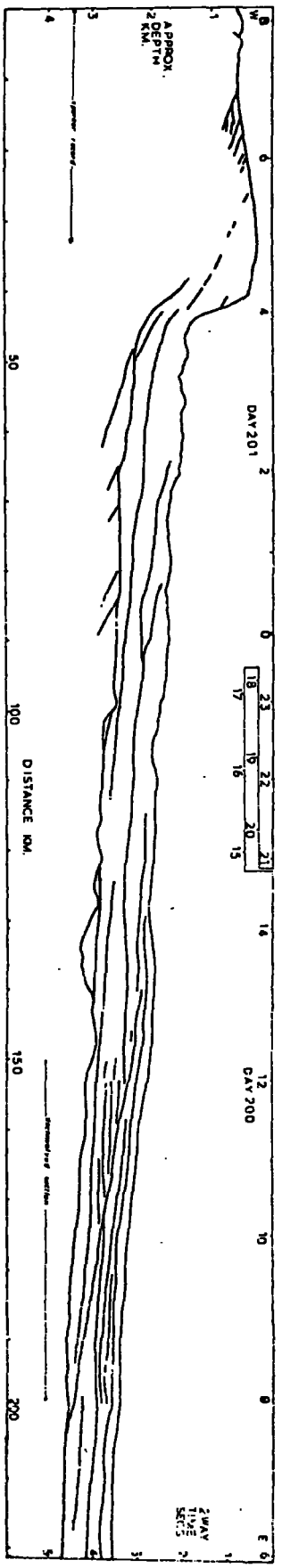

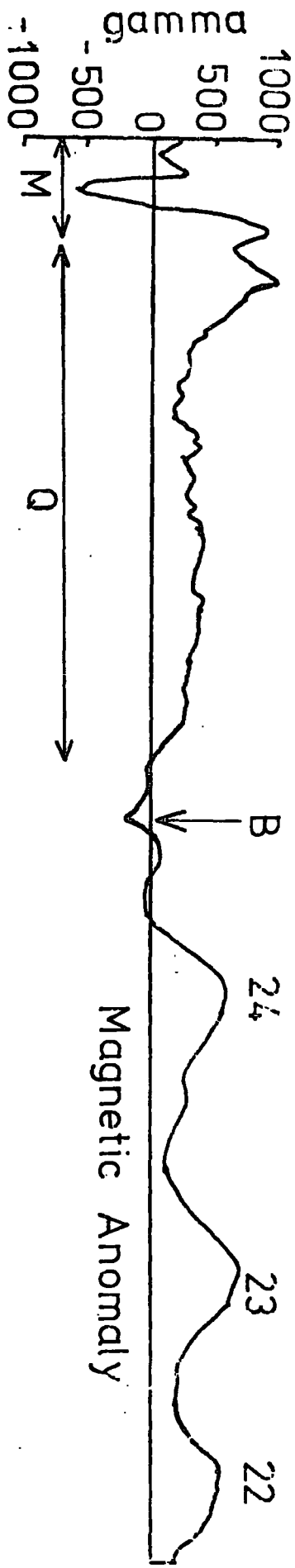

Fig. 5.8 Seismic profile line drawing from fig. 5.4a with associated magnetic anomaly from fig. 4.2, labelling as in fig. 4.2.

profile over the Eirik ridge (fig. 5.5) is interpreted as a continuation of the Farewell fracture zone that has been recognised at the eastern end of the Labrador Sea. This oceanic basement can be traced on seismic records from its outcrop at the Reykjanes ridge westwards into the region of study.

Further west, at a distance of between 30 and 80 km seaward of the continental scarp, depending on the profile, the depth to basement shallows and the nature of the pre-Tertiary surface changes. This change coincides with the western end of the oceanic magnetic anomalies and the start of the magnetic quiet zone which extends from here beneath rise, scarp and outer shelf (fig. 5.8). The topography of the pre-Tertiary surface becomes smoother and the reflection records show a group of strong reflectors beneath the Tertiary sediments identifiable on all airgun profiles across the margin (figs 5.4 and 5.9).

These reflectors show an apparent dip towards the east of approximately 15^{o}, assuming a sediment velocity of 4 km s^{-1}, and are unconformably overstepped by the early Tertiary marginal sediments of the continental rise. The observable extent of the reflectors (fig. 5.3) shows that the sub-Tertiary outcrop is at least 80 km wide, and that it is traceable along strike for 500 km. The reflectors may extend further west than is shown in fig. 5.3, but they

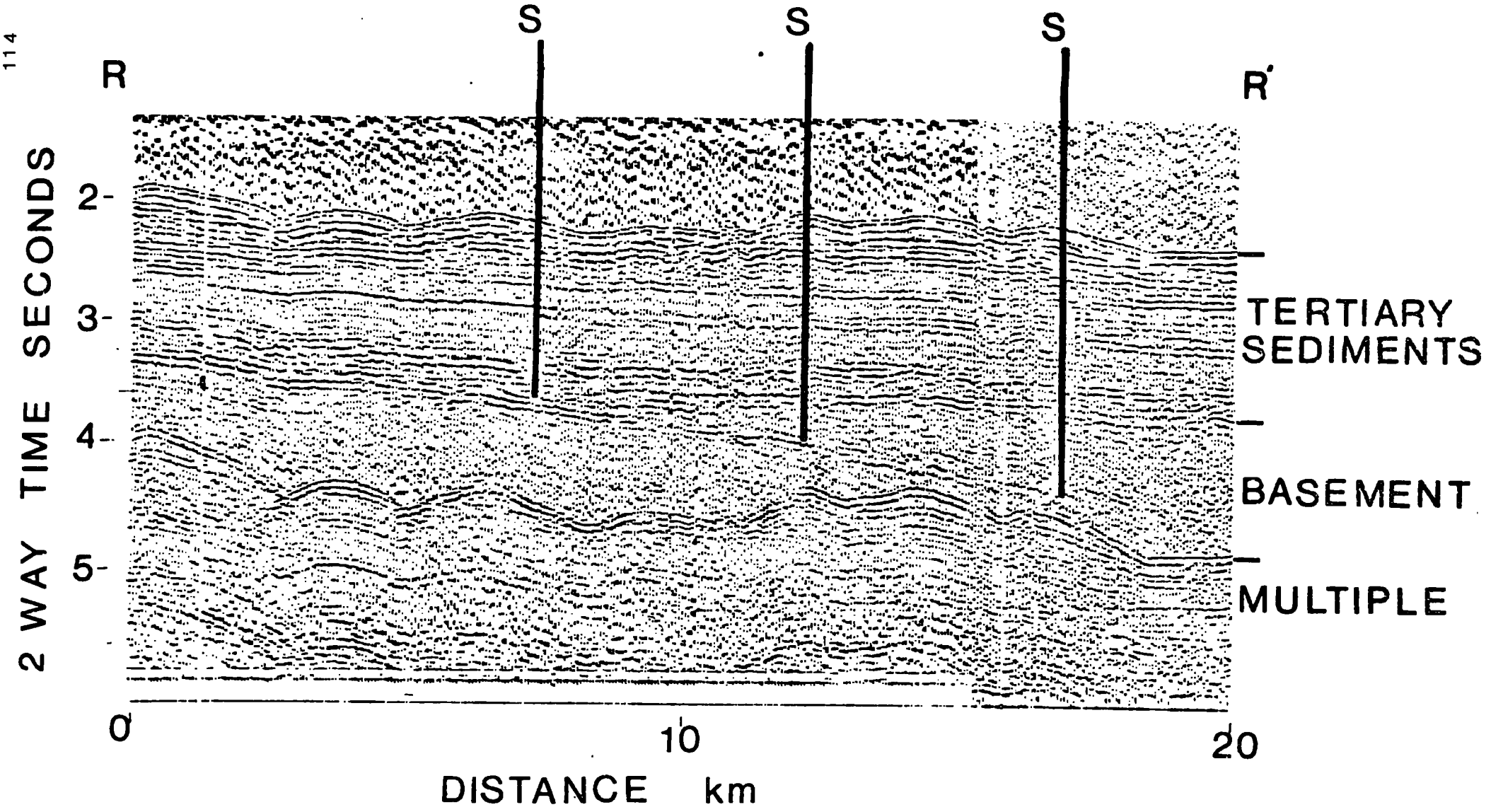

Fig. 5.9 Airgun profile showing prominent sub-Tertiary reflector, labelled S along R'-R' (fig. 5.4a), deconvolved to improve definition.

cannot be recognised beneath the upper slope and shelf because of the shallow water multiples. These reflectors, which are remarkably flat and widely spaced, are interpreted as sediments. Similar structures in deep water off the Voring Plateau (Talwani and Eldholm 1974) were found by drilling, however, to be a lava sequence (D.S.D.P. hole 338). Because of the lateral extent and continuity of the Greenland reflectors this explanation is thought unlikely, however the magnetic profiles of this area do indicate the occurrence of some igneous material, probably in the form of dykes or other minor intrusives within the sequence.

Fig. 5.10 shows the transition between the two types of basement. The exact position and nature of the junction is not clear on fig. 5.10 as it lies beneath approximately 1.5 km of Tertiary sediments. Faulting, volcanic intrusion or localised volcanic extrusions are all possible explanations of such an apparently abrupt change in basement type. The pre-Tertiary sediments are at least 2 km thick, which is the depth below the Tertiary to which reflectors can be traced assuming a velocity of 4 km s^{-1}. They are overlain by, and predate, the marginal sequence of the rise which is interpreted as late Palaeocene and Eocene in age. Deposition, tilting and erosion of the older sediment pile between the onset of spreading in the mid-Palaeocene (anomaly 24) and the start of deposition of the marginal sequence is thought

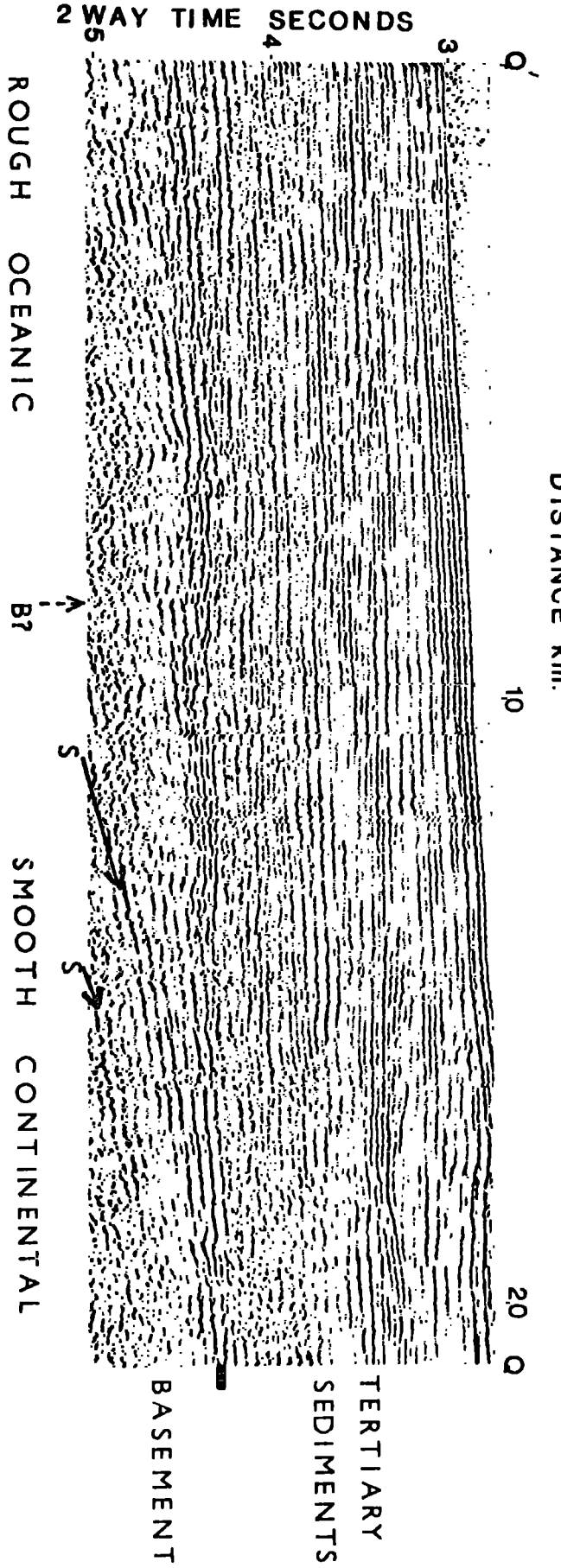

Fig. 5.10 Airgun profile showing interpreted position of the ocean-continent crustal boundary, labelled B and sub-Tertiary reflectors labelled S along Q-Q' (fig. 5.4C). Note that the profile is reversed relative to fig. 5.4.

to be unlikely. It would appear, therefore, that the older sediments predate the onset of spreading and formation of ocean crust at the time of anomaly 24. Thus the boundary between the basement types, whether it is caused by faulting, intrusion or extrusion, is likely to have formed at the onset of spreading.

The 2 km thickness of the pre-Tertiary sediments is a minimum estimate, as the bottom of the sediment pile is not seen. The sequence has a sub-Tertiary outcrop width of 80 km, with an average apparent dip of 15^{o} to the east. Normal faulting can be seen to affect the older sediments particularly near to the margin on the southern profiles (fig. 5.4c); this may repeat the succession, thus invalidating any estimate of thickness from outcrop width. Thus the reflectors are interpreted as sediment layers within a pre-Tertiary sedimentary basin of unknown thickness which formed prior to the continental split.

The recognition of this basin, truncated at its eastern edge by later oceanic crust, prompted a search for similar reflectors on the eastern side of the Atlantic that might represent the eastern part of the basin. Fig. 5.11 is a continental reconstruction of the area, after Tarling (pers. comm.) at anomaly 24 times, showing that the Greenland pre-Tertiary sedimentary basin abutted against the western margin of Hatton bank. On two profiles over Hatton bank, similar

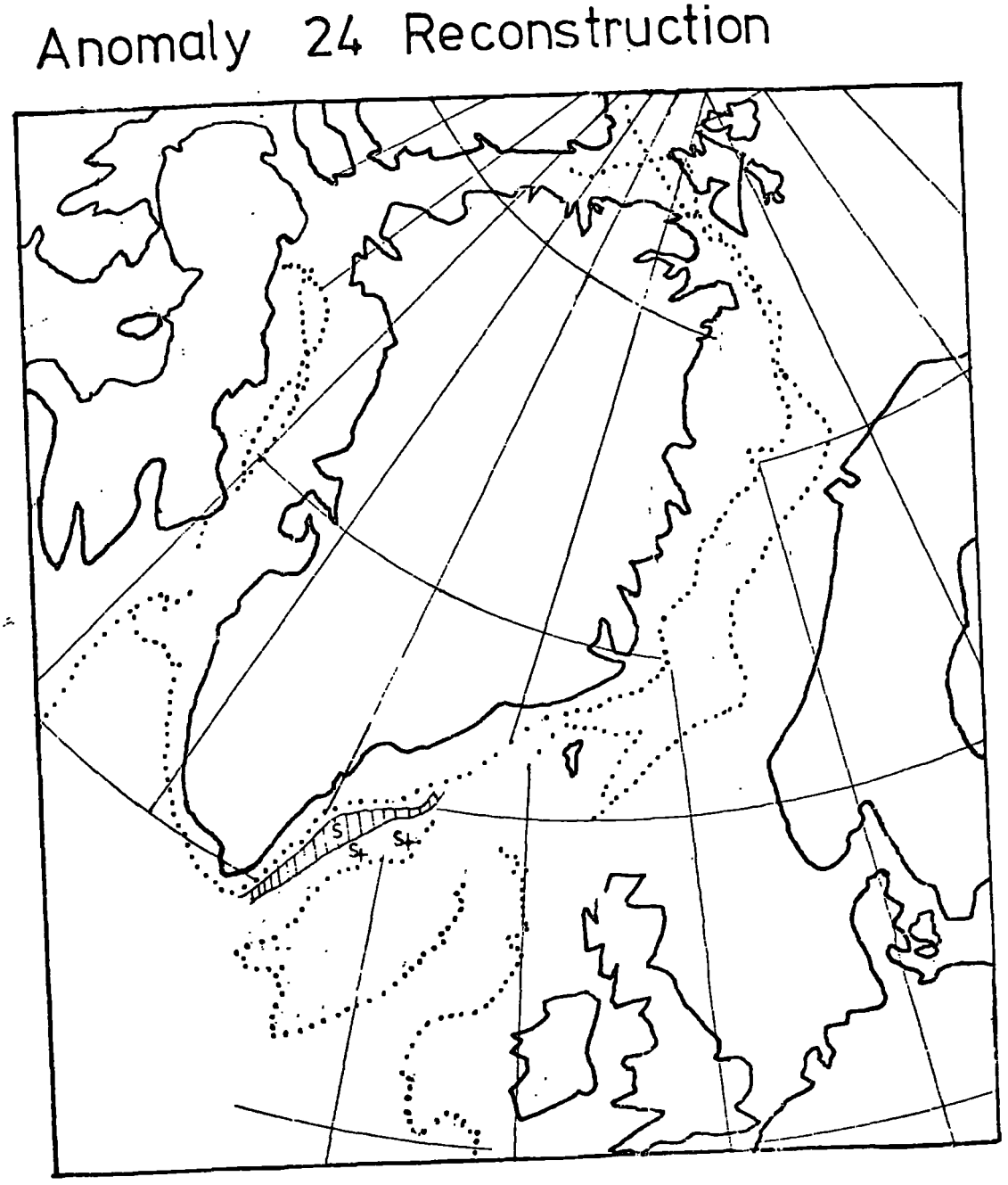

Fig. 5.11 Palaeogeographic reconstruction of the positions of the continents at the time of anomaly 24, recomputed from Tarling (pers. comm.). Euler poles and rotations are (1) North America 42.5°N. 136.4°E. - 11.1, (2) Greenland 43.2°N. 121.9°E. - 9.9°. Shaded area S is area of observed sub-Tertiary reflectors (fig. 5.3). S+ marks the position of observed reflectors on the Rockall margin (Peacock pers. comm.).

reflectors have been noticed by Mr. J.H. Peacock (pers. comm.). These reflectors do not cover such an extensive area as their East Greenland counterparts and are not as well developed; their position is shown in fig. 5.11; they also dip to the east, at a steeper angle than those of the Greenland margin, and are buried beneath a thin Tertiary sediment cover. Watts et al. (1975) record pre-split sediments of possible Cretaceous age dredged from the Rockall scarp just north of where the sub-Tertiary reflectors have been identified, and these may come from a local outcrop of this pre-Tertiary basin. These older sediments on both sides of the north Atlantic appear to have been deposited in an elongate north-south sedimentary basin, fault bounded either on both sides to form a graben-like structure, or on the eastern edge only to form a wedge-shaped basin. The early Tertiary continental split appears to have formed near the eastern faulted margin of this basin, leaving most of the sediments on the Greenland side but a narrow remnant strip adhering to the Rockall margin.

The age of the older sediments is not known. Laughton (1972) did not recognise the reflectors but suggested that a Cretaceous geosyncline existed in this area. The coast immediately adjacent to this area is composed of metamorphic rocks. To the south around Juliannehaab there is a sequence of Eocambrian sandstones (Escher et al. 1970) of restricted

extent. To the north of Kangerdlugssuaq for over 1500 km (fig. 5.12), there is a thick sediment sequence ranging from Cambrian to Cretaceous (with minor Tertiary). Calloman et al. (1973), Haller (1970) and Wager (1947) have shown that this sediment pile can be divided into an old Caledonian belt of highly folded and thrust sediments of Lower Palaeozoic age and a post-Caledonian sequence, starting in the Permian but reaching its zenith in Jurassic times, of gently tilted and faulted marine sediments. The younger sediments formed in a north-south trending basin as shown in fig. 5.12, the structure being dominated by Upper Jurassic block-faulting. This basin extends from 78°N. southwards to 70°N., becoming wider towards the south, until it disappears beneath Tertiary flood basalts. A small window in the basalts located just north of Kangerdlugssuaq indicates that the sediments continue beneath the basalts and probably extend onto the shelf areas of the Denmark Strait. The basalts, from magnetic studies, appear to extend only a few kilometres offshore (Johnson et al. 1975b).

The sedimentary basin described from the survey area occurs some 800 km south of the one on land described above (fig. 5.12) and extrapolation over this distance, as in table 5.1, is tenuous. However, between the two areas Johnson et al. (1975b) report the result of dredges up the continental scarp (located in fig. 5.13). Dredges 72-11,

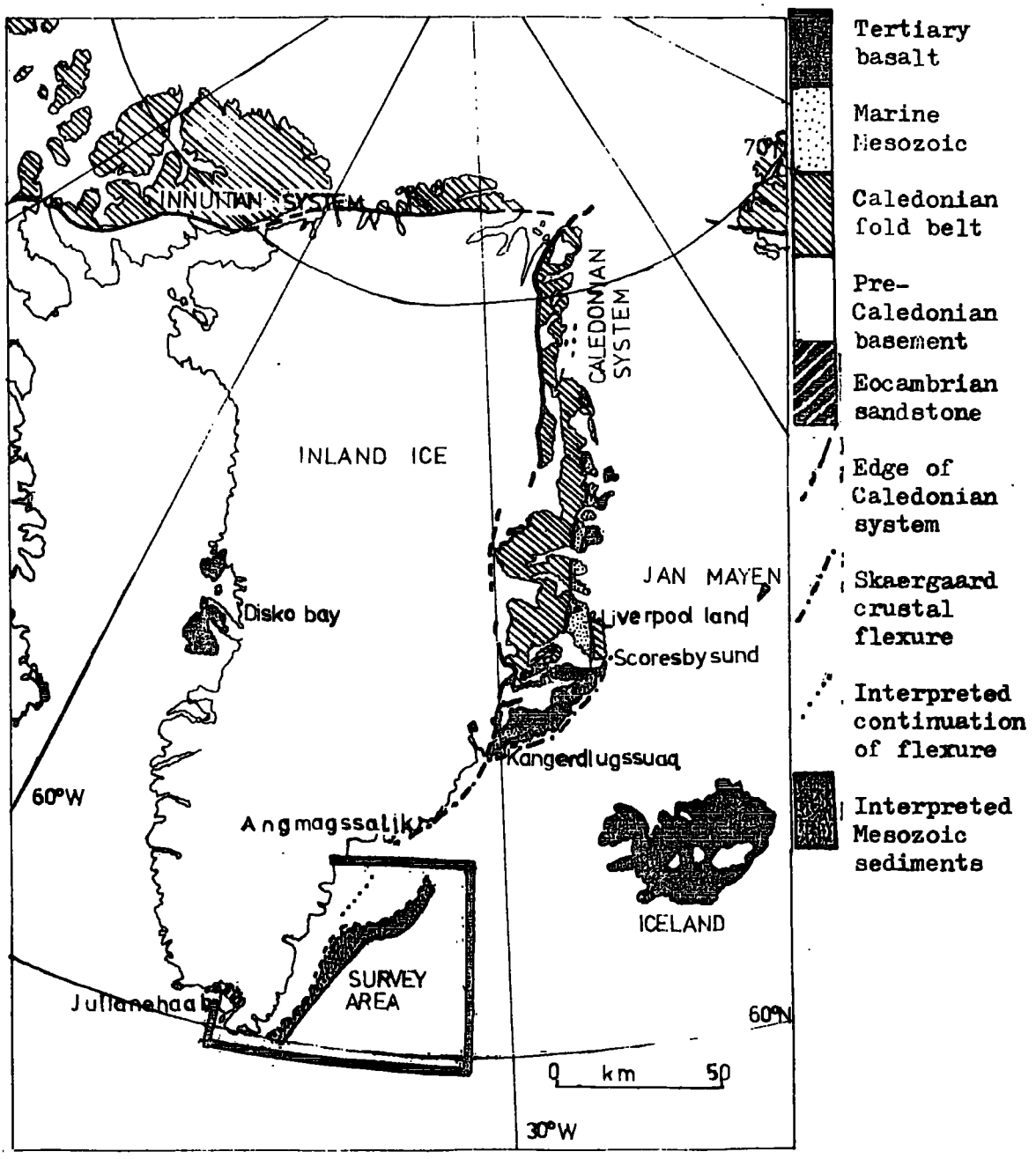

Fig. 5.12 Summary geological map of Greenland, redrawn from Haller (1970) including the area of observed sub-basement reflectors from fig. 5.3.

72-12, 72-13 and 72-15 (Table 5.2) contained Upper Devonian to Lower Carboniferous sandstones, and Johnson et al. suggest that this indicates that "the Palaeozoic Caledonides may extend as outliers beneath the wider portion of the Greenland shelf between 63° and 66°N.". Dredge sample 72-14 contains Middle Triassic sediments, indicating that the Upper Palaeozoic and Mesozoic block faulted basin may exist also beneath the shelf. Dredge sample 71-53 on the southern tip of Greenland contained shallow water or non-marine evaporites of indeterminate age, but tentatively correlated by Johnson et al. with Zechstein (Permian) evaporites that occur at the base of the block faulted basin on land. Fig. 5.4d shows the nearest seismic profile to this dredge, and it can be seen that the sub-Tertiary sediments almost outcrop at the base of the scarp, and may locally do so at the locality of the dredge.

Thus it would appear that Upper Palaeozoic and Mesozoic sediments outcrop in a graben-like basin on land between 78°N. and 70°N., extend beneath the basalts from 70°N. to 68°N., beneath the shelf from 68°N. to 63°N. and beneath the rise from 63°N. to 60°N. It is probably an over-simplification to suggest that all these sediments formed within a single sedimentary basin 2000 km long. They may, however, be part of a graben system that formed on or near the site of eventual continental split, as a result of

TABLE 5.2 Details of dredges from the Greenland scarp after Johnson et al. (1975b)

EAST GREENLAND DREDGES

DREDGE	LAT. (N)	LONG. (W)	DEPTH (M)	AGE	REMARKS
71-53	60°28.7'	41°40.0'	460-820	Indeterminate	shallow or nonmarine evaporitic
72-11	65°24.8'	29°55.9'	820-830	Famennian (Upper Devonian) to Lower Carboniferous	silty argillite 3 samples
72-12	65°25.5'	29°57.9'	801-805	Famennian (Upper Devonian) to Lower Carboniferous	silty argillite to fine sandstone
72-13	65°32.4'	32°03.7'	538	Famennian (Upper Devonian) to Lower Carboniferous	dolomicrite
72-14	64°38.7'	35°00.9'	695	Middle Triassic	lava/sediment mixture (2) silty argillite (1)
72-15	64°39.0'	35°01.6'	450-475	Famennian to Lower Carboniferous	fine sandstone
73-46	62°42.1'	40°37.7'	600-870	Upper Eocene to Oligocene	greywacke
73-46	62°42.1'	40°37.7'	600-870	Oligocene	soft argillaceous sandstone
73-48	61°25.8'	41°12.1'	860-1100	Upper Oligocene	greywacke
73-48	61°25.8'	41°12.1'	860-1100	Upper Eocene to Oligocene	fine grained micaceous sandstone

Fig. 5.13 Position of dredges in table 5.2, after Johnson et al. 1975b

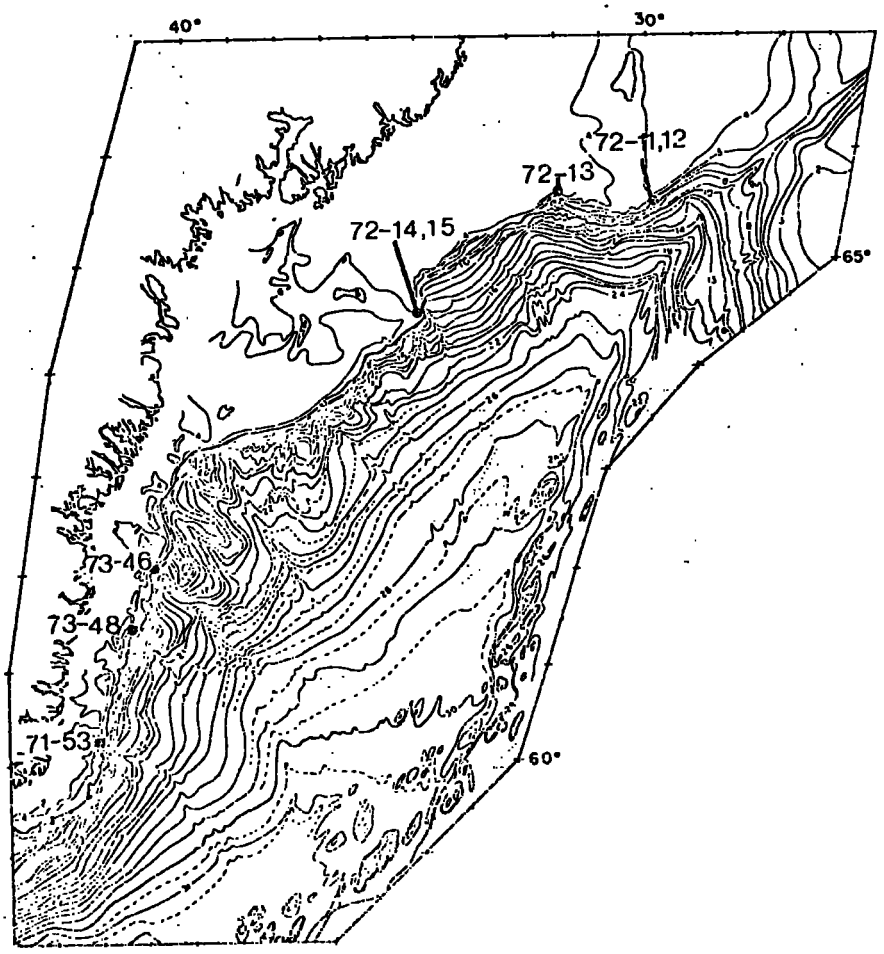

tensional stress and crustal thinning prior to separation. Such marginal graben basins have been described from many of the world's passive margins.

The sediments on land dip mainly to the west at about 10^{o} in a series of antithetic block faults (Haller 1970). Easterly dipping blocks are reported from Liverpoolland (Coe 1971), where they may represent the eastern margin of the graben system on land. The reflectors observable beneath the rise in the survey area all dip to the east at approximately 15^{o}. This possibly indicates that the reflectors are merely the eastern half of the graben and that the Mesozoic sediments continue to the west beneath the shelf, although these dips are likely to have been modified by later differential crustal subsidence. In the seismic profiles, the reflectors cannot be observed beneath the shelf due to the shallow water multiples, but there is no indication that the reflectors stop at the continental scarp. If the older sediments do occur beneath the shallow water of the shelf they may have economic potential as possible hydrocarbon accumulations (Johnson et al. 1975b, Stevens and Perch-Nielsen 1972).

These results imply that the observed reflectors lie on subsided continental crust. The alternative explanation is that the sediments were deposited, independently from those on land, on oceanic crust formed as a result of an

earlier pre-Tertiary continental separation. The former view is strengthened by the lack of distinctive oceanic magnetic anomalies, the shallow water depths of the rise (Johnson et al. 1975) and the mismatch of continental reconstructions in the area (Laughton 1972), (fig. 5.11).

The process of subsidence appears in the south of the survey area to have been one of normal faulting. Such normal faults can be seen near the scarp to have throws of up to 300m, with occasional horst blocks, fig. 5.4c. In the north of the survey area such faulting is not observed, and the subsidence appears to have been more gentle with the pre-Tertiary basement sloping gradually from its outcrop on the shelf down into the ocean basin. This apparent change in subsidence characteristics may reflect an increase in temperature northwards caused by proximity to the anomalously hot area of the Denmark Strait (Haigh 1973) and the associated extrusives on land. A similar change in tectonic style on land to the north of the Denmark Strait has been noted (Haller 1970) and attributed to the same cause.

CHAPTER 6

GRAVITY ANOMALIES

6.1 Introduction

The gravity field of the Greenland margin reflects the major structural elements and the deep crustal structure, and study of the gravity anomalies should be able to answer some of the questions posed in the preceding chapters. The gravity results from both the 1973 and 1974 cruises are shown as a contoured free air anomaly map in fig. 6.1. To the east in the ocean basin the free air anomaly is at a fairly constant level of between 0 and +20 mgal, the minor fluctuations in level being a result of local changes in water depths and Tertiary sediment thicknesses. Passing westwards across the continental scarp the free air anomaly increases rapidly. South of 63.5^{o}N. the anomaly rises westwards to a sharp peak value of +100 mgal over the shelf break, west of which it immediately falls nearly as steeply as it has risen to reach a value of about +30 mgal at the western end of the profiles, (fig. 6.3). North of 63.5^{o}N. the gravity anomaly again rises steeply westward over the scarp to a value of approximately 100 mgal but then remains at about that level, for up to 80 km, before

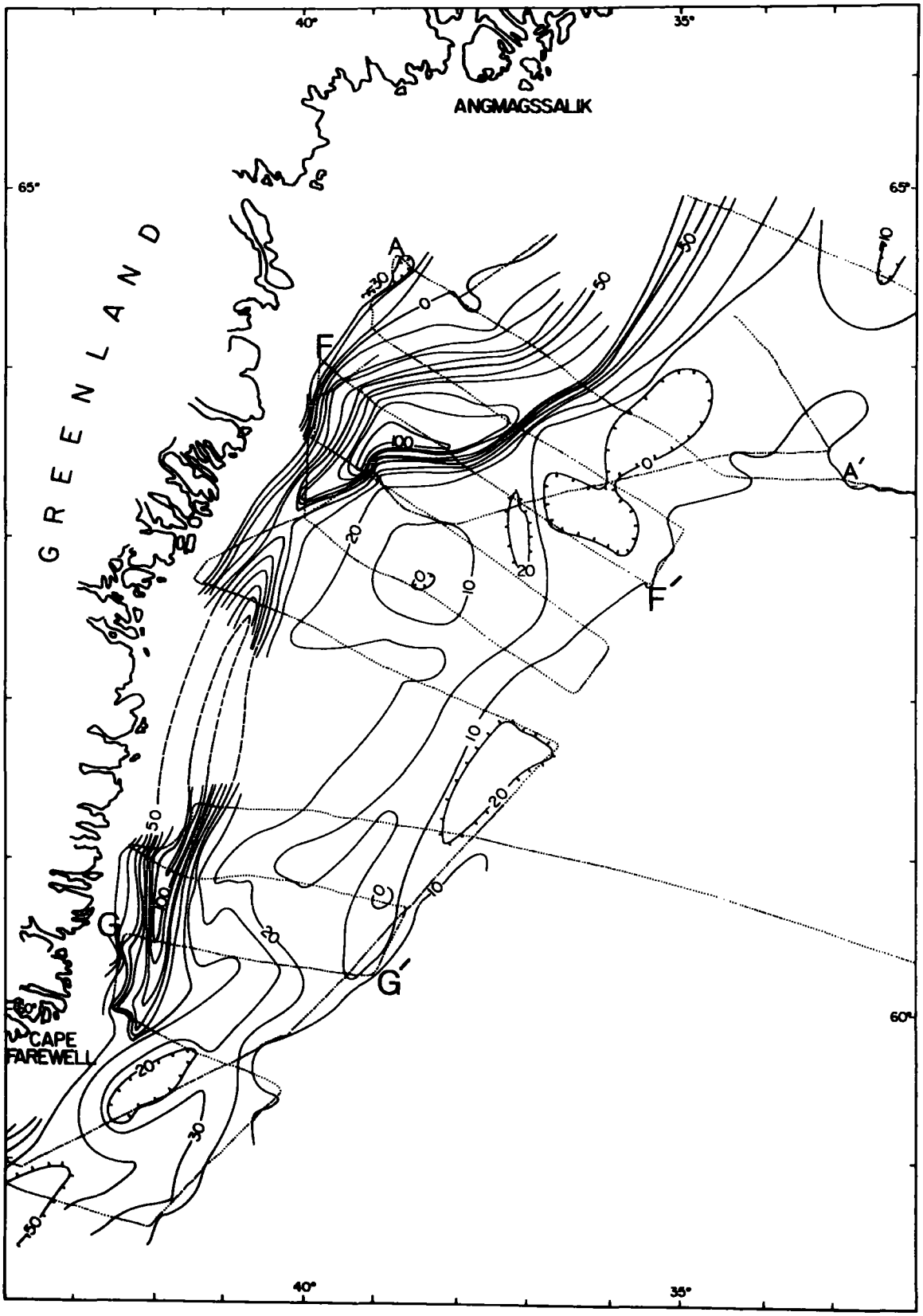

Fig. 6.1 Free air gravity anomaly map of the south-east Greenland margin. Contour interval 10 mgal, ship's track as dotted lines.

dropping steadily to a value of about -30 mgal at the western end of the profiles, (fig. 6.5). Land gravity data is known from Cape Farewell (Kejlso 1958) but none is known from the east coast between Cape Farewell and Angmagssalik, and so the landward extension of the gravity gradients at the western end of the profiles is unknown.

6.2 The expected gravity field over a continental margin

To understand the gravity anomaly field of the survey area it is worthwhile comparing it with the anomaly expected over a standard continental margin. Fig. 6.2a shows the anomaly produced by a vertical bathymetric scarp. Average water depths are used from the Greenland margin and the densities used are adapted from Worzel (1974). The gravity effect of the scarp is a very sharp, step-like rise in gravity anomaly on proceeding from ocean to continent.

However, beneath a continental margin there is also a change in Moho depth which has an equally important gravity effect. Fig. 6.2b shows the anomaly produced by a vertical increase in Moho depth; wherever values for Moho depth are given in this thesis they refer to the total depth to the Mohorovicic discontinuity measured from sea-level. The depth to Moho beneath the ocean basin adjacent to the south-east Greenland margin is not

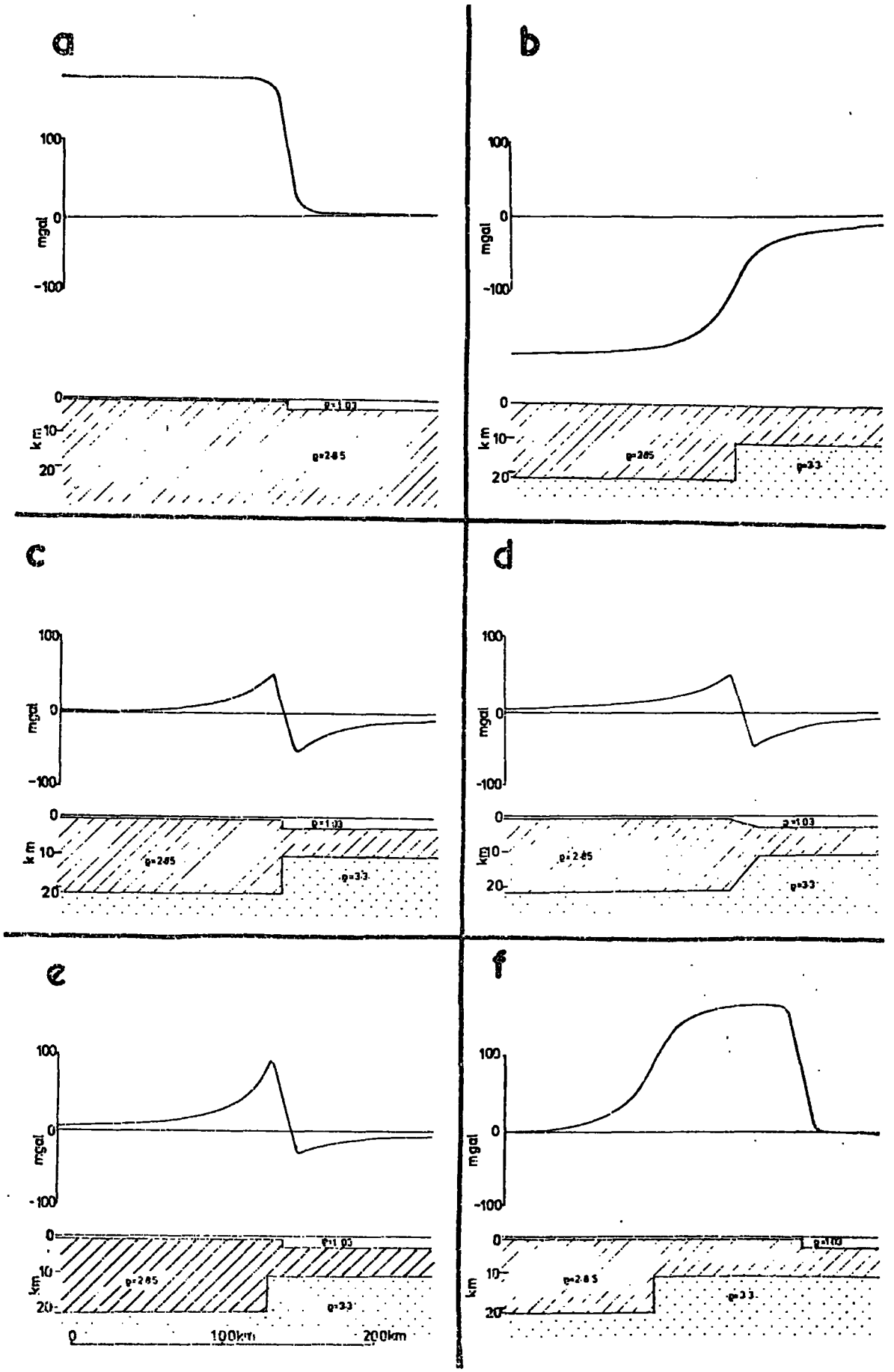

Fig. 6.2 The free air gravity effect of a continental margin and its component parts. ρ is the bulk rock density in g cm^{-3}.

known directly. Refraction measurements (Ewing and Ewing 1959) have given a mean depth to Moho of 11.25 km from the ocean basins of the western Atlantic and a depth to Moho of 9.95 km is recorded for the nearest refraction line (F-1) which lies 500 km south-east of Cape Farewell. However, these values may be an over-estimate of the depth to Moho, as measurements on the other side of the Reykjanes ridge, which is the complementary basin of the same age (line E-5) have given depths to what may be the Moho of 6.23 km, although this may be affected by proximity to the nearby spreading ridge. The oceanic Moho depth is taken as 11 km throughout this thesis, and if this is seriously in error other depths to Moho calculated from this assumption will show a similar systematic error. However, the relative differences in Moho depth and the general shape of the Moho calculated from this assumption will not significantly change. The densities used in fig. 6.2b are again adapted from Worzel (1974). The continental crustal thickness of 21.5 km has been calculated assuming that the continent and ocean are in isostatic equilibrium. This assumption leads to an unusually low value for the continental crustal thickness. This is in part due to the fact that the effects of the Tertiary sediments have been omitted in the simplified isostatic model, but mainly reflects the anomalously shallow oceanic

depths of the Greenland margin, as is discussed in the next section. The gravity effect of the increase in Moho depth is a gentle fall in free air anomaly moving from ocean to continent. The fall is of the same amplitude as the rise in value caused by the scarp, but spread over a wider lateral extent.

If the increase in Moho depth lies immediately beneath the scarp (fig. 6.2c), as appears to be the case over most of the world's passive margins, the addition of these two effects gives; zero anomaly over the ocean basin, a gentle fall in gravity value to a low some 10 km on the ocean side of the scarp, a rapid rise in value to a sharp peak above the shelf break and a more gentle fall in gravity value, immediately following the rise, towards zero anomaly well away from the scarp over the continental shelf.

The effect of a more realistic sloping scarp and gradual increase in Moho depth (fig. 6.2d) is to slightly decrease the amplitude of both the positive and negative anomalies, but the two anomalies are of equal magnitude provided the scarp and increase in Moho depth are co-incident. However, if the scarp and increase in Moho depth are slightly offset (fig. 6.2e) the amplitudes of the positive and negative anomalies become unequal, thus the relative amplitude of the positive and negative anomalies over a continental margin is a very sensitive measure of

the relative positions of the scarp and increase in Moho depth.

If the margin is, however, abnormal in that the increase in Moho depth lies a great distance landward of the scarp, a platform exists between the sharp rise in gravity value due to the scarp and the gentler fall in value due to the crustal thickening (fig. 6.2f).

6.3 Modelling the anomaly south of 63.5°N.

The gravity anomaly south of 63.5°N. (fig. 6.3) shows the main features described above for a near coincident scarp and increase in Moho depth; the gravity high over the shelf is, however, larger than the low over the rise, indicating that the increase in Moho depth may lie slightly landward of the scarp. An interpretation of the structure based on the gravity evidence is given in fig. 6.3. The water depths have been taken from the reduced bathymetric profiles, and the Tertiary sediment structure from the seismic reflection records. A velocity of 1.9 km s^{-1} has been used to convert sediment travel time to thickness as indicated by disposable sonobuoy results (C.D.T. Walker pers. comm.), and the sediment density of 2.1 g cm^{-3} was derived by modelling the anomaly over a bathymetric feature at different sediment densities to find the density that gives the best fit to the observed anomaly (Nettleton's

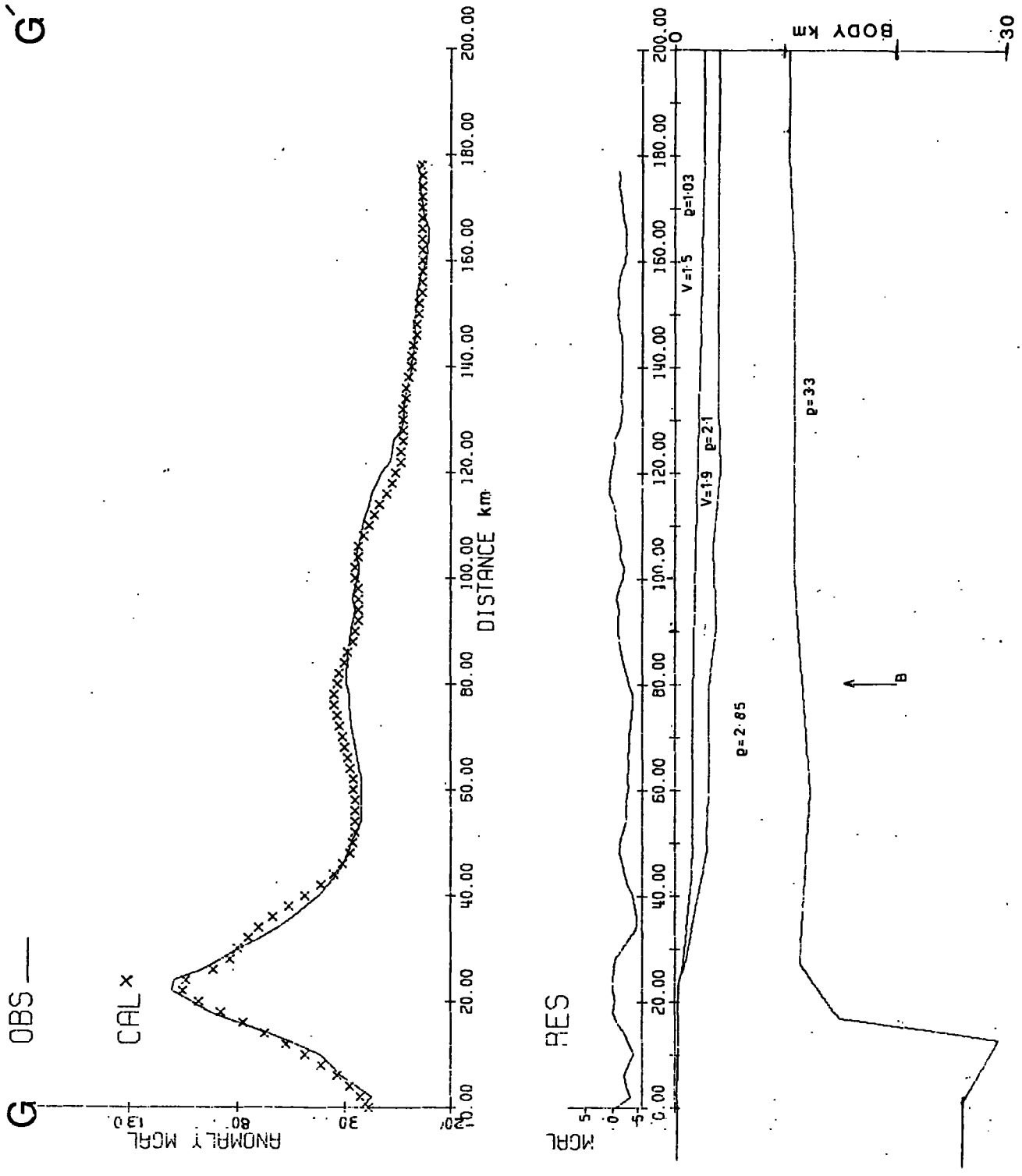

Fig. 6.3 Gravity model south of 63.5°N., along line G-G' (fig. 6.1). ρ is the bulk rock density in g cm^{-3}, V is the velocity in km s^{-1}, OBS is the observed anomaly, CAL the calculated anomaly and RES the residuals. B is the position of the inferred continent-ocean boundary (fig. 4.1).

method). When deriving the model the following assumptions were made:

(1) That the Moho depth is 11 km beneath the ocean basin.

(2) That there is no internal crustal structure beneath the Tertiary sediments and that both oceanic and continental crust have a constant density of 2.85 g cm^{-3}.

(3) That there is a constant mantle density of 3.3 g cm^{-3}.

(4) That the section can be approximated by a two dimensional body.

The method used to derive the model was first to calculate the gravity effect of the water and Tertiary sediments using the semi-infinite slab method of Talwani et al. (1959) and subtract this from the observed anomaly. Thus the residual gravity effect was found and this was attributed to changes in Moho depth. The best fit depth to Moho was then calculated at a set of points using an iterative vertical slab method (Bott 1960). These depths were then included in the semi-infinite slab model and manually adjusted to give a good fit to the observed anomaly. Minor adjustments to the Tertiary sediment structure were made to remove short wavelength residual errors. The residuals in all the gravity models of this thesis are less than $\pm$ 5 mgal.

The model of fig. 6.3 shows that south of 63.5°N. the assumed Moho depth of 11 km in the ocean basin continues beneath the rise with slight thickening to 12 km approximately at the continent-ocean boundary inferred from magnetic and seismic evidence. The Moho continues at this depth beneath the area thought from magnetic and seismic evidence to be subsided continental crust, and then thickens rapidly beneath the scarp to give a calculated Moho depth of approximately 27 km beneath the shelf, the apparent lip of continental crust just landward of the increase in Moho depth may not be a real feature.

This subcontinental Moho depth of 27 km is unusually shallow when compared with a standard continental depth of 33.7 km (Worzel 1974) although refraction experiments have shown that the Moho beneath Britain is approximately at this shallower depth. However, the model assumes a uniform mantle density beneath continent and ocean: In fact the sub-oceanic mantle will be hotter and therefore less dense than the sub-continental mantle, and thus the calculated continental crustal thickness will be erroneously small. The variation of mantle density is particularly marked in this area, as the margin is younger than most other Atlantic margins, and thus the sub-oceanic lithosphere will be hotter. Also, Haigh (1973) has noted a consistent northward shallowing of water depths in the ocean basins of the North Atlantic

which he has attributed to a rise in lithosphere temperatures with proximity to the Iceland-Faeroe-Greenland ridge which lies just to the north of the survey area. The elevated lithosphere temperatures, and therefore low mantle densities are reflected in the shallow water depths of the rise and ocean basin (fig. 5.1). The shallowness of the rise may be affected by the presence of subsided continental crust (Johnson et al. 1975a), but in the ocean basin the water depths are still considerably shallower than the standard oceanic depth of 4.8 km (Worzel 1974).

A rough estimate of the density of the hot sub-oceanic mantle can be obtained by assuming that the total mass above the base of the lithosphere is the same for both standard ocean structure and the ocean structure of the Greenland margin. Table 6.1 shows that, assuming reasonable water depths and sediment thicknesses from the Greenland margin, and assuming a 70 km thick lithosphere, the masses will approximately balance for a sub-oceanic mantle density of 3.22 g cm^{-3}. This lower density mantle material is included in fig. 6.4, which assumes that the junction between the hot sub-oceanic and cold sub-continental mantle is abrupt, vertical, and lies directly beneath the scarp. Fig. 6.4 shows that the Moho depth originally modelled at 27 km beneath the shelf is increased to 38 km by including the change in mantle density. This figure is in better

TABLE 6.1 Mass balance for standard oceanic structure and the Greenland margin structure, assuming a 70 km thick lithosphere

Standard Oceanic structure adapted from Worzel (1974)

Water	4.8 km x 1.03 g cm^{-3}	=	4.94 x 10^5 g cm^{-2}
Sediment	0.8 km x 1.90 g cm^{-3}	=	1.52 x 10^5 g cm^{-2}
Crust	6.45 km x 2.85 g cm^{-3}	=	18.38 x 10^5 g cm^{-2}
Mantle	57.95 km x 3.3 g cm^{-3}	=	191.34 x 10^5 g cm^{-2}
TOTAL	70.00 km		216.15 x 10^5 g cm^{-2}

Greenland margin ocean structure

Water	2.5 km x 1.03 g cm^{-3}	=	2.58 x 10^5 g cm^{-2}
Sediment	1.3 km x 2.1 g cm^{-3}	=	2.73 x 10^5 g cm^{-2}
Crust	7.2 km x 2.85 g cm^{-3}	=	20.52 x 10^5 g cm^{-2}
Mantle	59.0 km x 3.22 g cm^{-3}	=	189.98 x 10^5 g cm^{-2}
TOTAL	70.0 km		216.11 x 10^5 g cm^{-2}

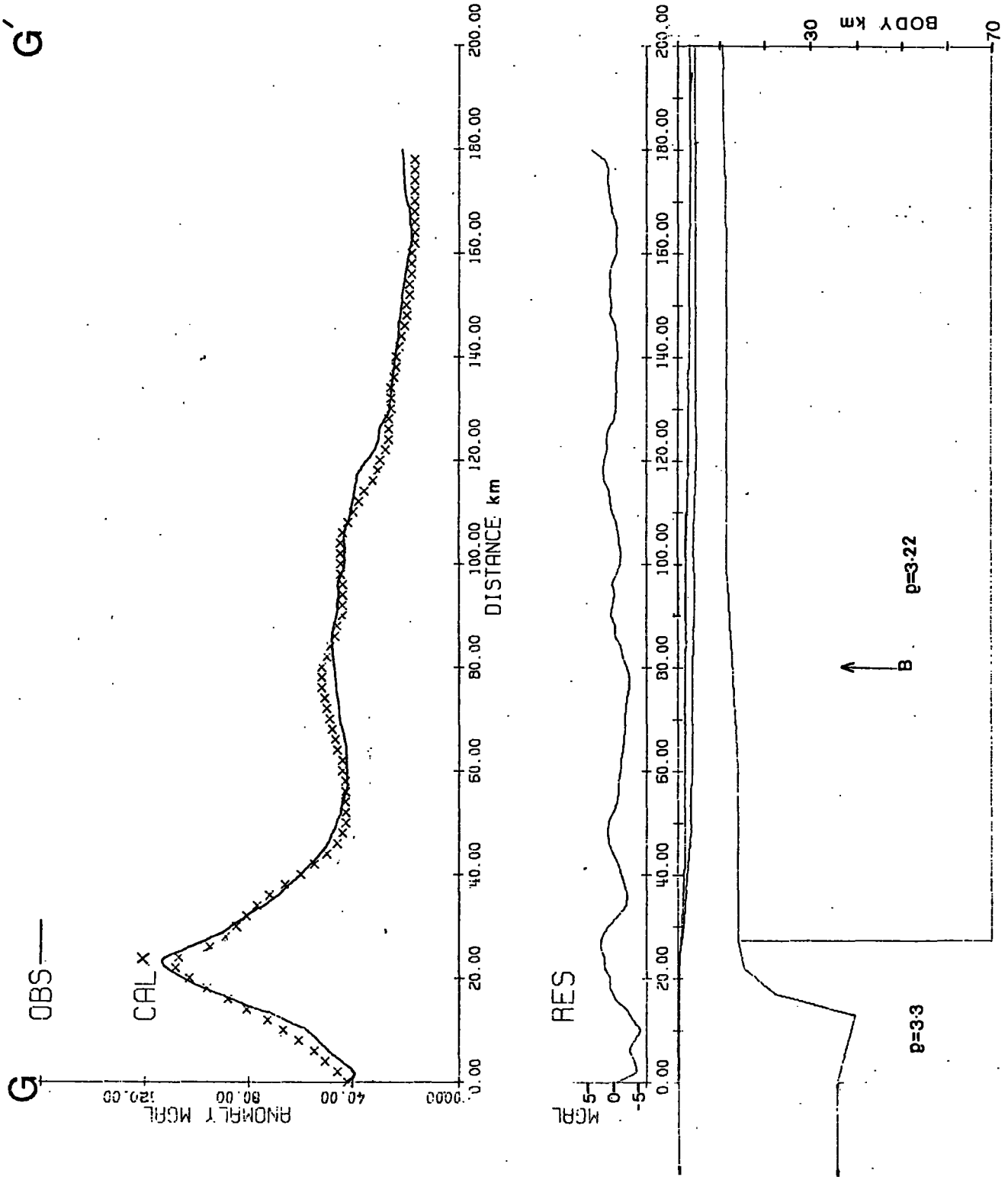

Fig. 6.4 Gravity model as fig. 6.3 but including a lateral change in mantle density. Labelling and densities as in fig. 6.3.

agreement with the crustal thickness of 42.7 km derived for the whole of Greenland from surface wave dispersion studies (Gregersen 1971). The contact between the high and low density mantle material is likely to be gradational rather than abrupt, and thus the crustal thickness in the transition zone between hot and cold mantle, which probably includes the shelf, will lie between 27 and 38 km.

Thus south of 63.5°N. the true continental crustal thickness beneath the shelf is likely to lie between 27 and 38 km. Also the increase in crustal thickness occurs approximately beneath the scarp. The area of inferred subsided continental crust to the east of the scarp is of little more than oceanic crustal thickness.

6.4 Modelling of the anomaly north of 63.5°N.

North of 63.5°N. the gravity anomaly over the margin is not the sharp peak expected over a normal continental margin; instead there is a platform up to 80 km wide with an anomaly of 100 mgal landward of the shelf break (fig. 6.5). The interpretation of this anomaly, shown in fig. 6.5, is derived using the methods and assumptions given in the preceding section with a constant mantle density of 3.3 g cm^{-3}. It shows that the Moho depth, fixed at 11 km in the ocean basin, deepens slightly to 13.5 km at the inferred continent-ocean boundary. It remains at that depth beneath the rise, scarp

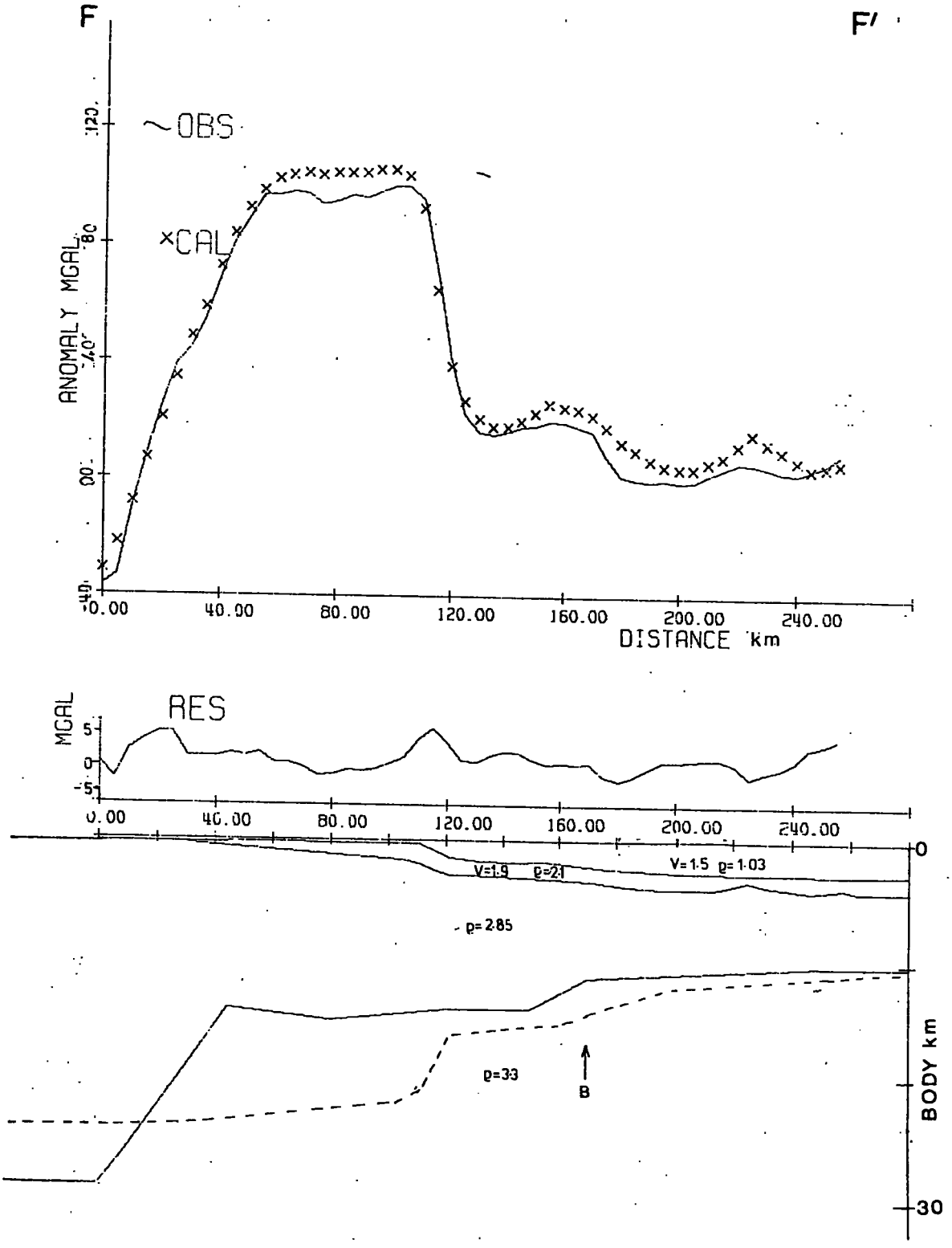

Fig. 6.5 Gravity model north of 63.5°N., along line F-F' (fig. 6.1), dotted line is the expected Moho shape assuming an Airy isostatic model, other labelling as in fig. 6.3.

and outer shelf and then deepens rapidly to 28 km beneath the inner shelf. This sub-continental Moho depth of 28 km is likely to be an under-estimate as explained in the preceding section. Thus the rapid change in crustal thickness does not coincide with the scarp but occurs some 80 km landward of it, the change in thickness being reflected in the gravity anomalies by the downward trending values at the western end of the profiles.

The staggered nature of the continental scarp and increase in Moho depth, of which a further example is given in fig. 7.2, is initially surprising, but is the natural consequence of the assumptions given in the preceding section. Perhaps the most dubious assumption is that of a constant oceanic and continental crustal density, with no internal sub-Tertiary crustal structure. The reflection records indicate the presence of a sub-Tertiary sedimentary basin of unknown thickness beneath the rise, and possibly extending beneath the shelf, that has not been included in the gravity model. The inclusion of this sedimentary basin, which will have a lower density than the surrounding crust, will slightly reduce the modelled Moho depth beneath the rise. The westward drop of 120 mgal over the inner shelf could be explained either by thickening of this basin, the presence of an additional basin or the presence of a large granite intrusion, although an unlikely 15 km thick basin

or granite is required assuming a suitable density of 2.4 g cm^{-3}. However, the presence of low density material beneath the inner shelf increases rather than decreases the lateral extent of the thinned crust beneath the shelf. If there is to be an increase in crustal thickness between the ocean basin and the continental shelf at the western end of the profiles, it must lie approximately 80 km inland from the scarp.

Thus north of 63.5°N. there are 3 zones of differing crustal thickness:

(1) Beneath the inner shelf the continental Moho depth is likely to be between 28 and 40 km. (2) Beneath the outer shelf, scarp and rise there is an area thought to be thinned continental crust with a Moho depth modelled as 13.5 km, although inclusion of the observed sub-Tertiary sedimentary basin, which lies within this area, in the gravity model will slightly reduce this Moho depth perhaps to a normal oceanic depth of 11 km. (3) Beneath the ocean basin the Moho depth has been fixed in the model at 11 km. The rapid change in Moho depth from near oceanic to near continental thickness occurs some 80 km landward of the scarp.

6.5 The thinned continental crust

The gravity results, when combined with the magnetic and seismic interpretations, have thus yielded information

on the crustal thickness and crustal type of various portions of the margin. It has been shown that south of 63.5°N. an area of thinned continental crust up to 80 km wide lies seaward of the scarp. North of 63.5°N. the width of this area of thinned continental crust, seaward of the scarp, decreases northwards to 40 km at 64°N. and even smaller further north, but in addition there is up to a further 80 km of thinned crust landward of the scarp. The scarp north of 63.5°N. coincides with neither the continent-ocean boundary nor with the increase in crustal thickness. The scarp is rather an erosional feature in Tertiary sediments. The base of the sediment pile north of 63.5°N. shows little expression of the overlying scarp, but slopes down smoothly from its outcrop on the shelf into the ocean basin. The scarp therefore does not reflect any major structural feature but is the present erosional front in the early Tertiary marginal sediments, the erosion being caused by rapid contour currents. The margin is therefore out of isostatic equilibrium, with the rapid variation in Tertiary sediment thickness at the scarp not fully compensated in the local sense. The shape of the Moho expected, assuming the Airy isostatic hypothesis, is shown in figs 6.5 and 7.3.

The increase in Moho depth is reflected in the gravity anomalies by the westward drop in gravity values over the

shelf. South of 63.5°N. the westward drop parallels, and occurs just landward of the north-south trending scarp. At 63.5°N. the scarp swings eastward, but the position of the westward drop in gravity values continues northward, running towards Angmagssalik, but becoming gradually more spread out and poorly defined (fig. 6.1). The westward drop and therefore the increase in crustal thickness roughly coincides with the emergence of the basement from beneath the Tertiary sediments, discussed in Chapter 5, and the onset of the short wavelength high amplitude magnetic anomalies, discussed in Chapter 4. The magnetic anomalies have been interpreted as a continuation of the dyke swarm that runs along the coast between Skaergaard and Angmagssalik (Wager 1934). The dykes are injected along the axis of a massive crustal flexure with a total vertical movement of 9 km (Wager 1947, Nielsen 1975), downwarping towards the east. It is suggested that this massive crustal flexure on land is the surface expression of the change in crustal thickness noticed from the survey area to the south. This interpretation follows that of Wager (1940) who, before the advent of plate tectonics, recognised that the subsidence and flexuring of the continental crust was in isostatic response to drastic crustal thinning (fig. 6.6).

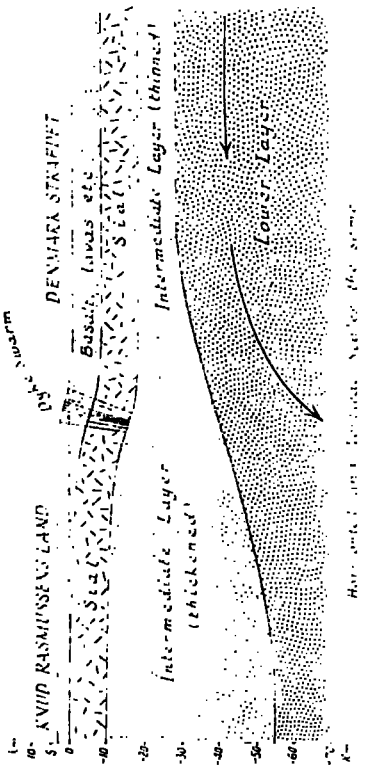

Fig. 6.6 Deep structure of the Skaergaard crustal flexure after Wager (1940).

The line of the crustal flexure has been attributed to the reactivation of Caledonian lines of weakness (Haller 1970) and possibly defines the western limit of the Caledonian fold belt, (fig. 5.11). These lines of weakness trend approximately north-south and are also thought to have controlled the shape of the graben basin on land to the north. It is suggested that the line of the increase in Moho depth and also possibly the line of continental split may reflect the imprint of an earlier Caledonian orogeny.

CHAPTER 7

CONCLUSIONS AND DISCUSSION

7.1 Introduction

The preceding chapters have demonstrated,using differing geophysical methods, that the survey area exhibits some of the features expected over an Atlantic-type continental margin, but certain aspects of the spreading history, sedimentary history, and in particular the nature of the continent-ocean transition, are anomalous. These aspects are summarised in sections 7.2, 7.3 and 7.4.

The geological history of the margin, summarised in section 7.5 is dominated by the processes of continental separation, and the tectonics largely reflect the tensional forces involved in the split of Greenland and Rockall. Many of the unusual features of the margin are due to the proximity of the anomalous Iceland-Faeroe-Greenland ridge, which is thought to have been the site of unusually elevated temperatures that affected the surrounding margins and ocean basins during their formation. The potential of the margin as a source of hydrocarbons is discussed in section 7.6.

7.2 Spreading history

The earliest linear oceanic magnetic anomaly adjacent to the south-east Greenland margin is anomaly 24, which trends south-west north-east from the southern tip of Greenland to 63°N., and lies up to 80 km east of the scarp. North of 64°N., anomaly 21 is the earliest observed, and anomalies 22, 23 and 24 appear to be cut out as the shelf widens and the scarp swings eastward. A complementary widening of the zone of oceanic crust, between anomaly 21 and the scarp, is observable on the opposite margin of the Atlantic, just north of Hatton bank. This is attributed to a local westward migration of the spreading axis prior to the time of anomaly 21.

Igneous intrusives within the Tertiary sediments of the margin post-date the onset of spreading by several million years. This throws some doubt on recent attempts to change the dating of anomaly 24 by correlating dated volcanic activity on the land north of 68°N., with the split. The older Heirtzler time-scale is used in this thesis, dating anomaly 24, and hence the onset of spreading between Greenland and Rockall, as 60 my (mid-Palaeocene). The volcanic activity of east Greenland is thought to have occurred after the split, and is possibly associated with the westward jump in spreading axis at the time of anomaly 21 (50 my, early Eocene). Since this time, spreading has

continued to the present day about the nearly linear Reykjanes ridge, with minor changes in spreading rate as the Labrador sea opening slowed down and stopped.

7.3 Tertiary sediment structure

The sediments which form the south-east Greenland margin are summarised in fig. 7.1. The Tertiary sediments can be subdivided into an early Tertiary marginal sequence and a younger Miocene to Recent oceanic sequence. The marginal sequence, which is acoustically transparent, outcrops north of 62°N., on the outer shelf, the scarp and the inner rise, and is interpreted as a series of pelagic limestone oozes, perhaps containing turbidites, of late Palaeocene, Eocene and possible Oligocene age that formed during seaward subsidence of the margin in the initial stages of continent separation. These sediments are overlain at oceanic depth by a highly stratified oceanic sequence, which outcrops on the outer rise, in the ocean basin and, south of 62°N., on the inner rise.

North of 62°N. the junction between the two sediment types is a shallow, easterly dipping, erosional plane of unconformity, thought to have been cut at oceanic depths by fast flowing contour currents that started in the Miocene, when subsidence of the Iceland-Faeroe-Greenland ridge below

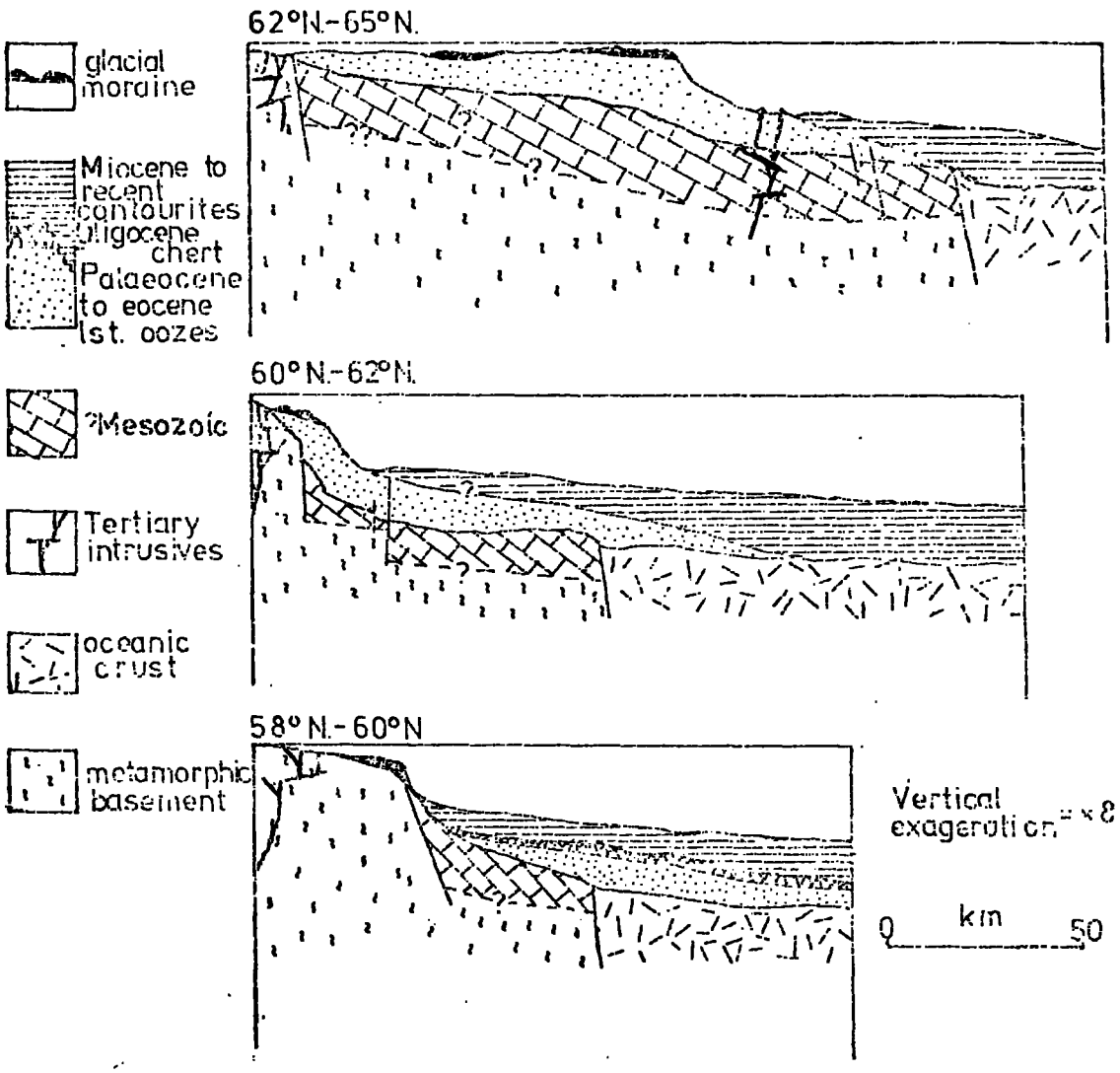

Fig. 7.1 Summary schematic cross sections of the margin showing the sediment structure

sea-level allowed the overflow of cold Norwegian sea-water into the north Atlantic. South of 60°N., a sediment sequence containing irregular reflectors, interpreted as Oligocene cherts by analogy with similar reflectors on the Rockall margin, occurs between the lower marginal and upper oceanic sequences.

The present continental scarp is an erosional feature cut in the early Tertiary marginal sediments, the erosion being caused by the rapid contour currents that first cut the mid-Tertiary unconformity, and now flow southward down the Greenland margin cutting back the scarp and preventing sedimentation on the rise. This is a striking example of the erosional effect of a contour current, reported elsewhere, on a smaller scale, from the Blake-Bahama ridge (Schneider et al. 1967) and the Rockall area (Roberts 1975).

7.4 The continent-ocean transition

Fig. 7.2 summarizes the geophysical evidence from one of the profiles over the margin. The Tertiary sediments described in the previous section blanket the transition from continental to oceanic crust. The surface on which the Tertiary sediments rest exhibits two distinct styles. To the east, in the ocean basin, the pre-Tertiary surface has a rough structureless topography which is associated with oceanic layer 2, as indicated by the presence of character-

Fig. 7.2 Cross section of margin showing the interrelation of the gravity, magnetic and seismic results, along A-A' (located in fig. 6.1). Labelling of magnetic anomalies as in fig. 4.1 and gravity model as in fig. 6.3, G is the modelled Moho depth, I the depth expected assuming an Airy isostatic model.

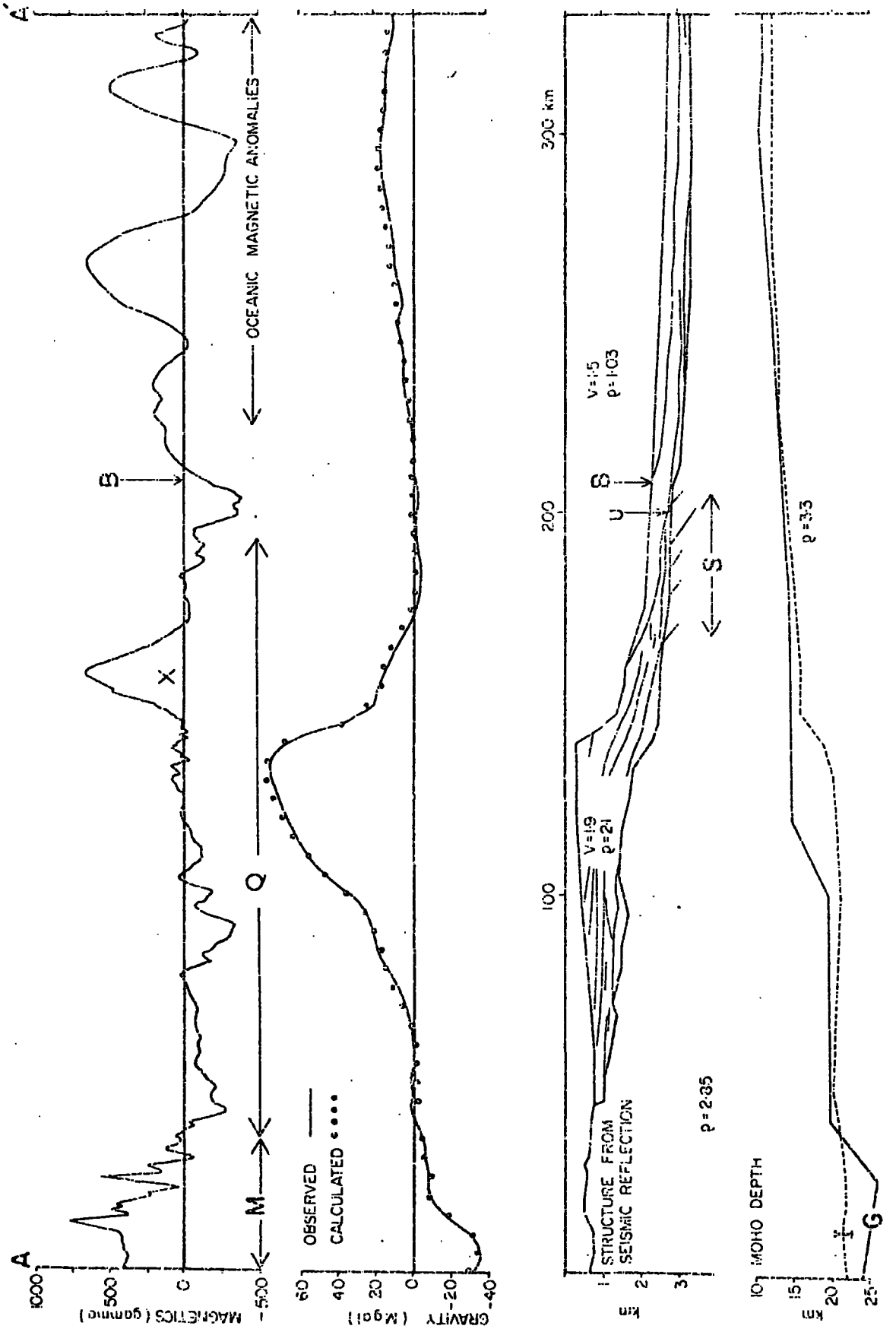

istic linear oceanic magnetic anomalies (fig. 7.2). Beneath the rise, at a distance of between 30 and 80 km east of the continental scarp, depending on the profile, the rough pre-Tertiary surface becomes abruptly smoother with a slight rise in level. This change in pre-Tertiary basement topography coincides with the end of the oceanic magnetic anomalies and the onset of a magnetic quiet zone. Between this point and the scarp there is a series of strong, widely-spaced reflectors within the sub-Tertiary basement, which dip to the east at approximately 15^{o} and are interpreted as reflective layers within a pre-Tertiary (and pre-continental split) sedimentary basin of unknown thickness. The basin may continue beneath the shelf but the structure is obscured by multiples. The sub-Tertiary reflectors are abruptly terminated to the east by new oceanic crust, and similar reflectors on the western margin of Hatton bank may represent the eastern edge of the basin. The sediments are thought to have been deposited in a north-south elongate graben-like basin, which formed during the early stages of crustal thinning, the final continental split occurring at the eastern faulted margin of this graben.

These pre-Tertiary sediments may be correlated with a large, late Palaeozoic and Mesozoic sedimentary pile, which outcrops in a graben-like basin on the east Greenland coast between 78^{o}N. and 70^{o}N., and is buried by flood basalts

between 70°N. and 68°N. The sediments also possibly outcrop on the scarp at 64.5°N.

Modelling of the gravity results (fig. 7.2) shows that the Moho, assumed to be at a depth of 11 km below sea-bed in the ocean basin at the eastern end of the profile, may thicken slightly beneath the pre-Tertiary basin to about 13 km. South of 63.5°N. the crust thickens rapidly beneath the scarp to reach a nearly standard continental thickness of 27 to 38 km beneath the shelf (depending on whether allowance is made for a hot, low density, sub-oceanic lithosphere). North of 63.5°N. there is no rapid crustal thickening beneath the scarp, and the Moho depth of about 13 km, beneath the rise, continues with only slight crustal thickening beneath the outer shelf for up to 80 km, before deepening rapidly to a more standard continental crustal thickness beneath the inner shelf.

The increase in crustal thickness beneath the shelf north of 63.5°N. approximately coincides with the onset of short-wavelength magnetic anomalies, which are interpreted as indicating the continuation across the shelf of the Skaergaard dyke swarm. This dyke swarm which follows the coast between Kap Brewster and Angmagssalik, before running out to sea, is intruded along the axis of a large scale crustal flexure with a total vertical movement of 9 km.

This flexure is interpreted as overlying a rapid change in crustal thickness similar to the change observable from the gravity results to the south.

There is therefore an area of dubious crustal type and intermediate crustal thickness stretching up to 80 km on either side of the continental scarp. It is bounded by oceanic crust on the eastern side (as indicated by the linear magnetic anomalies) and by continental crust to the west (as indicated by the increased crustal thickness); it includes the area to the east of the scarp containing the pre-Tertiary reflectors, and also (north of 63.5°N.) an area to the west of the scarp of magnetically quiet continental shelf. The scarp itself, north of 63.5°N., does not reflect any major structural feature, but is the present erosional front in the Tertiary marginal sediments.

The area of dubious crustal type is interpreted as attenuated continental crust rather than thickened oceanic crust. This is indicated by:

(1) The lack of recognisable linear magnetic anomalies.

(2) The presence of a tilted and eroded pre-Tertiary sedimentary basin of at least 2 km thickness within the area of dubious crustal type, which must therefore lie on crust (whether oceanic or continental) considerably older than the present phase of spreading, which started 60 million years ago.

(3) The shallow water depths of the rise.

(4) The mismatch of continental reconstructions, which show that the area of dubious crustal type lies in a gap between Greenland and Rockall when the continents are reconstructed on their pre-split positions. This local gap cannot simply be explained by a period of pre-Tertiary spreading.

(5) The presence of a magnetic low just landward of the last oceanic magnetic anomaly ('B' in fig. 7.2) which can be interpreted as being caused by the junction of highly magnetic oceanic crust against more weakly magnetised continental crust.

The change in character of the sub-Tertiary basement from rough to smooth topography is therefore interpreted as marking the continent-ocean boundary (fig. 7.2). Similar continent-ocean boundaries, and areas of attenuated crust beneath the rise, have been reported from the Atlantic margins of west Africa (Rabinowitz 1972), the Blake-Bahama region (Rabinowitz 1974), the Voring Plateau (Talwani and Eldholm 1974), and the Labrador sea (van der Linden 1975b) and it has been suggested that such a zone of attenuated crust may be the norm rather than the exception (Hallam 1976). This thesis has shown that the three major features expected at a continental margin, which are the continental scarp, the continent-ocean crustal boundary and the rapid increase

in crustal thickness, do not necessarily coincide, and in the case of south-east Greenland are separated by as much as 120 km.

7.5 Geological history

The earliest rocks outcropping on the south-east Greenland margin are probably of Precambrian age, and similar to the metamorphic rocks which outcrop on land to the west of the survey area, and are present as derived fragments in the glacial material of cores C1 and C2 (Appendix 1). Correlation of these rocks with the shield areas of the Baltic and north America or with the metamorphic rocks of similar age in Scotland and those drilled from the Rockall plateau has been attempted but may not be very meaningful (Callomon et al. 1972). Superimposed on this metamorphic basement is the north-south trending Caledonian fold belt, which occurs on land north of 70°N. and is a complex of lower Palaeozoic rocks that have been intensely folded and thrust in an orogeny which started abruptly during the Silurian (420-400 my), but continued during the Devonian and Carboniferous (400-270 my) (Haller 1970). Rocks of Devonian and Carboniferous age have been dredged from the south-east Greenland scarp between 64.5°N. and 65.5°N. (Johnson et al. 1975b), indicating that the fold belt probably continues southwards in to the survey area, beneath

the Tertiary sediments of the shelf.

It has been suggested that the pre-Silurian sediments formed in a lower Palaeozoic proto-Atlantic ocean which later closed, but during the Devonian and Carboniferous there is no good evidence for the existence of such an ocean (Callomon et al. 1972). The end of the Carboniferous marked the waning of the Caledonian compressive phase and by the late Permian, gradual subsidence had started in a gently subsiding basin that stretched at least as far south as Scotland and opened into the North Sea (Callomon et al. 1972). This gradual subsidence continued through the Triassic, with continental red-bed sedimentation and marine incursions being dominant in the thin Triassic basin exposed on the east coast of Greenland. Dredges of Triassic material from the scarp indicate that sedimentation continued at least as far south as 64.5°N., and evaporitic deposits, tentatively correlated with evaporites of Permian age on land (Johnson et al. 1975b), have been dredged from the scarp at 60.5°N.

Sedimentation became more rapid during the Jurassic, the sediments being deposited in a north-south trending marine graben, that is witnessed in the survey area by the pre-Tertiary reflectors beneath the rise, and outcrops on land north of 70°N. in a 3 km thick basin (Haller 1970). At this time the Atlantic had started to open south of the Azores,

and the general tensional stress and crustal thinning over the north Atlantic region is witnessed by the regional downwarping, and development of thick sedimentary basins in Britain (Roberts 1974), and the formation of a similar graben-like basin in the North Sea (Ziegler 1975). Towards the end of the Jurassic, there was a period of intense block faulting that can be seen both in Greenland (Haller 1970) and the British Isles (Roberts 1974); the block faulting follows the same north-south trend as the earlier Caledonian fold belt in Greenland, and may have been influenced by underlying Caledonian lines of weakness. The block faulting may have culminated in the abortive split of Rockall from Europe, which possibly occurred during the Cretaceous (Roberts 1975), thus relieving some of the tension. The early Cretaceous of east Greenland is characterised by tilting and erosion, followed in the late Cretaceous by a series of marine transgressions. At this time the Labrador Sea started to open and, as with the south-east Greenland margin, this was preceded by a phase of crustal thinning and the formation of Mesozoic basins beneath the shelf areas and the rise (Hood and Bower 1974).

Crustal thinning beneath south-east Greenland and Rockall continued with normal faulting as the dominant mechanism visible on land, until, in the mid-Palaeocene, Greenland and Rockall finally split to form the Reykjanes

ridge. The split was accompanied by volcanic activity in the Faeroes and Hebridean region. The line of the initial split and early spreading appears to have been sinuous and was possibly governed by underlying Caledonian structures.

As the spreading continued, and the thinned crust subsided, pelagic sedimentation built up a thick early Tertiary pile of sediments on both sides of the spreading ridge. On the Rockall margin these are represented by the pre-R4 series, drilled from the Hatton-Rockall basin, and on the Greenland margin they are represented by the marginal sediments of the shelf, scarp and rise, and possibly also by the Kangerdlugssuaq formation, visible on land to the north. To the south of 63.5°N., the subsidence appears to have been fault-bounded and restricted to the area that now lies west of the scarp, and this may indicate a continued subsidence of the Mesozoic graben during the Tertiary. North of 63.5°N., the subsidence appears to have been more widespread, and flexuring rather than faulting appears to be dominant, possibly as a result of a higher crustal temperature, caused by the suggested hot spot now under Iceland. During the early stages of spreading the centre of the hot spot may have been located beneath the Greenland margin rather than beneath the spreading ridge, as the sinuous initial split may not have

exactly coincided with the axis of maximum heat flow. Thus, between the times of anomalies 24 and 21 (60 to 50 my) the base of the Greenland lithosphere overlying the centre of the hot spot between about 68°N. and 70°N., may have been abnormally heated. Approximately 50 my ago this area experienced a short period of intense volcanic activity, with a total thickness of 9 km of basalt extruded in the space of a few million years, extrusion approximately keeping pace with subsidence of the crust, as indicated by the shallow-water beds of the Kangerdlugssuaq formation just beneath the basalts, and the Kap Dalton formation on top of the lava pile (Soper et al. 1976). Traces of this volcanic activity can be found as dykes in the early Tertiary marginal sediments of the survey area. Brown and Whitley (1976) have pointed out that this large volume of basalt is "well in excess of the estimated maximum discharge of the mantle plume model". It is suggested that this volcanic pile resulted from the release of lava from within the area of preheated lithosphere, and that subsidence of the crust occurred in order to fill the space left by the erupting lava. The release of lava, which occurred 50 my ago, at the time of anomaly 21, may have been triggered by a westward migration of the spreading axis, which straightened the initially sinuous split. From the time of anomaly 21 to the present day, spreading has continued

about the nearly linear Reykjanes ridge with only minor changes of spreading rate, as the Labrador Sea opening slowed during the mid-Eocene, and finally stopped during the late-Oligocene (Kristoffersen and Talwani 1974).

The final stage of subsidence appears to have occurred after extrusion of the basalts and to have been in the form of the Skaergaard crustal flexure with its associated dyke-swarm. This crustal flexure followed the line of maximum crustal thinning and may extend southward beneath the shelf into the survey area. Since the crustal flexure, which occurred during the early Oligocene, tectonic activity on land has been restricted to minor normal faulting at the end of the Oligocene (Haller 1970); this faulting can be seen to affect the marginal sediments of the survey area.

During the Eocene, sedimentation of the marginal sequence continued and, at some time during the Oligocene, the pelagic sedimentation gave way to deposition of a chert sequence, possibly indicating an increase in water depth. The Iceland-Faeroe-Greenland ridge, which had remained elevated as a land-link separating the Atlantic from the Norwegian-Greenland seas, finally subsided below sea-level at the start of the Miocene, allowing a radical change in the ocean circulation patterns, and initiating the rapid contour currents that now sweep along the Greenland margin. These contour currents first cut the mid-Tertiary unconformity, seen north of 62°N., but, as subsidence continued

and the water depth increased, sediment drift deposits were laid down, onlapping this erosional plane to form the oceanic sequence of the survey area.

The contour currents have continued to erode in shallow water, cutting back the early Tertiary marginal sediments to form the scarp, and preventing any sedimentation on the rise. Sedimentation has continued in the ocean basin to the present day.

The effects of the Pleistocene glaciation can be seen as ice-scoured plateaus on the inner shelf and glacially accumulated banks and saddles on the outer shelf, representing terminal moraines and therefore the outer limit of glaciation.

7.6 The potential of the margin as a source of hydrocarbons

The tectonics and history of development of the south-east Greenland margin is linked to that of the North Sea and the two areas are remarkably similar in many ways. Both areas show a Mesozoic graben basin that is now tilted, eroded and deeply buried by Tertiary sediments. Such an environment would seem favourable for the accumulation of commercial quantities of hydrocarbons as is witnessed by the current activities in the North Sea, and "numerous oil companies have expressed interest in the sedimentary basin of central East Greenland and the continental shelf off

East Greenland" (Henderson 1974). This thesis has shown that the sedimentary basin continues along the south-east Greenland margin beneath the rise. The water depths of the rise, however, (approximately 2 km) will make drilling very difficult with present technology, and the hostile weather conditions, the presence of icebergs and the remoteness of Greenland from any potential oil users are likely to prevent any exploitation of the rise in the near future.

If, however, the basin does exist beneath the shelf and cannot be seen merely because of shallow water multiples, then the area may be worthy of further examination. The basin is most likely to exist north of 63.5^{o}N., beneath the part of the shelf that is magnetically quiet, although volcanic activity may have been significant in this area, and intrusions within the Mesozoic graben may seriously affect the hydrocarbon potential.

The readiness of the Danish government, who control the Greenland shelf, to grant licences is perhaps indicated by the fact that allocations have already been made of concession blocks on the western Labrador Sea margin of Greenland.

The Mesozoic graben basin outcrops along the east Greenland coast, and one mining company holds an exclusive concession, including petroleum rights, over the sedimentary

area on land (Henderson 1974). Sampling of some of these sediments has been carried out for oil source rock analysis (Stevens and Perch-Nielsen 1972) and one sample was determined to be a good source rock, while another may contain traces of migrated oil. The basin on land may, however, never have been buried deeply enough to produce useful quantities of hydrocarbons. No offshore exploration licences or concessions had been granted prior to 1974 (Henderson 1974) and none are known of since. Further geophysical surveys of the Greenland margin are, however, being planned by several companies and research institutes, and it is hoped that they will lead to a more accurate knowledge of the structure of the margin and a better understanding of the reasons why the south-east Greenland margin is apparently so unusual.

REFERENCES

Anonymous, 1972. Formats for marine geophysical data exchange, Natn. Acad. Sci. - Natn. Res. Coun., 19 pp.

Avery, O.E., Burton, G.D., & Heïrtzler, J.R., 1968. An aeromagnetic survey of the Norwegian Sea, J. geophys. Res., 73, 4583-4600.

Avery, O.E., Vogt, P.R., & Higgs, R.H., 1969. Morphology, magnetic anomalies and evolution of the northeast Atlantic and Labrador Sea, part II, Magnetic anomalies, E.O.S. (Trans. Am. Geophys. Un.), 50, 4, p.184.

Avilov, I.K., 1965. Bottom contours and nature of grounds and their significance for trawl fishing, I.C.N.A.F. Environ. Symp. Int. Comm. Northwest Atlantic Fish., Spec. Pub., 6, 781-789.

Beckinsale, R.D., Brooks, C.K., & Rex, D.C., 1970. K-Ar ages for the Tertiary of East Greenland, Bull. Geol. Soc. Den., 20, 27-37.

Berggren, W.A., 1972. A Cenozoic time scale - some implications for regional geology and Paleobiogeography, Lethaia, 5, 195-215.

Bott, M.H.P., 1960. The use of rapid digital computing methods for direct gravity interpretation of sedimentary basins, Geophys. J.R. astr. Soc., 3, 63-67.

Bott, M.H.P., 1974. Deep structure, evolution and origin of the Icelandic transverse ridge, in Geodynamics of Iceland and the North Atlantic area, ed. L. Kristjansson, 33-47, Reidel, Dordrecht & Boston.

Bott, M.H.P., Browitt, C.W.A., & Stacey, A.P., 1971. The deep structure of the Iceland-Faeroe ridge, Mar. Geophys. Res., 1, 328-351.

Brooks, C.K., 1973. Tertiary of Greenland - a volcanic and plutonic record of continental break-up, in Arctic geology, ed. M.G. Pitcher, 150-160, (Am. Ass. Petrol. Geol., Mem. 19), Tulsa, Okla.

Brown, P.E., & Whitley, J.E., 1976. Eastern Greenland basalts and their supposed plume origin, Nature, Lond., 260, 232-234.

Bullard, E., Everett, J.E., & Smith, A.G., 1965. The fit of the continents around the Atlantic, Phil. Trans R. Soc., A258, 41-51.

Callomon, J.H., Donovan, D.T., & Trümpy, R., 1972. An annotated map of the Permian and Mesozoic formations of East Greenland, Meddr. Grønland, 168, 3, 35pp.

Coe, K., 1971. Faulting in the western part of Liverpool land, East Greenland, Bull. Geol. Soc. Den., 20, 260-264.

Coron, S., 1972. Bureau Gravimetrique International, Information Bulletin, No. 29.

Davies, T.A., & Laughton, A.S., 1972. Sedimentary processes in the North Atlantic, in Laughton, A.S., Berggren, W.A., et al., Initial Reports of the Deep Sea Drilling Project, 12, 905-934, U.S. Government Printing Office, Washington.

Deitrich, G., 1959. Zur Topographie und Morphologie des Meeresbodens im Nordlichen Nord Atlantischen Ozean, Dt. hydrogr. Z. Erganzungsch. Reihe B, 3, 26-34.

Deitrich, G., 1965. New hydrographical aspects of the Northwest Atlantic, I.C.N.A.F. Environ. Symp. Int. Comm. Northwest Atlantic Fish., Spec. Pub., 6, 29-51.

Egloff, J., & Johnson, G.L., 1975. Morphology and structure of the Southern Labrador Sea, Can. J. Earth Sci., 12, 2111-2133.

Escher, A., Henriksen, N., Dawes, P.R., & Weidick, A., 1970. Tectonic/Geologic map of Greenland, by the Geological Survey of Greenland, Kümmerley & Frey, Berne.

Evans, A.L., Fitch, F.J., & Miller, J.A., 1973. Potassium - Argon age determinations on some British Tertiary igneous rocks, J. geol. Soc., Lond., 129, 419-443.

Ewing, J.I., & Ewing, M., 1959. Seismic-refraction measurements in the Atlantic Ocean basins, in the Mediterranean Sea, on the Mid Atlantic ridge and in the Norwegian Sea, Bull. Geol. Soc. Am., 70, 291-318.

Falconer, R.K.H., Srivastava, S.P., & Johnson, G.L., 1975. Movement of Greenland with respect to European and North American plates, E.O.S. (Trans. Am. Geophys. Un.), 56, 6, p.456.

Faller, A.M., 1975. Palaeomagnetism of the oldest Tertiary basalts in the Kangerdlugssuaq area of East Greenland, Bull. Geol. Soc. Den., 24, 173-178.

Featherstone, P.S., Bott, M.H.P., & Peacock, J.H., 1976. The structure of the south-east Greenland continental margin, Geophys. J. R. astr. Soc., in press.

Fleischer, V., 1974. The Reykjanes Ridge - a summary of geophysical data, in Geodynamics of Iceland and the North Atlantic area, ed. L. Kristjansson, 17-31, Reidel, Dordrecht & Boston.

Godby, E.A., Baker, R.C., Bower, M.E., & Hood, P.J., 1966. Aeromagnetic reconnaissance of the Labrador Sea, J. geophys. Res., 71, 511-517.

Gregerson, S., 1971. Surface wave dispersion and crust structure in Greenland, Geophys. J. R. astr. Soc., 22, 29-39.

Haigh, B.I.R., 1973. North Atlantic oceanic topography and lateral variations in the upper mantle, Geophys. J. R. astr. Soc., 33, 405-420.

Hailwood, E.A., & Mitchell, J.G., 1971. Palaeomagnetic and radiometric dating results from Jurassic intrusions in South Morocco, Geophys. J. R. astr. Soc., 24, 351-364.

Hailwood, E.A., Tarling, D.H., Mitchell, J.G., & Løvlie, R., 1973. Preliminary observations on the palaeomagnetism and radiometric ages of the Tertiary basalt sequence of Scoresby Sund, East Greenland, Rapp. Grønlands geol. Unders., 58, 43-47.

Hallam, A., 1976. How closely did the continents fit together? Nature,Lond., 262, 94-95.

Haller, J., 1970. Tectonic map of East Greenland 1:500,000, Meddr. Grønland, 171, 5, 286pp.

Harvey, J.G., 1961. Overflow of cold deep water across the Iceland-Greenland ridge, Nature, Lond., 189, 911-913.

Heezen, B.C., 1974. Atlantic type continental margins, in The geology of continental margins, eds. C.A. Burk & C.L. Drake, 13-24, Springer-Verlag, Berlin, Heidelberg & New York.

Heirtzler, J.R., Dickson, G.O., Herron, E.M., Pitman, W.C. III, & Le Pichon, X., 1968. Marine magnetic anomalies, geomagnetic field reversals and motions of the ocean floor and continents, J. geophys. Res., 73, 2119-2136.

Heirtzler, J.R., & Hayes, O.E., 1967. Magnetic boundaries in the North Atlantic Ocean, Science, 157, 185-187.

Henderson, G., 1974. Developments in petroleum exploration in and around Greenland 1969-1974, Rapp. Grønlands geol. Unders., 75, 13-16.

Holmes, A., 1918. The Basaltic rocks of the Arctic region, Mineralog. Mag., 18, 180-223.

Hood, P., & Bower, M.E., 1973. Low-level aeromagnetic surveys of the continental shelves bordering Baffin Bay and the Labrador Sea, Geol. Surv. Pap. Can., 71-23, 573-598.

Institute of Oceanographic Sciences, 1974. Computer system for reduction, display and storage of navigation, gravity, magnetic and depth data recorded in continental shelf or deep-ocean areas, Manuals 1 to 12.

Johnson, G.L., Campsie, J., Rasmussen, M., & Dittmer, F., 1974. Mesozoic rocks from the Labrador Sea, Nature, Lond., 247, 413-414.

Johnson, G.L., & Eckhoff, O., 1966. Bathymetry of the North Greenland Sea, Deep Sea Res., 13, 1161-1173.

Johnson, G.L., Egloff, J., Campsie, J., Rasmussen, M., Dittmer, F., & Frietag, J., 1973. Sedimentary distribution and crustal structure of the southern Labrador Sea, Bull. Geol. Soc. Den., 22, 7-24.

Johnson, G.L., McMillan, N.J., & Egloff, J., 1975b. East Greenland continental margin, in Canada's continental margins and offshore petroleum exploration, eds. C.J. Yorath, E.R. Parker, & D.J. Glass, 205-224, (Can. Soc. Petrol. Geol., Mem. 4,) Calgary, Alberta.

Johnson, G.L., & Schneider, E.D., 1969. Depositional ridges in the North Atlantic, Earth planet. Sci. Lett. (Neth.), 6, 416-422.

Johnson, G.L., Sommerhoff, G., & Egloff, J., 1975a. Structure and morphology of the west Reykjanes basin and the southeast Greenland continental margin, Mar. Geol., 18, 175-196.

Jones, E.J.W., Ewing, M., Ewing, J.I., & Eittreim, S.L., 1970. Influences of Norwegian Sea overflow water on sedimentation in the northern North Atlantic and Labrador Sea, J. geophys. Res., 75, 1655-1680.

Kejlso, E., 1958. Gravity measurements in Western Greenland 1950-1952, Geod. Inst. Skr. (Kbh.), 3, 27,69 pp.

Kristoffersen, Y., & Talwani, M., 1974. Extinct triple-junction south of Greenland, E.O.S. (Trans. Am. Geophys. Un.), 55, 4, p.295.

Larsen, B., 1974. Marine geophysical survey of the East Greenland shelf south of Angmagssalik, Rapp. Grønlands geol. Unders., 75, 87-88.

Laughton, A.S., 1971. South Labrador Sea and the evolution of the North Atlantic, Nature, Lond., 232, 612-617.

Laughton, A.S., 1972. The southern Labrador Sea. A key to the Mesozoic and early Tertiary evolution of the North Atlantic, in Laughton, A.S., Berggren, W.A., et al., Initial Reports of the Deep Sea Drilling Project, 12, 1155-1179, U.S. Government Printing Office, Washington.

Laughton, A.S., Berggren, W.A., et al., 1972. Initial Reports of the Deep Sea Drilling Project, 12, U.S. Government Printing Office, Washington, 1243 pp.

Le Pichon, X., Hyndman, R.D., & Pautot, G., 1971. Geophysical study of the opening of the Labrador Sea, J. geophys. Res., 76, 4724-4743.

MacIntyre, R.M., McMenamin, T., & Preston, J., 1975. K-Ar results from Western Ireland and their bearing on the timing and siting of Thulean magmatism, Scott. J. Geol. 11, 227-249.

Masson-Smith, D., Howell, P.M., & Abernethy-Clark, A.B.D.E., 1974. The national gravity reference net 1973, Ord. Surv. Prof. Pap. New Ser., No. 26, 22 pp.

Matthews, D.J., 1939. Tables of the velocity of sound in pure water and sea water for use in echo sounding and sound ranging, Admiralty Office, London, 52pp.

Mead, G.D., 1970. International Geomagnetic reference field 1965.0 in Dipole Co-ordinates, J. geophys. Res., 75, 4372-4374.

Mussett, A.E., Brown, G.C., Eckford, M., & Charlton, S.R., 1972. The British Tertiary igneous province: K-Ar ages of some dykes and lavas from Mull, Scotland, Geophys. J. R. astr. Soc., 30, 405-414.

Nielsen, T.F.D., 1975. Possible mechanism of continental break-up in the North Atlantic, Nature, Lond., 253, 182-184.

Noe-Nygaard, A., 1974. Cenozoic to Recent volcanism in and around the North Atlantic basin, in The Ocean Basins and Margins: II, The North Atlantic, eds. A.E.M. Nairn & F.G. Stehli, 391-443, Plenum Press, New York & London.

Pitman, W.C. III, & Talwani, M., 1972. Sea floor spreading in the North Atlantic, Bull. geol. Soc. Am., 83, 619-646.

Rabinowitz, P.D., 1972. Gravity anomalies on the continental margin of Angola, Africa, J. Geophys. Res., 77, 6327-6347.

Rabinowitz, P.D., 1974. The boundary between oceanic and continental crust in the western North Atlantic, in The geology of continental margins, eds. C.A. Burk & C.L. Drake, 67-84, Springer-Verlag, Berlin, Heidelberg & New York.

Roberts, D.G., 1974. Structural development of the British Isles, the continental margin, and the Rockall plateau, in The geology of continental margins, eds. C.A. Burk & C.L. Drake, 343-359, Springer-Verlag, Berlin, Heidelberg & New York.

Roberts, D.G., 1975. Marine geology of the Rockall plateau and trough, Phil. Trans. R. Soc., A278, 447-509.

Robinson, E.A., 1967a. Statistical communication and detection with special reference to digital data processing of radar and seismic signals, Griffin, London, 362pp.

Robinson, E.A., 1967b. Multichannel time series analysis with digital computer programs, Holden-Day, San Francisco, Cambridge, London, Amsterdam, 298pp.

Schneider, E.D., Fox, P.J., Hollister, C.D., Needham, H.D., & Heezen, B.C., 1967. Further evidence of contour currents in the western north Atlantic, Earth planet. Sci. Lett. (Neth.), 2, 351-359.

Scrutton, R.A., 1972. The crustal structure of Rockall plateau microcontinent, Geophys. J. R. astr. Soc., 27, 259-275.

Sommerhoff, G., 1973. Formenschatz und morphologische Gleiderung des südostgrönländischen Shelfgebeites und kontinental Abhanges, "Meteor" Forsch-Ergebnisse, C15, 1-54.

Soper, N.J., Higgins, A.C., Downie, C., Matthews, D.W., & Brown, P.E., 1976. Late Cretaceous-early Tertiary stratigraphy of the Kangerdlugssauq area, East Greenland, and the opening of the north-east Atlantic, J. geol. Soc. Lond., 132, 85-102.

Stacey, A.P., Gray, F., Allerton, H.A., & Sewart, D.I., 1972. A logger and mobile computer system for marine data aquisition and reduction, Proc. Oceanology International.

Stevens, N.B.H., & Perch-Nielsen, K., 1972. Sampling for oil source rock analysis, Scoresby Sund region, Central East Greenland, Rapp. Grønlands geol. Unders, 55, 47-48.

Talwani, M., Worzel, J.L., & Landisman, M., 1959. Rapid gravity computations for two-dimensional bodies with application to the Mendocino submarine fracture zone, J. geophys. Res., 64, 49-59.

Talwani, M., & Eldholm, O., 1974. Margins of the Norwegian - Greenland Sea, in The geology of continental margins, eds. C.A. Burk & C.L. Drake, 361-374, Springer-Verlag, Berlin, Heidelberg & New York.

Tarling, D.H., 1970. Palaeomagnetic Results from the Faeroe Islands, in Palaeogeophysics, ed. S.K. Runcorn, 193-208, Academic Press.

Tarling, D.H., & Gale, N.H., 1968. Isotopic Dating and Palaeomagnetic Polarity in the Faeroe Islands, Nature, Lond., 218, 1043-1044.

Tarling, D.H., & Mitchell, J.G., 1976. Revised Cenozoic Polarity Time Scale, Geology, 4, 133-136.

Tucker, M.J., Smith, N.D., Pierce, F.E., & Collins, F.P., 1970. A Two-Component Electromagnetic Ship's Log, J. Inst. Navig., 23, 3, 302-316.

Ulrich, J., 1960. Zur Topographie des Reykjanes-Rücken, Kieler Meeresforsch., 16, 155-173.

van der Linden, W.J.M., 1975a. Mesozoic and Cainozoic opening of the Labrador Sea, the North Atlantic and the Bay of Biscay, Nature, Lond., 253, 320-324.

van der Linden, W.J.M., 1975b. Crustal attenuation and sea-floor spreading on the Labrador Sea, Earth planet. Sci. Lett. (Neth.), 27, 409-423.

Vogt, P.R., 1970. Magnetised basement outcrops on the south-east Greenland continental shelf, Nature, Lond., 226, 743-744.

Vogt, P.R., 1972. The Faeroe-Iceland-Greenland aseismic ridge and the western boundary undercurrent, Nature, Lond., 239, 79-81.

Vogt, P.R., Anderson, C.N., Bracey, D.R., & Schneider, E.D., 1970. North Atlantic magnetic smooth zones, J. geophys. Res., 75, 3955-3968.

Vogt, P.R., & Avery, O.E., 1974. Detailed magnetic surveys in the northeast Atlantic and Labrador Sea, J. geophys. Res., 79, 363-389.

Vogt, P.R., Ostenso, N.A., & Johnson, G.L., 1970. Magnetic and bathymetric data bearing on sea-floor spreading north of Iceland, J. geophys. Res., 75, 903-920.

Wager, L.R., 1934. Geological investigations in East Greenland, Part I, from Angmagssalik to Kap Dalton, Meddr. Grønland, 105, 2, 1-46.

Wager, L.R., 1940. Epeirogenic earth movements in East Greenland and the depth of the earth, Nature, Lond., 145, 938-939.

Wager, L.R., 1947. Geological investigations in East Greenland, Part IV, The Stratigraphy and Tectonics of Knud Rasmussen Land and the Kangerdlugssauq region, Meddr. Grønland, 134, 5, 1-64.

Wager, L.R., & Deer, W.A., 1938. A dyke swarm and crustal flexure in East Greenland, Geol. Mag., 75, 39-46.

Watkinson, N.D., 1976. Polarity Subcommission sets up some guidlines, Geotimes, 21, 4, 18-20.

Watts, A.B., Schreiber, B.C., & Habib, D., 1975. Dredged rocks from Hatton Bank, Rockall plateau, J. geol. Soc. Lond., 131, 639-646.

Williams, C.A., 1973. A fossil triple junction in the N.E. Atlantic west of Biscay, Nature, Lond., 244, 86-88.

Williams, C.A., 1975. Sea-floor spreading in the Bay of Biscay and its relationship to the North Atlantic, Earth planet. Sci. Lett., (Neth.), 24, 440-456.

Worthington, L.V., & Volkmann, G.H., 1965. The volume transport of the Norwegian Sea overflow water in the North Atlantic, Deep Sea Res., 12, 667-676.

Worzel, J.L., 1974. Standard oceanic and continental structure, in The geology of continental margins, eds. C.A. Burk & C.L. Drake, 59-66, Springer-Verlag, Berlin, Heidelberg & New York.

Ziegler, P.A., 1975. North Sea basin history in the tectonic framework of North-Western Europe, in Petroleum and the continental shelf of North-West Europe, ed. A.W. Woodward, 131-148 Appl. Sci.

APPENDIX 1

DATA PRESENTATION

Data is presented as composite profiles and maps. The data is also stored on magnetic tape at 2-minute intervals for navigational, gravity and magnetic data and at 10-minute intervals for the bathymetric data. All the valid data is recorded and displayed.

The composite profiles that follow consist of:

Magnetic anomaly (gamma)

Free air gravity anomaly (mgal)

Bathymetry (m)

Speed (km hr^{-1})

Course (degrees)

Linear distance made good (km)

Time (hrs G.M.T.)

The profiles have been plotted to fit conveniently onto A4 sized paper. Consequently some of the longer lines are plotted onto separate consecutive pages. Gaps in the profiles are data breaks. When there is no data recorded for a particular parameter, the axes are still presented to indicate the data break.

The maps accompanying this thesis are at a scale of 1 to 1,000,000 plotted on a Mercator Projection (International

Spheroid) natural scale at latitude 65°N. Map 1 is the ship's track plotted between 2 minute fixes and is marked with a cross every hour. Time is annotated usually at 6 hourly intervals with hours minutes and Julian day. Core sites are marked on the map (C1-C4), the numbering indicates the chronological order in which they were carried out. Table A1.1 gives details of the coring results.

Map 2 shows the interpreted seismic profiles plotted along simplified ship's track. The track runs through the top of each profile. The vertical scale of each profile is marked, and represents a vertical exaggeration of about 7 to 1 at water velocities.

The data is stored in the Formats for Marine Geophysical Data Exchange (Anon. 1972) on ½ inch, 9 track, 800 B.P.I., NRZ, IBM compatible magnetic tape. The basic record length is a card image of 80 characters (the tape record has been padded out to 80 characters with blanks when necessary). Each record of 80 characters is separated by an inter-block gap (I.B.G.); the tapes are in the following formats:

Format 1. Geophysical data. A file-mark is written at the end of each data set (a data set consists of a header record followed by a time series for the

relevant parameter). '-1', followed by a file-mark, is written at the end of all the data on magnetic tape.

Format 2. Navigation data. All final adjusted 2 minute fix positions are recorded. There are no header records, and no file marks. The data is terminated on tape with '-1', followed by a file-mark.

Format 3. Merged-Merged format. This format combines bathymetry (corrected, uncorrected meters), free air gravity anomaly (0.1 mgal), total and residual magnetic intensity (gamma) and navigation data with time.

The magnetic tapes are stored on the NUMAC system at Newcastle as follows:

DGP451 Format 1 1973 Navigation time series

DGP452 Format 1 1973 Navigation time series

DGP453 Format 1 1973 Gravity time series

DGP454 Format 1 1973 Magnetic time series

DGP455 Format 1 1973 Topography time series

DGP456 Format 3 1973 Merged-Merged format

DGP457 Format 3 1973 Merged-Merged format

DGP482 Format 3 1974 Merged-Merged format

DGP483 Format 1 1974 Navigation time series

DGP484 Format 1 1974 Gravity time series, file mark,

Magnetic times series

DGP485 Format 2 1974 Navigation Topography merged

To mount and list the magnetic tapes:

```
£MOUNT DGP482 *TAPE* NV
£LIST *TAPE*
```

Table A1.1 Details of 1974 coring experiments

Core	Latitude	Longitude	location	depth m	day/time	length m	comments
C1	63°22.9'	39°18.4'	shelf	400	241/0050	-	gravel & fine clay in core catcher, probably glacial
C2	63°21.4'	39°15.6'	scarp	1600	241/0130	-	gravel in core catcher, probably glacial
C3	63°06.4'	38°14.8'	rise	1970	241/0820	1	dark clay, abundant recent foraminifera
C4	63°03.8'	38°08.8'	rise	2010	241/1135	1.6	1 m dark clay, 0.6 m light slightly cemented sand. Clay recent, sand not adequately dated (sample sent to B.M.)

Samples were collected by gravity coring and are stored in 60 mm diameter clear plastic tubes

Composite profile index

The start and end times of the composite profiles in Julian day/hours are listed below:

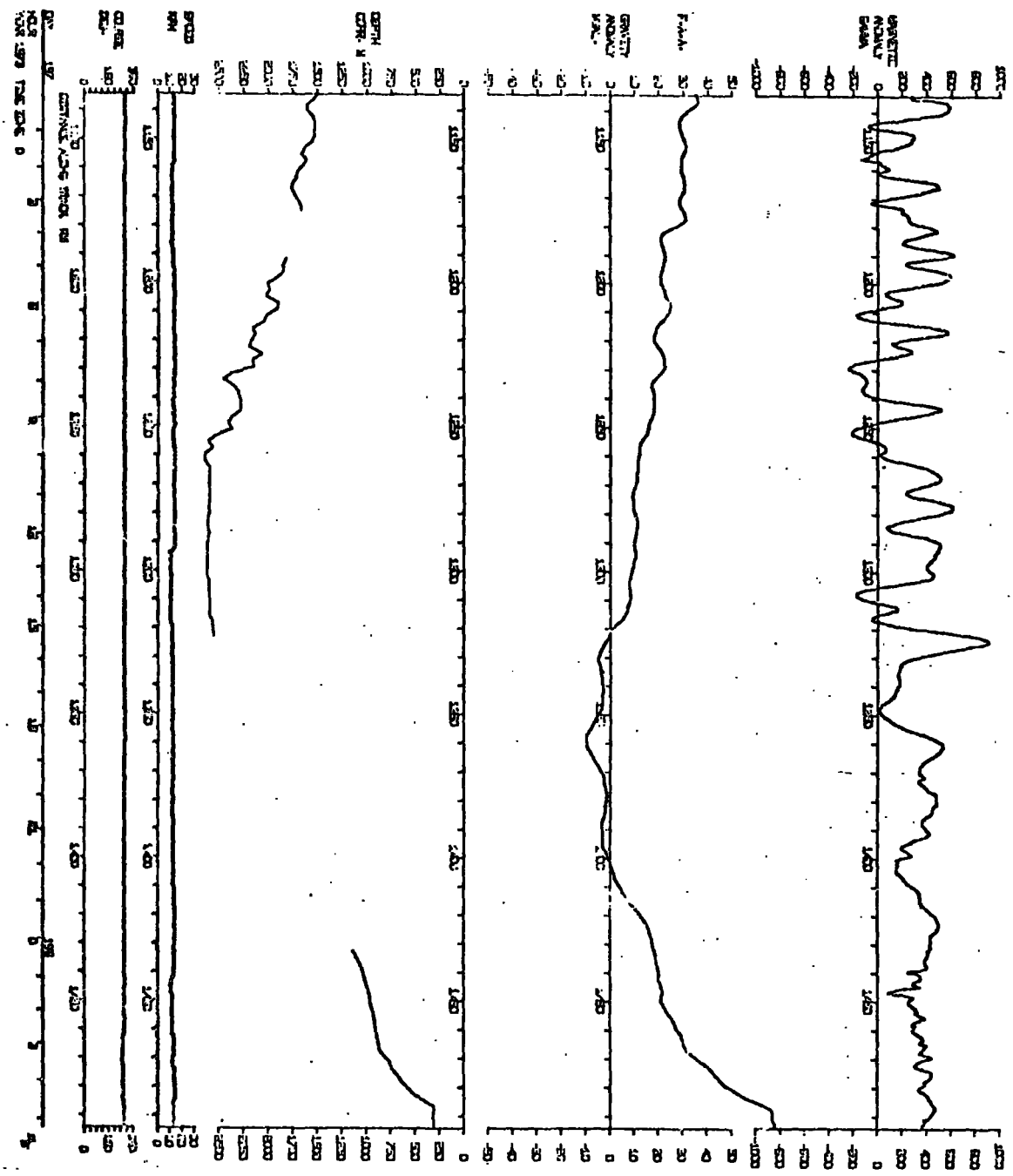

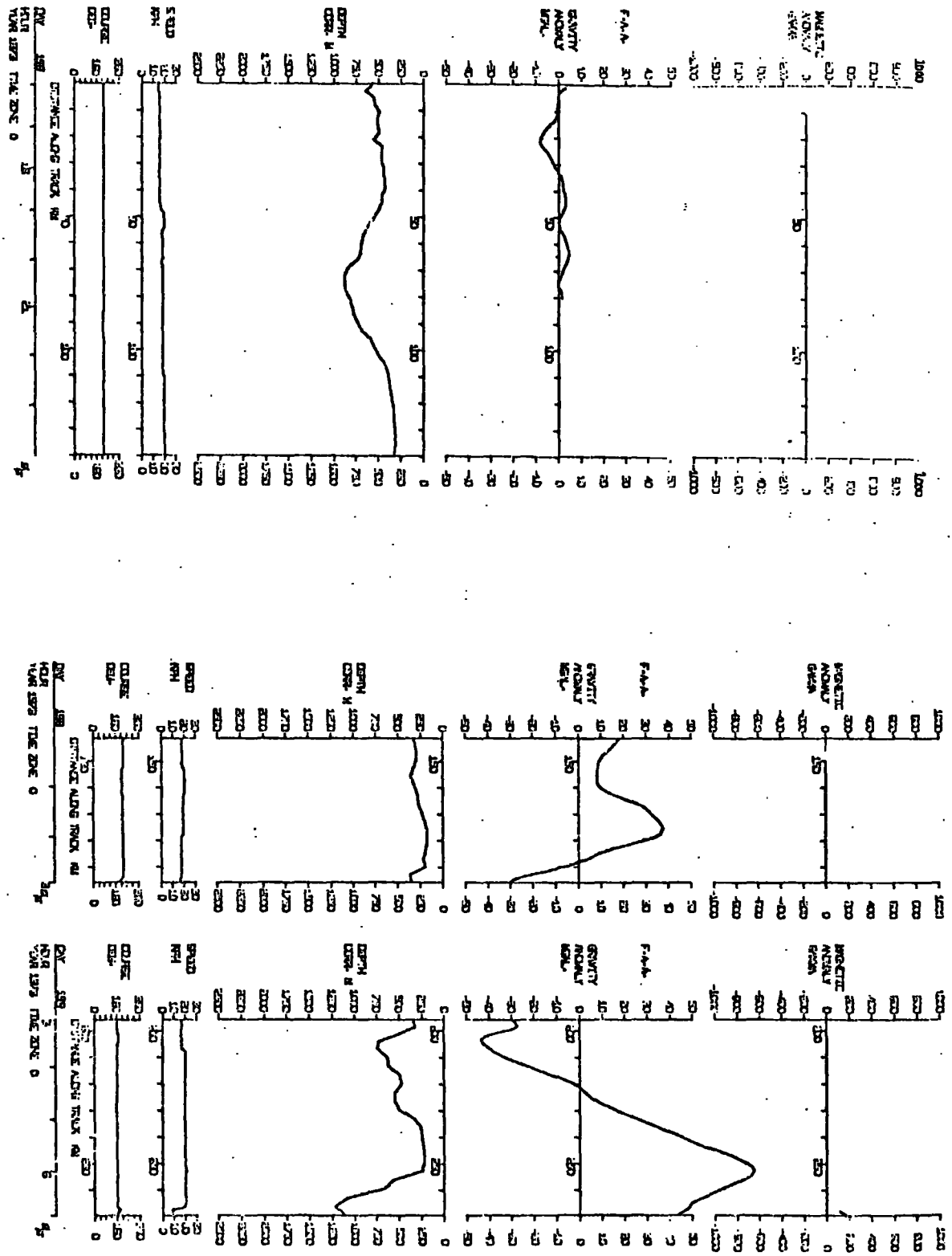

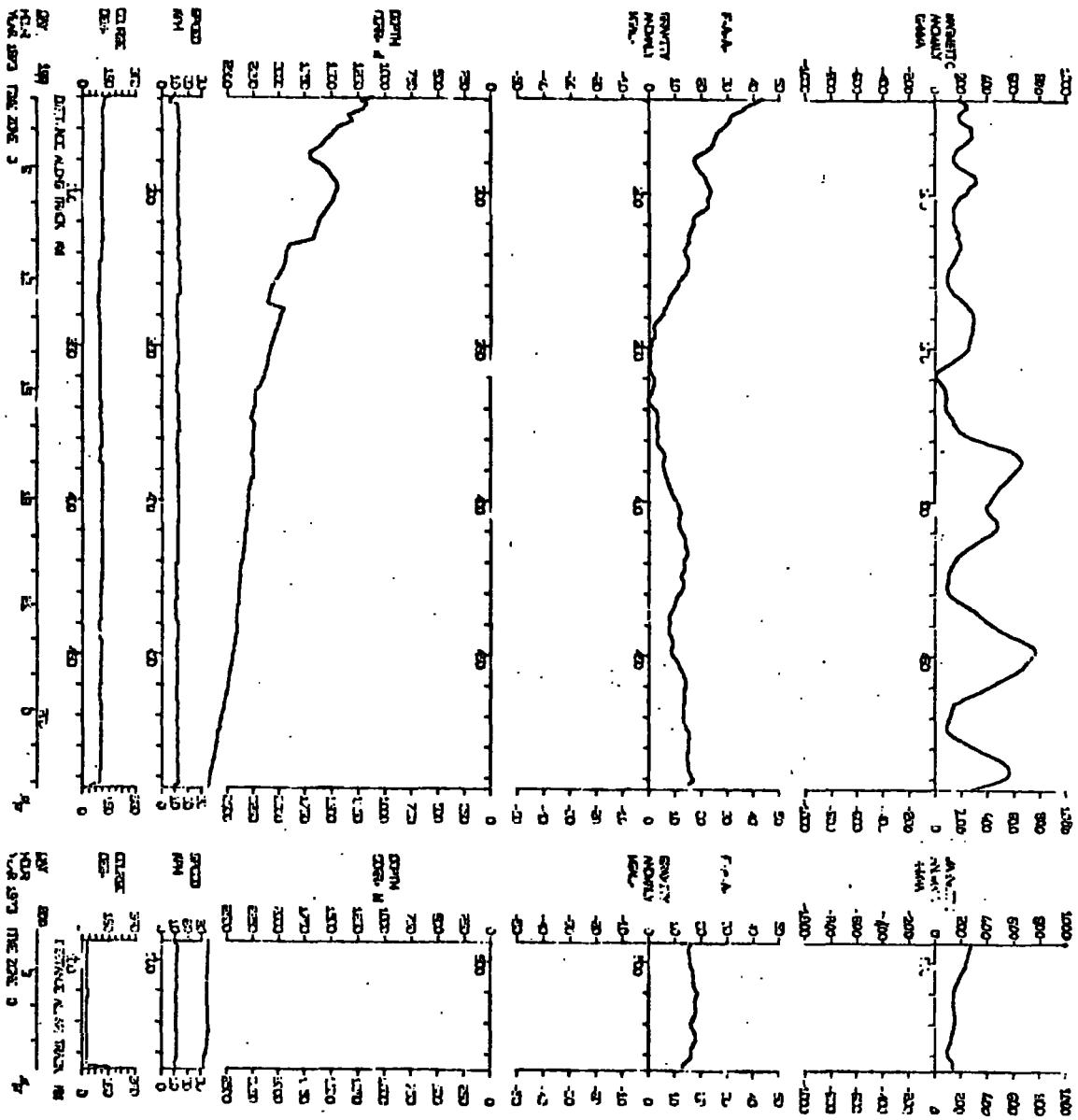

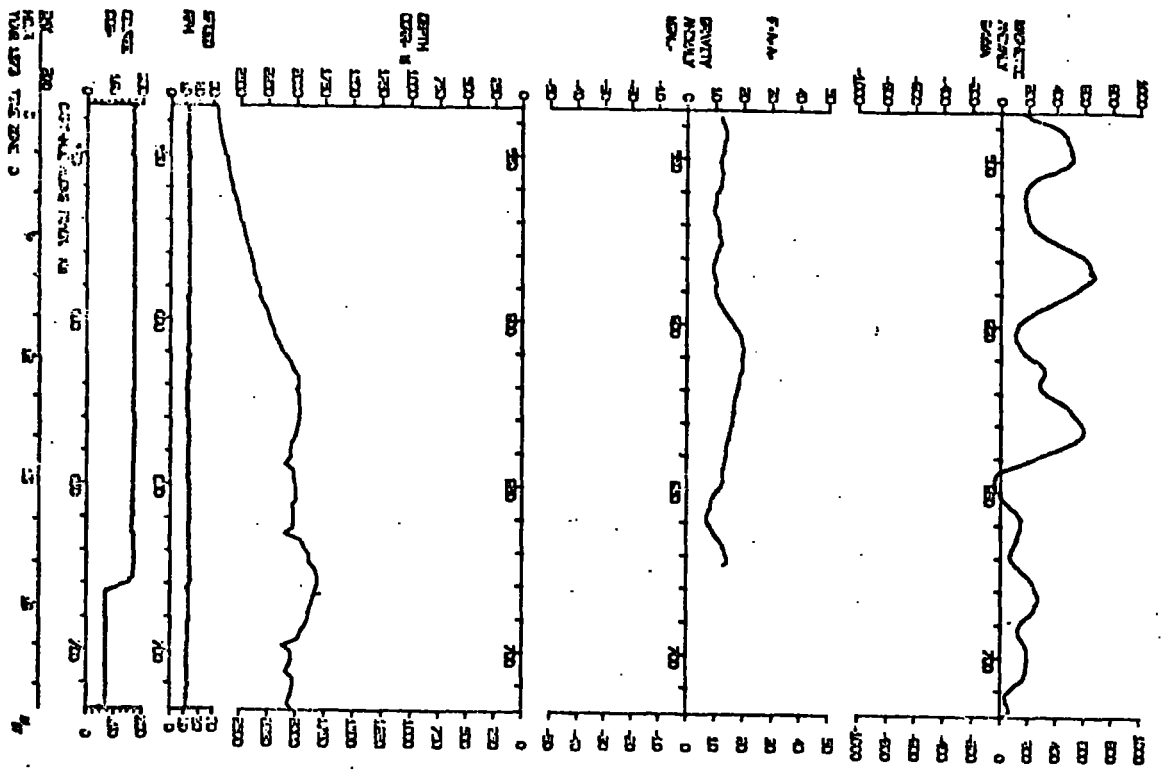

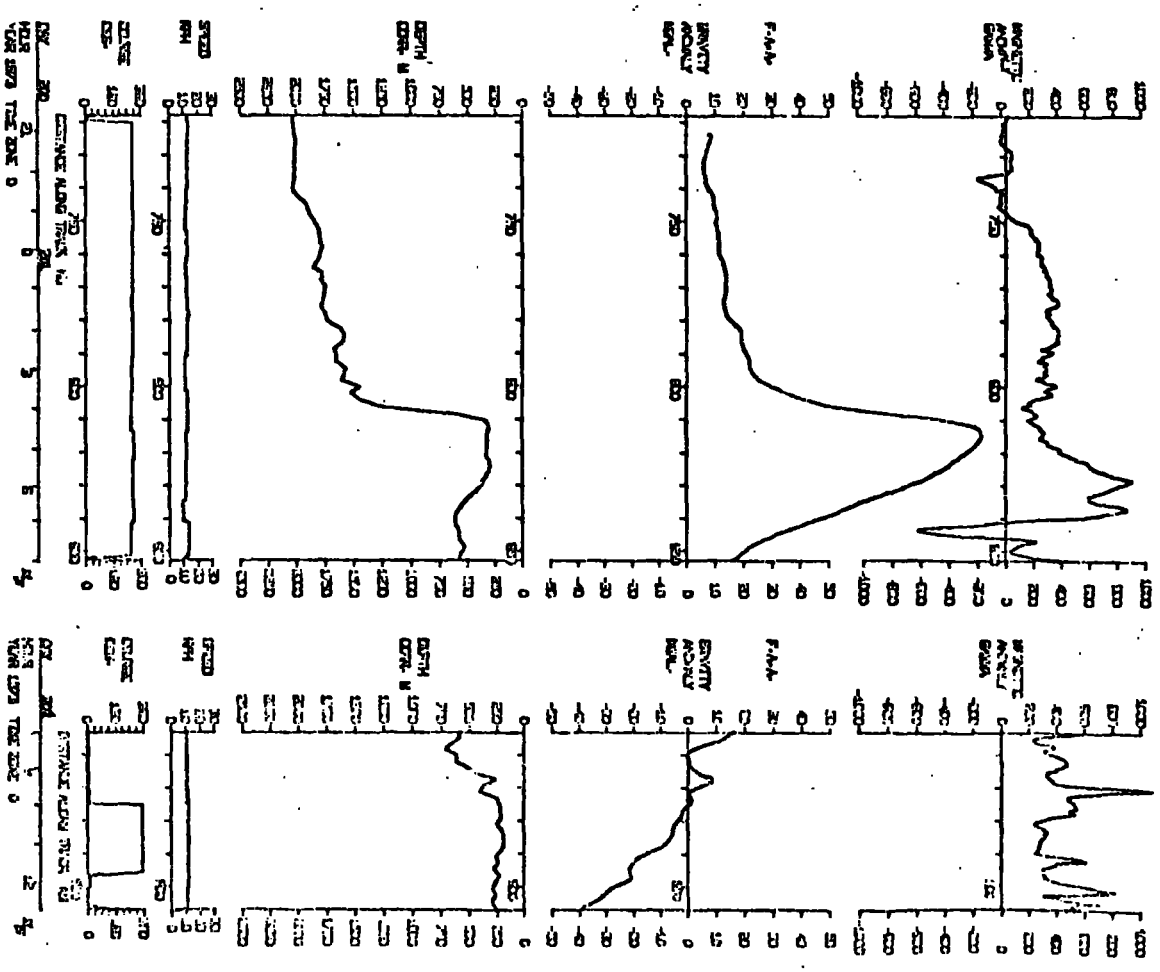

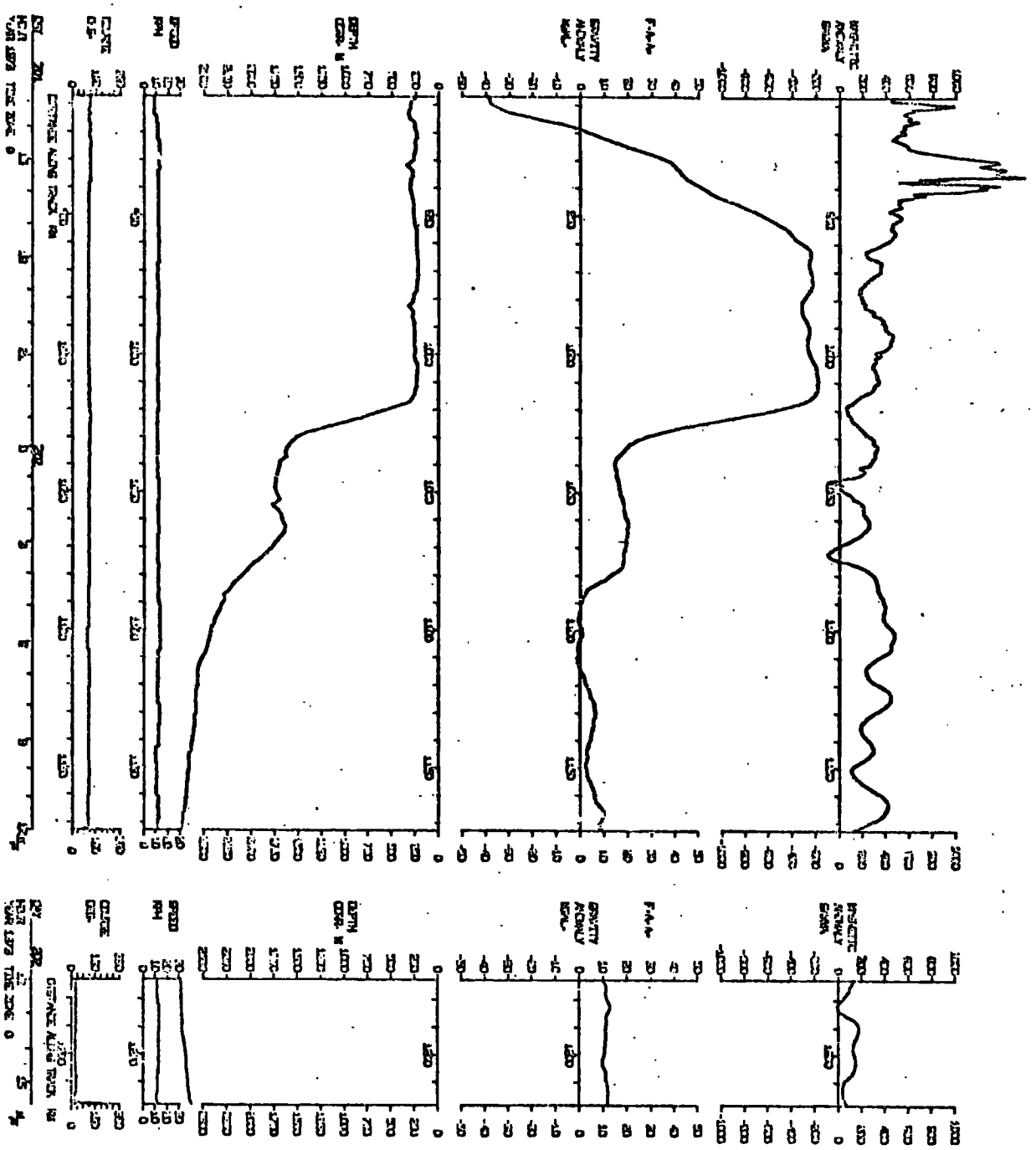

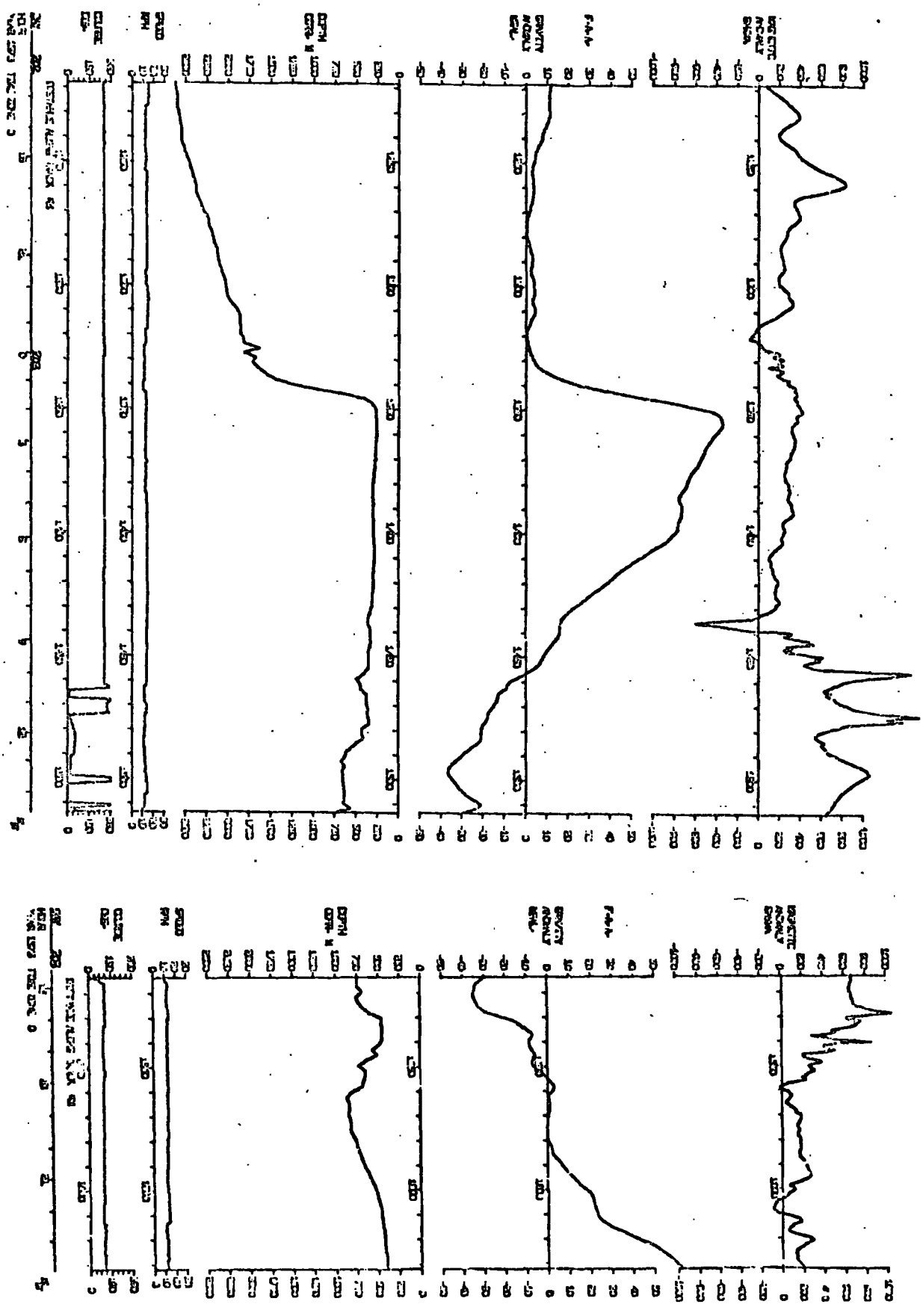

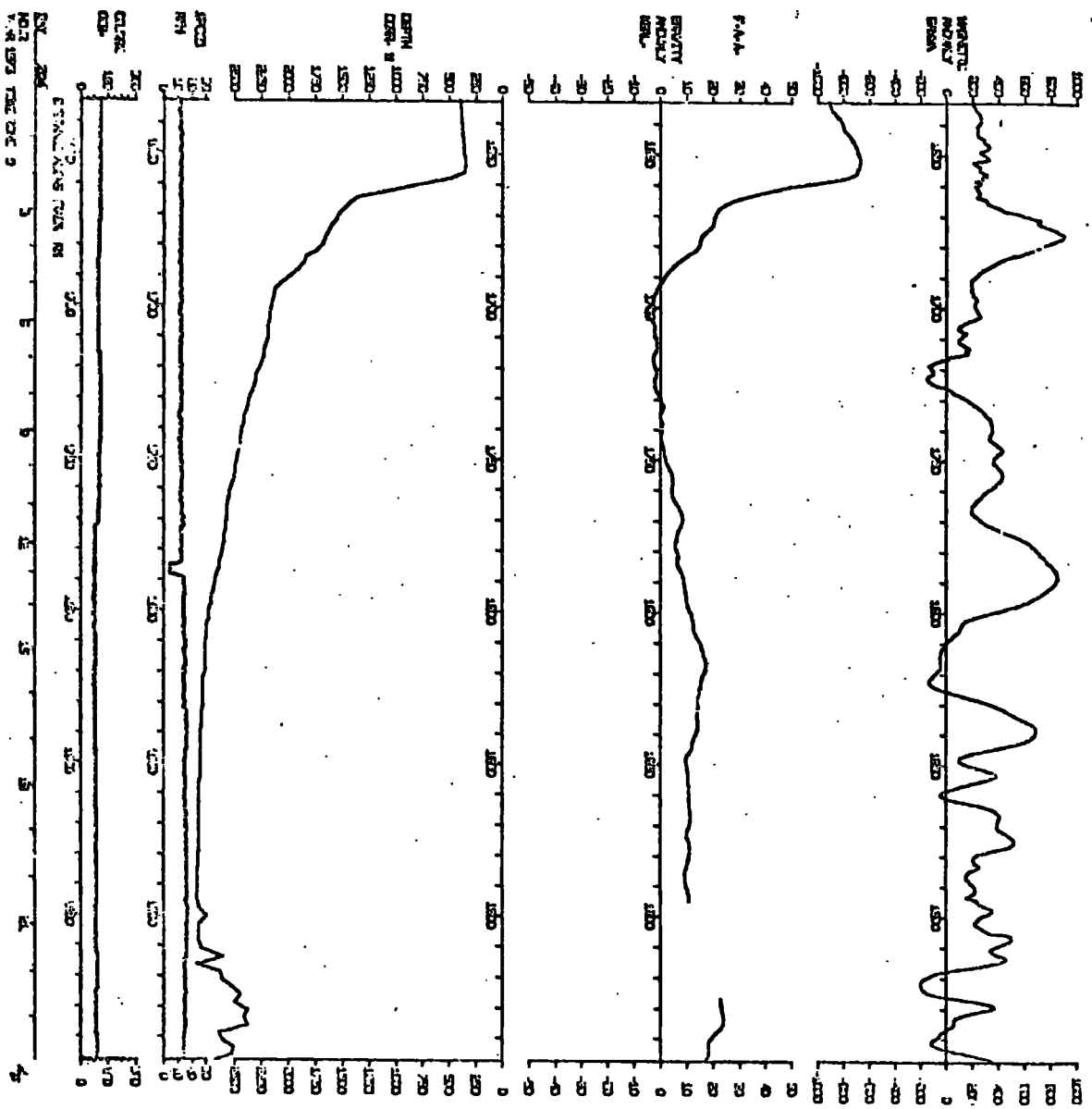

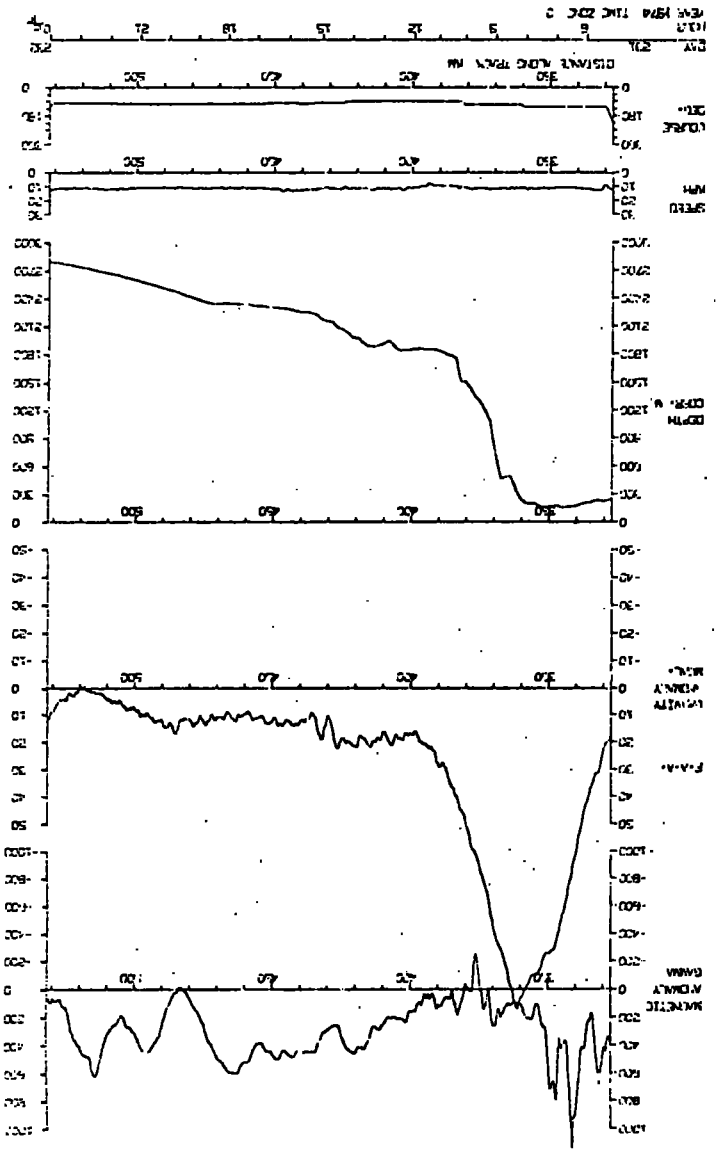

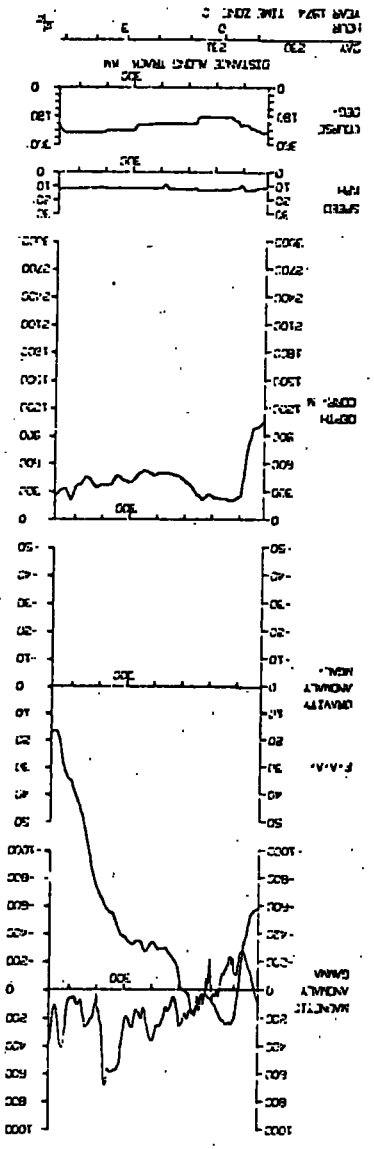

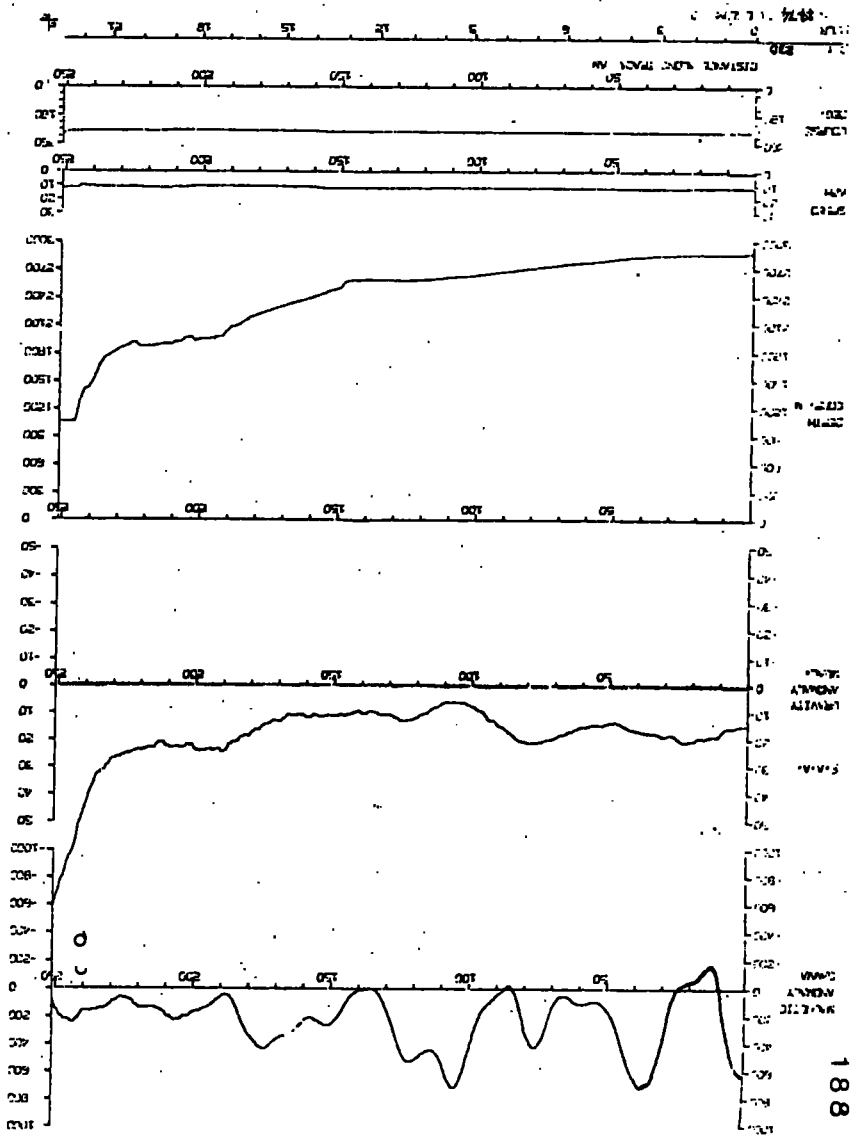

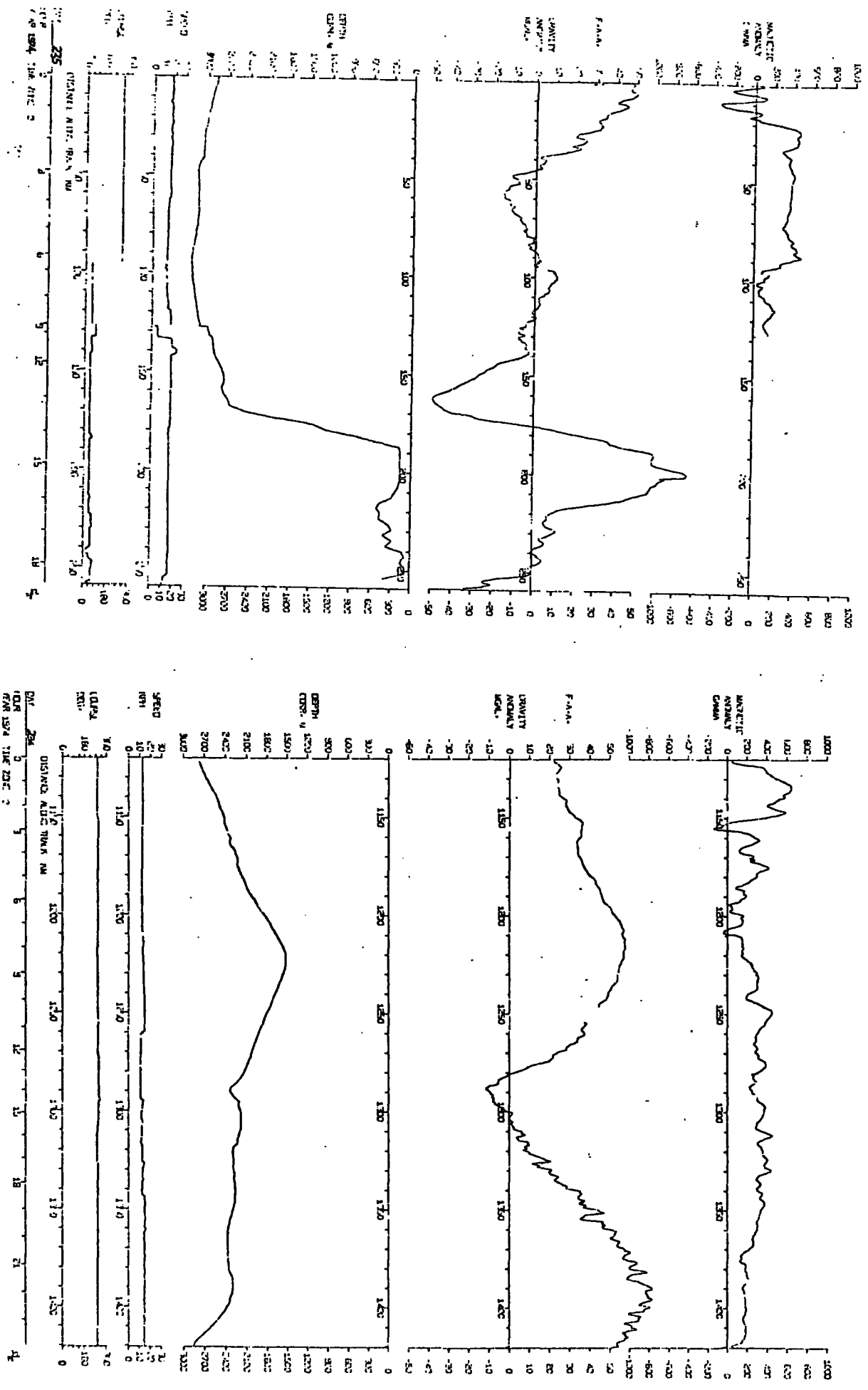

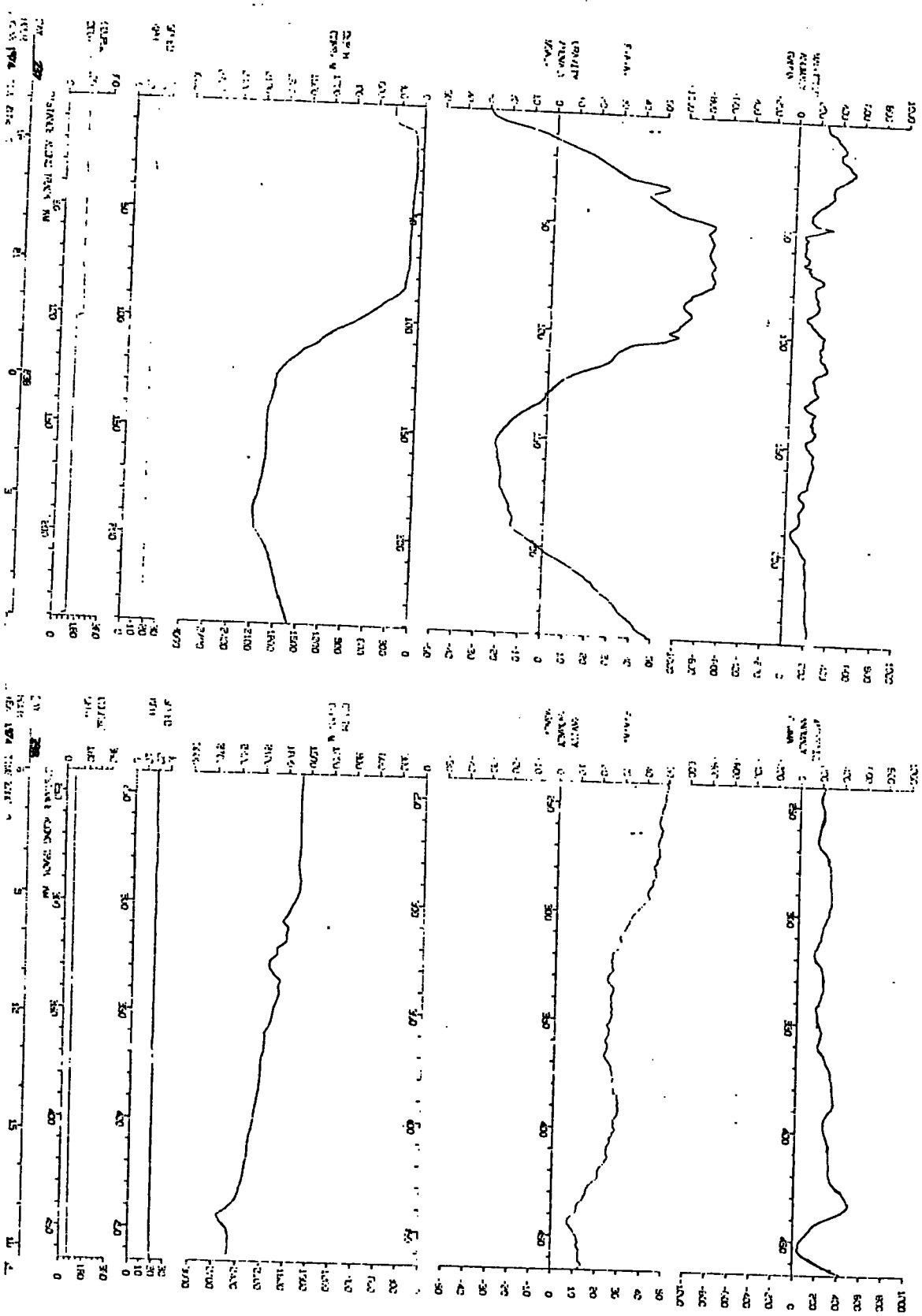

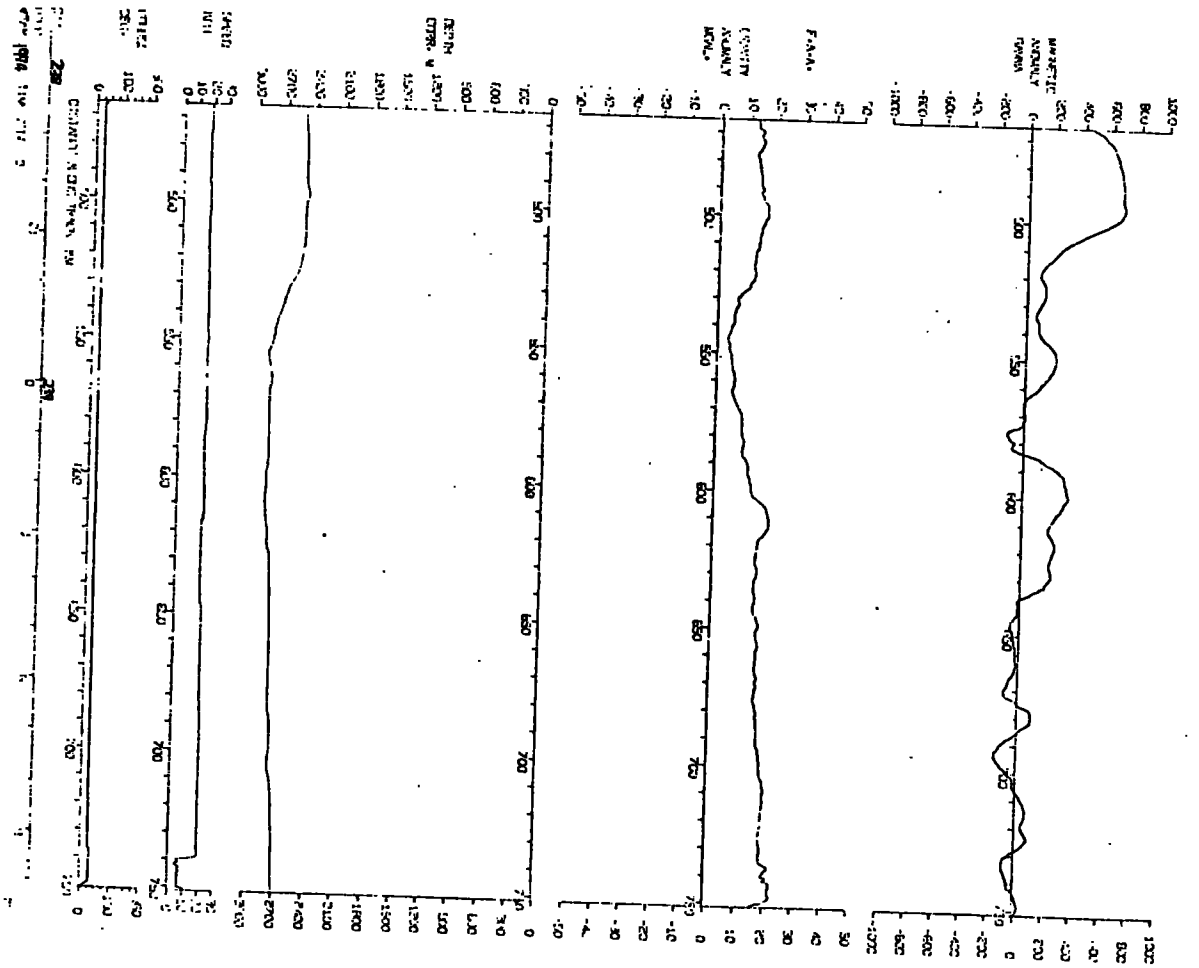

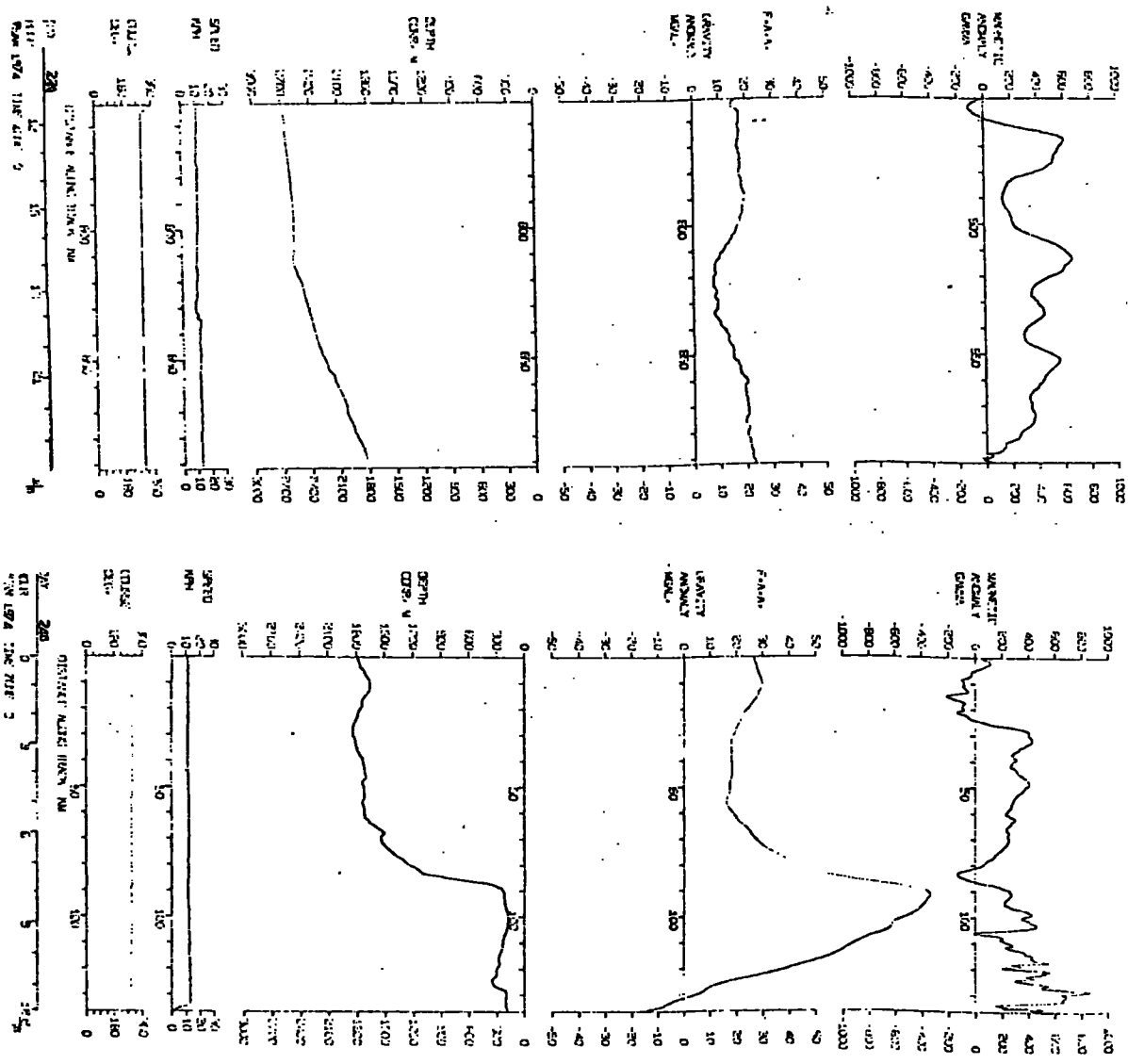

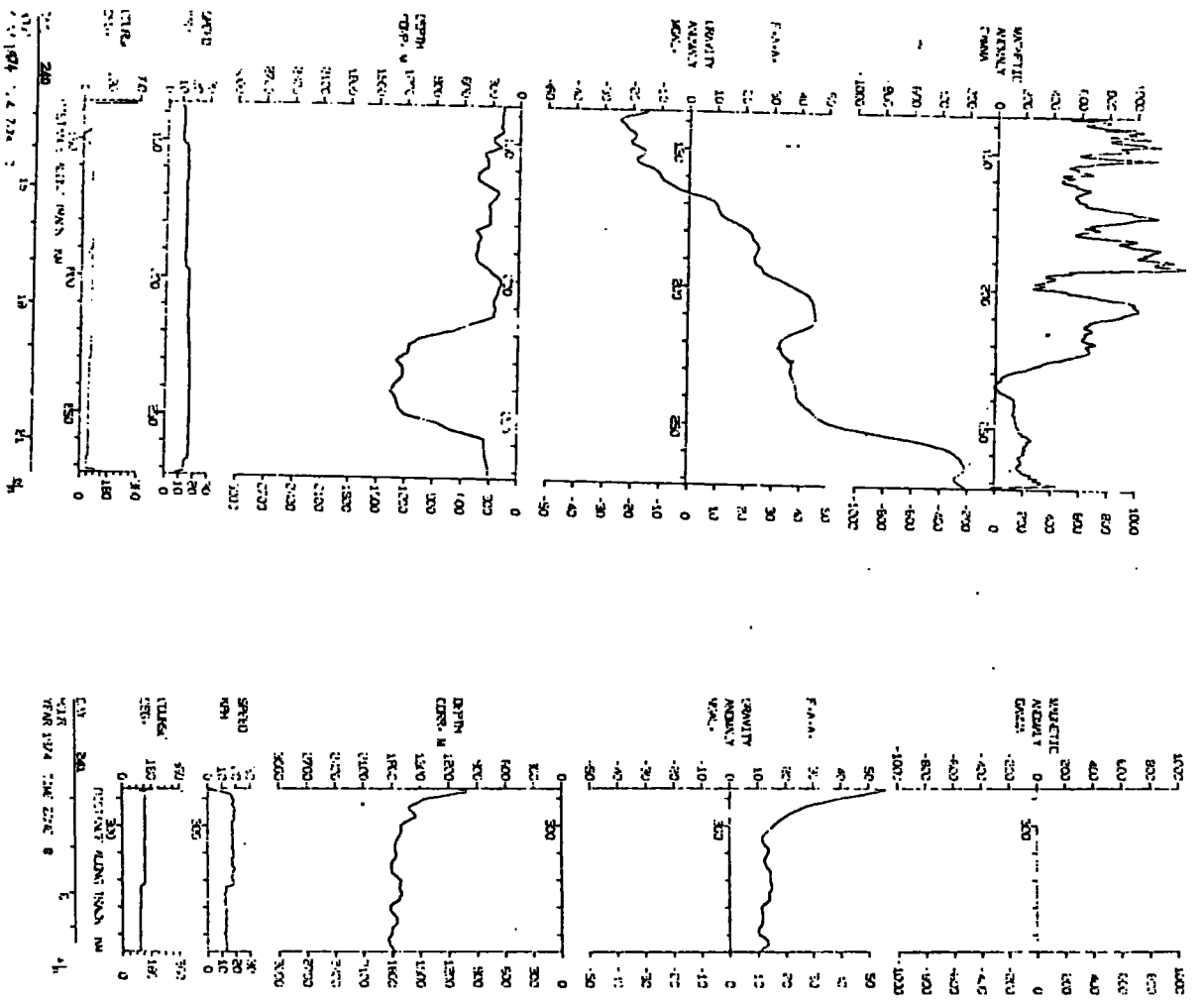

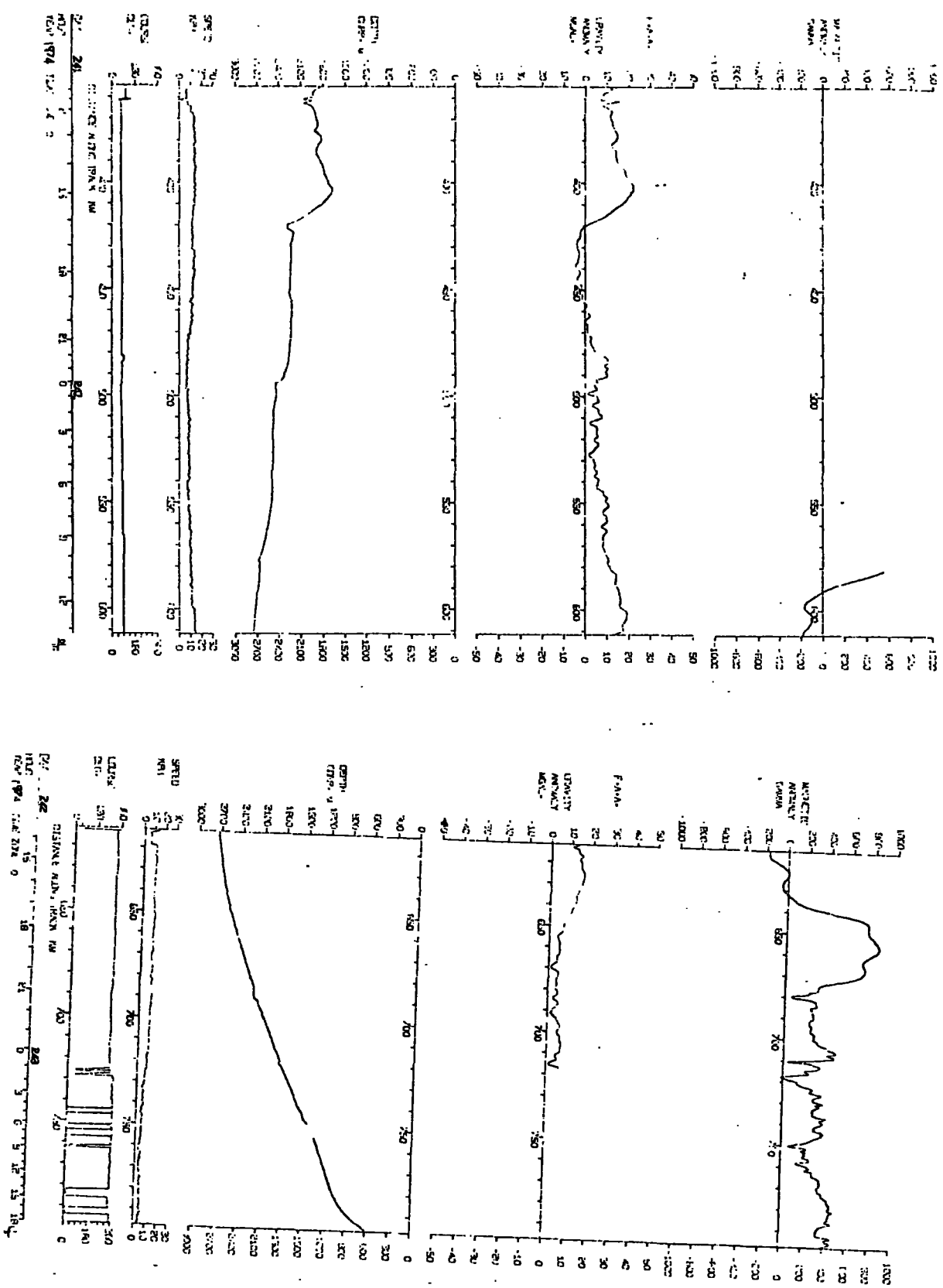

APPENDIX 2

COMPUTER PROGRAMS

The programs that follow were used in the processing of the seismic data of this thesis, and are referred to in Chapter 3. They are written in a variety of computer languages, and are reproduced in the hope that at least some of the techniques will be of further use in the future.

A2.1 RNSO

Routine RNSO, written in CTL assembler for the Modular 1, will remove normal moveout from a set of seismic channels. The theory is given in section 3.5, the arguments are:

RNSO; I_1, I_2.... I_n; X_s, Y_s; V; D; O_1, O_2 .... O_n;

I_n..... is the number of a channel that requires moveout correction. It must be a time series channel, with a system delay greater than the direct-wave arrival time for the shot-receiver separation and velocity used.

X_s,Y_s.. are the coordinates of the shot point, in km, on the same system as used to define the coordinates of the geophone array (opn.12).

V..... is the velocity, in km s^{-1}, to be used for movement calculation.

D..... is the delay, in seconds, between the shot-instant and the first sample of the seismic record, that has been inserted when the records were digitised.

O_n.... is the number of a channel that will receive the moveout corrected seismic signal, it need not be a time series channel.

The operation of the RNSO routine is in two sections; firstly during compilation of the program the shot-receiver distance is calculated, squared, and divided by V^2 to form a value 'K' for each channel that is constant throughout processing. The second section of the routine, which is within the square-root package, takes this value of K, calculates for each sample a time delay, and uses this time delay to transfer samples from the input queue to the output location. The two routines follow and are fully commented.

A 21

```
;PAGE

; C-BLOCK 2 - REMOVE NORMAL STEP OUT COMPILE ROUTINE

CBLK2:    PROCESS;

CRNS:     ADB L 1;                    INCREMENT AND STORE
          STB Y WKSP;                 RETURN ADDRESS

          LDB Y WKSP+8;               PICK UP DATA POINTER

          LDA YB DATA+4;              PICK UP
          SRE Y ESBRT+7;              CHECK (INDD)
          STA Y WKSP+6;               AND STORE VELOCITY

          LDB Y ARRAY;                PICK UP AND
          LDB YB ADAT+3;              STORE
          STB Y WKSP+1;               ARRAY ADDRESS

          LDB Y EWKSP+4;              PICK UP DATA POINTER
          LDW Y EWKSP+3;              PICK UP PARAM POINTER
          LDM L 0;                    SET CHANNEL
          SBM Y CBRT+1;               COUNT
R1:       STB Y WKSP+13;              STORE DATA POINTER
          TSTL M=0 INCM;              FINISHED? (INCREMENT)
          LDP Y WKSP;                 YES - EXIT

          STM Y WKSP+9;               NO - SAVE CHANNEL COUNT

          LDA YB DATA;                PICK UP CHANNEL NUMBER
          SRE Y ESBRT+7;              CHECK (INDD)
          MLS L 3;                    LOCATE ARRAY
          ADA Y WKSP+1;               OFFSET
          CPYL RB A1 EQV NOT1;        GET X CO-ORDINATE
          LDA YB DATA;                FROM ARRAY
          STA Y WKSP+2;               AND STORE
          LDA YB DATA+1;              DITTO WITH
          STA Y WKSP+3;               Y CO-ORDINATE

          STW Y WKSP+4;               SAVE PARAM POINTER
          LDW L 0;                    INITIALISE
          LDM X M1;                   POINTERS

R2:       STA Y WKSP+7;               SAVE CURRENT VALUE
          LDB Y WKSP+8;               PICK UP DATA POINTER
          LDA YB DATA+1;              PICK UP SHOT POINT CO-ORDINATE
          ADB L 1;                    INCREMENT AND STORE
          STB Y WKSP+8;               DATA POINTER
          SRE Y ESBRT+7;              CHECK CO-ORDINATE (INDD)
          CPY Y A=-A;                 NEGATE AND ADD
          ADA YW WKSP+2;              TO CHANNEL CO-ORDINATE
          STA YW WKSP+2;              AND SAVE

          LDB L 0;                    SQUARE DISTANCE
          MLD YW WKSP+2;              AND DIVIDE
          DIV Y WKSP+6;               BY VELOCITY
          LDB L 0;                    NORMALISE
          MLD L 100;                  AND DIVIDE BY
          DIV Y WKSP+6;               VELOCITY AGAIN
          ADW L 1;                    INCREMENT POINTER
          TST X M<0INCM;              FINISHED CO-ORDINATES? (INCREMENT)
          JMP R2;                     NO - GOTO DO NEXT

          ADA Y WKSP+7;               ADD CURRENT VALUE TO GIVE (D/V)**2
          LDW Y WKSP+4;               PICK UP PARAM POINTER
R3:       STA YW DATA+7;              AND STORE VALUE
          ADW Y CBRT+9;               INCREMENT PARAM POINTER
          LDB Y WKSP+13;              PICK UP INCREMENT AND
          ADB L 1;                    RESTORE DATA POINTER
          LDM Y WKSP+9;               PICK UP CHANNEL COUNT
          JMP R1;                     GOTO DO NEXT CHANNEL


M<0INCM:  TSTC M<0 INCM;
M1:       -1;

          RESERVE 7;

          END;
```

```
;PAGE

; BLOCK 10 - SQUARE ROOT AND REMOVE.NORMAL STEP OUT SUBROUTINES

BLK10:    PROCESS;

; SQUARE ROOT ROUTINE

FSQR:     LDA YWI 1;              PICK UP VALUE
          STP Y WKSP+1;           CALCULATE SQUARE
          JMP SQRT;               ROOT

          STA YWI 2;              STORE ROOT
          ADM L 3;                INCREMENT POINTER
          CPY Y P=W;              AND EXIT

; REMOVE NORMAL STEP OUT ROUTINE

FRNS:     LDA Y TBP;              PICK UP TIME
          TSTL ACO;               INSIDE SYSTEM DELAY?
          JMP L1;                 YES - BYPASS DELAY CALCULATIONS

          LDA YWI 1;              PICK UP DELAY
          LDB L 0;                AND CONVERT TO SAMPLES
          DIV Y NRCH;             FROM STORE OFFSET
          ADA Y TBP;              AND ADD TO THE TIME

          LDB L 0;                CONVERT TIME TO SECONDS
          MLD L 100;              BY DIVIDING BY
          DIV Y SAMRATE;          SAMPLING RATE
          STA Y WKSP+2;           AND STORE

          LDB L 0;                SQUARE TIME
          MLD Y WKSP+2;           NORMALISE
          DIV L 100;              AND
          STA Y WKSP+6;           STORE

          TST X AOVR;             OVERFLOW?
          EXEC L 16;              YES - EXIT FROM FILTER

L1:       ADM L 2;                INCREMENT POINTER
          LDB YWI 0;              PICK UP CHANNEL COUNT
L2:       TSTL B=0 INCB;          FINISHED? (INCREMENT)
          CPY Y P=MPONE;          YES - EXIT

          STB Y WKSP+7;           NO - SAVE CHANNEL COUNT

          LDA Y TBP;              PICK UP TIME
          TST X ACOSKP4;          INSIDE SYSTEM DELAY?
          LDA L 0;                YES - SET ZERO
          STA Y WKSP;             DELAY
          JMP L3;                 GOTO TRANSFER THIS CHANNEL

ACOSKP4:  TSTC ACO SKP4;

          LDA Y WKSP+6;           PICK UP T**2
          ADA YWI 3;              ADD (D/V)**2
          STP Y WKSP+1;           AND TAKE SQUARE
          JMP SQRT;               ROOT

          SBA Y WKSP+2;           SUBTRACT T TO GIVE DELAY (SECS)

          LDB L 0;                CONVERT DELAY
          MLD Y SAMRATE;          TO SAMPLES
          DIV L 100;              NORMALISE
          MLS Y NRCH;             CONVERT TO STORE OFFSET
          STA Y WKSP;             AND SAVE

          TST X AOVR;             OVERFLOW?
          EXEC L 16;              YES - REJECT

          SBA Y MMND;             DELAY OUTSIDE
          TSTL A>0 A=0;           SYSTEM DELAY?
          EXEC L 16;              YES - EXIT FROM FILTER

L3:       SBM Y WKSP;             NO - SUBTRACT DELAY
          LDA YWI 1;              PICK UP FROM I/P CHANNEL
          ADM Y WKSP;             RESTORE INDEX
          STA YWI 2;              STORE IN O/P CHANNEL
          ADM L 3;                INCREMENT POINTER
          LDB Y WKSP+7;           PICK UP CHANNEL COUNT
          JMP L2;                 GOTO DO NEXT CHANNEL

; SQUARE ROOT SUBROUTINE

SQRT:     LDB L 152;              REJECT NEGATIVE
          TSTL ACO;
          EXEC L 72;

          STA Y WKSP;
          STM Y WKSP+5;           SQRT(X)=(X/N+N)/2
          LDM X M6;               (7TIMES)
          LDA L 100;

S1:       STA Y WKSP+3;
          LDB L 0;
          LDA Y WKSP;
          MLD L 100;
          DIV Y WKSP+3;
          ADA Y WKSP+3;
          SFTL S L R 1;
          TST X M<OM>0INC1;
          JMP S1;

          LDB Y WKSP+1;
          LDM Y WKSP+5;
          CPY Y P=BPONE;

AOVR:     TSTC AOVR;
M6:       -6;
M<OM>0INC1:TSTC M<0 M>0 INC1;

          RESERVE 2;

          END;
```

A2.2 FOAM1

Program FOAM1, written in Fortran IV for the IBM 360/370, will translate a file of a 4 channel Modular 1 seismic data tape into a form readable by other Fortran programs.

```
:C TO MOUNT READY FOR TRANSLATION THE
:C 50TH FILE ON MODULAR 1 TAPE DGP48M
:C $MOUNT DGP48M *TAPE* NV FMT=FB(512,256) POSN=*51*
:       INTEGER*2 JIM(256)
:       NBLK=0
:   13  READ(5,10,END=3)(JIM(I),I=1,256)
:   10  FORMAT(128A2/,128A2)
:       NBLK=NBLK+1
:       K=2
:       IF(NBLK.EQ.1)K=42
:       DO12I=K,255,8
:       WRITE(6,11)(JIM(I+J),J=0,3)
:   11  FORMAT(4(I10,14X))
:   12  CONTINUE
:       GOTO13
:    3  STOP
:       END
```

A2.3 DELSTORE

Program DELSTORE, written for the Modular 1, will store four channels of seismic data on digital magnetic tape.

```
40;;
SPP;
SET THRESHOLD LEVEL;
ASK;
INS; 149; 159;
SPP;
DELAY(SA.MS);
ASK;
INS; E; 159;
SPP;
RECORD(SA.MS);
ASK;
INS; 150; 159;
SPP;
NUMBER OF RECORDS;
ASK;
INS; 148; 159;
SPP;
START FILENO;
ASK;

ADD; 159, 148; 102;
INS; B; 159;

DO; A; B; 0.01; C;
SET; 151; 0;
INP;;; 13, 14, 15, 16, 17, 18; 1, 2, 3, 4, 5, 6;

IF; CC(1.51, 0)=1;
   GOTO; 30;
ELSE;

IF; CC(0.06, 0)<CC(1.49, 0);
   GOTO; 19;
ELSE;

SET; 151; 1;

DO; D; 0.01; 0.01; E;
INP;;; 13, 14, 15, 16, 17, 18; 1, 2, 3, 4, 5, 6;
CONTINUE;

IF; TRP>CC(1.50, 0);
   GOTO; 35;
ELSE;

OUT; A;; 1, 2, 3, 4; 1, 2, 3, 4;
IGOTO; 19;
EVA; TRP=0;
CONTINUE;

EVA; TRP=0;
FGOTO; 1;;
END;
```

A2.4 FILIP

Program FILIP, written for the Modular 1, will convolve single channel seismic data, from a digital magnetic tape, with a predesigned 50 sample spiking filter and output the results to an analogue display.

```
45;.2;
SPP;
SPIKE FILTER;
VIN;;;;
SPP;
CHANNEL;
ASK;
INS;C;159;
SPP;
STARTFILE;STOPFILE;
ASK;
DEL;159;;153;
ASK;
DEL;159;;157;
SPP;
DELAY;
ASK;

IF;C(1.59,0)>C(1.57,0);
   EX;;
ELS;
INS;T;153;
LINK;;29;;

INP;T;;C;1;
IF;TRP>C(1.59,0);
   IF;TRP<C(1.59,0)+1;
      SET;16;5;
      GOT;26;
   ELS;
ELS;
SET;16;0;

FIL;1;;5;
OUT;;;5,6,7;5,16,1;
IGO;19;

IF;TRP>25;
   EVA;C(1.58,0)=C(1.58,0)+.01;
   INS;T;158;
   FGO;13;;
ELS;
INP;;;;;
IGO;29;

END;
```

Specimen spiking filter (shown in fig. 3.2 and used to produce fig. 3.3) that can be used with program FILIP.

```
-7.46;2.32;4.19;.64;-1.36;-1.42;1.78;1.17;-.62;-.65;
.11;.08;-.27;.23;1.30;1.46;.25;-1.04;-1.20;-.31;
0.34;.16;-.27;-.29;.10;.36;.24;-.02;-.21;-.29;
-.25;-.05;.25;.40;.25;-.04;-.15;-.01;.12;.06;
-.09;-.13;-.04;.05;.06;.00;-.10;-.21;-.18;.21;
```

A2.5 SPIFIL

Program SPIFIL, written for the Modular 1, will convolve 4 channel seismic data from digital magnetic tape, store the spiked output on disc and then link to program STAFIL.

```
35;.2,.2,.2,.2;
SPP;
SPIKING FILTER;

VIN;1,2,3,4;;;
SPP;
STARTFILE;STOPFILE;
ASK;
DEL;159;;158;
ASK;
DEL;159;;157;

FGC;9;1;
SET;151;;
EVA;C(1.51,0)=C(1.51,0)-.01;
EVA;C(1.56,0)=TBP;

IF;C(1.58,0)>C(1.57,0);
   EXI;
ELS;
INS;T,F;158,151;
LINK;;33;;

IF;C(.99,0)>0;
   IF;TBP>C(.99,0);
      EVA;C(1.58,0)=C(1.58,0)+.01;
      INS;T;158;
      FGC;10;1;
   ELS;
   INP;;;1,2,3,4;1,2,3,4;
   GOT;30;
ELS;

INP;T;;1,2,3,4;1,2,3,4;
IF;TBP<0;
   IGC;26;
ELS;

FIL;1,2,3,4;1,2,3,4;5,6,7,8;
OUT;F;;1,2,3,4;5,6,7,8;
IGC;17;

EVA;C(.99,0)=TBP-C(1.56,0);
GOT;17;

END;
```

A2.6 STAFIL

Program STAFIL, written for the Modular 1, and entered via program SPIFIL, will take spiked seismic data from disc, CDP stack the channels, and output them to an analogue display.

```
35;;
SPP;
STACK VEL;
ASK;
INS;V;159;
SPP;
DEL(SA.MS);
ASK;
DEL;159;;149;

SET;148,147;-.1,-.11;
FGO;9;;
GOTO;1;

INS;A,B;148,147;
LINK;;33;;

INP;-.01;;1,2,3,4;1,2,3,4;
IF;TBP<0;
   IGO;12;
ELS;

IF;TBP=0;
   EVA;TBP=C(1.49,0);
ELS;

INP;A;;1,2,3;5,6,7;

IF;TBP<C(1.49,0)+1;
   SET;19;10;
   GOTO;25;
ELS;
SET;19;0;

PNS;1,2,3,4;,;V;;11,12,13,14;
ADD;12,5;3;
ADD;13,6;9;
ADD;14,7;10;
WEI;10;.5;;0;

OUT;P;;1,2,3;11,3,9;
OUT;;;5,6;10,19;
IGO;12;

DEL;147,148,146;;146,147,145;
FGO;12;;

END;
```

A2.7 DEEPSTACK

Program DEEPSTACK, written for the Modular 1, will perform a static common depth point stack, of 4 seismic channels, from digital tape and output them to an analogue display. The static time corrections are entered when declaring the array coordinates (opn. 12).

```
45;;
SPP;
STARTING FILE;
ASK;
INS; D; 159;
SPP;
TERMINATING FILE;
ASK;
INS; E; 159;

SET; 1,2,3,6;,,,;
SET; 20,21;-.1,-.11;
INS; A; 20;
LINK;;13;;

OUT; A;;1,2,3;1,2,3;
IGOTO; 11;

DO; C; D; .01; E;
INS; A,B; 20,21;
EVA; TRp=0;
LINK;;30;;

INp; C,A;,;1,2,3,4,25,26,27;1,2,3,4,5,6,7;
IF; TRp<1.0;
    SET; 6; 5.0;
    GOTO; 23;
ELSE;
SET; G; 0;

ADD; 2,5;8;
ADD; 3,6;9;
ADD; 4,7;10;
WEI;10;.25;10;

OUT; F;;1,2,3;1,8,9;
OUT;;;5,6;10,6;
IGOTO; 17;

IF; TRp<25;
   INp;;;;;
   IGO; 30;
ELSE;

DEL; 20,21,22;;22,20,21;
CONTINUE;
EXIT;
END;
```

A2.8 VELVET

Program VELVET, written for the Modular 1, will perform moveout correction at a series of velocities on sequential channels of seismic data, each shot being stored on disc file.

```
60;;
SPP;
NO.FILES;
ASK;
DEL;159;;134;
SPP;
STARTV;STEP;ENDV;;
ASK;
DEL;159;;139;
ASK;
DEL;159;;139;
ASK;
DEL;159;;137;
SPP;
DEL(SA.MS);
ASK;
DEL;159;;132;

SET;136,135;-.01,.14;
SUB;134;136;133;

LINK;;34;;
INS;V,B,C;139,136,135;

INP;;;1,2,3,4;1,2,3,4;

INP;B;;1,2,3,4;1,2,3,4;

IF;TRP<0;
   IGO;19;
ELS;

IF;TRP=0;
   EVA;TRP=C(1.32,0);
ELS;

IF;TRP<C(1.32,0)+1;
   SET;6;5;
   GOTO;31;
ELS;

SET;6;;
INS;1,2,3,4;;V;;11,12,13,14;
OUT;;;5,6;C,6;
IGO;19;

EVA;C(1.35,0)=C(1.35,0)-.01;
IF;C(1.35,0)<.11;
   SET;135;.14;
   EVA;C(1.36,0)=C(1.36,0)-.01;
   IF;C(1.36,0)=C(1.33,0);
      SET;136;-.01;
      SPP;
;
      CPP;139;
      ADD;139,134;139;
      IF;C(1.39,0)>C(1.37,0);
         EXI;
      ELS;
   ELS;
ELS;
IF;TRP<25;
INP;;;;;
IGO;48;
ELS;
IGO;13;;

END;
```

A2.9 JUSTINTIME

Program JUSTINTIME, written for the Modular 1, will digitise data from analogue tape and store it on disc. It will then cause an external hardware switch to interchange the clock signal governing the sampling rate by altering the D.C. levels of output channels 7 and 8 and replay the digitised seismic signal, convolving it with a predesigned spiking filter and outputting it to an analogue display.

```
60;.2;
SPP;
SPIKING FILTER;
VIN;;;;
SPP;
THRESHOLD LEVEL;
ASK;
INS;149;159;
SPP;
CHANNEL(+.12);
ASK;
INS;C;159;
SPP;
DELAY (SA.MS);
ASK;
INS;E;159;
SPP;
RECORD (SA.MS);
ASK;
SET;152,153;-.01,10;

INS;F;152;

INP;;;18;6;
CUT;;;7,8;152,153;
IF;C(.06,0)<C(1.49,0);
   GOT;16;
ELS;

SPP;;
EVA;TRP=0;
DO;154;.01;.01;5;
   INP;;;;;
   CUT;;;7,8;152,153;
CON;

INP;;;C;1;
IF;TRP>C(1.59,0);
   GOT;34;
ELS;
CUT;F;;1;1;
CUT;;;7,8;152,153;
IGO;27;

INS;G;152;
DO;150;.01;.01;1;
INP;;;;;
CUT;;;7,8;153,152;
CON;

EVA;TRP=0;

IF;TRP<C(1.59,0);
   INP;G;;1;1;
   FIL;1;;5;
   IF;TRP<1;
      SET;16;5;
      GOT;48;
   ELS;
   SET;16;0;
   CUT;;;5,6,7,8,9;5,16,153,152,1;
    IGO;40;
ELS;
GOT;15;
END;
```

NORTH ATLANTIC GEOPHYSICAL SURVEY 1973-4 DURHAM UNIVERSITY R.R.S. SHACKLETON

AREA I — SHIPS TRACK

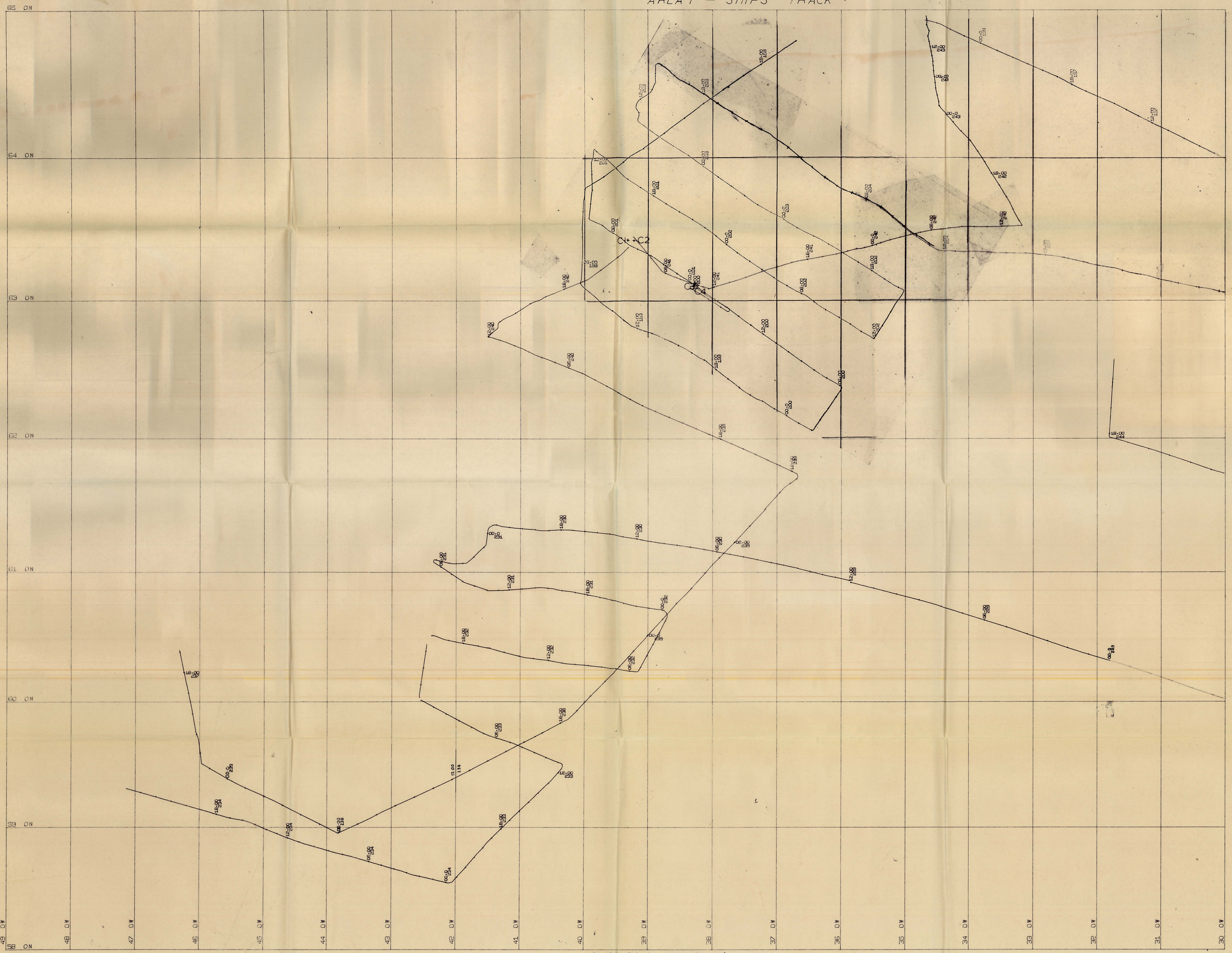

SHIPS TRACK MARKED WITH CROSS EVERY HOUR
TIME IN HOURS MINUTES AND JULIAN DAY

MERCATOR PROJECTION
SCALE 1 TO 1000000. (NATURAL SCALE AT LAT. 65)
INTERNATIONAL SPHEROID

NORTH ATLANTIC GEOPHYSICAL SURVEY 1973-4 DURHAM UNIVERSITY R.R.S. SHACKLETON

46°W 44°W 42°W 40°W 38°W 36°W 34°W 32°W

64°N 63°N 62°N 61°N 60°N 59°N

Seismic profiles along simplified ships track

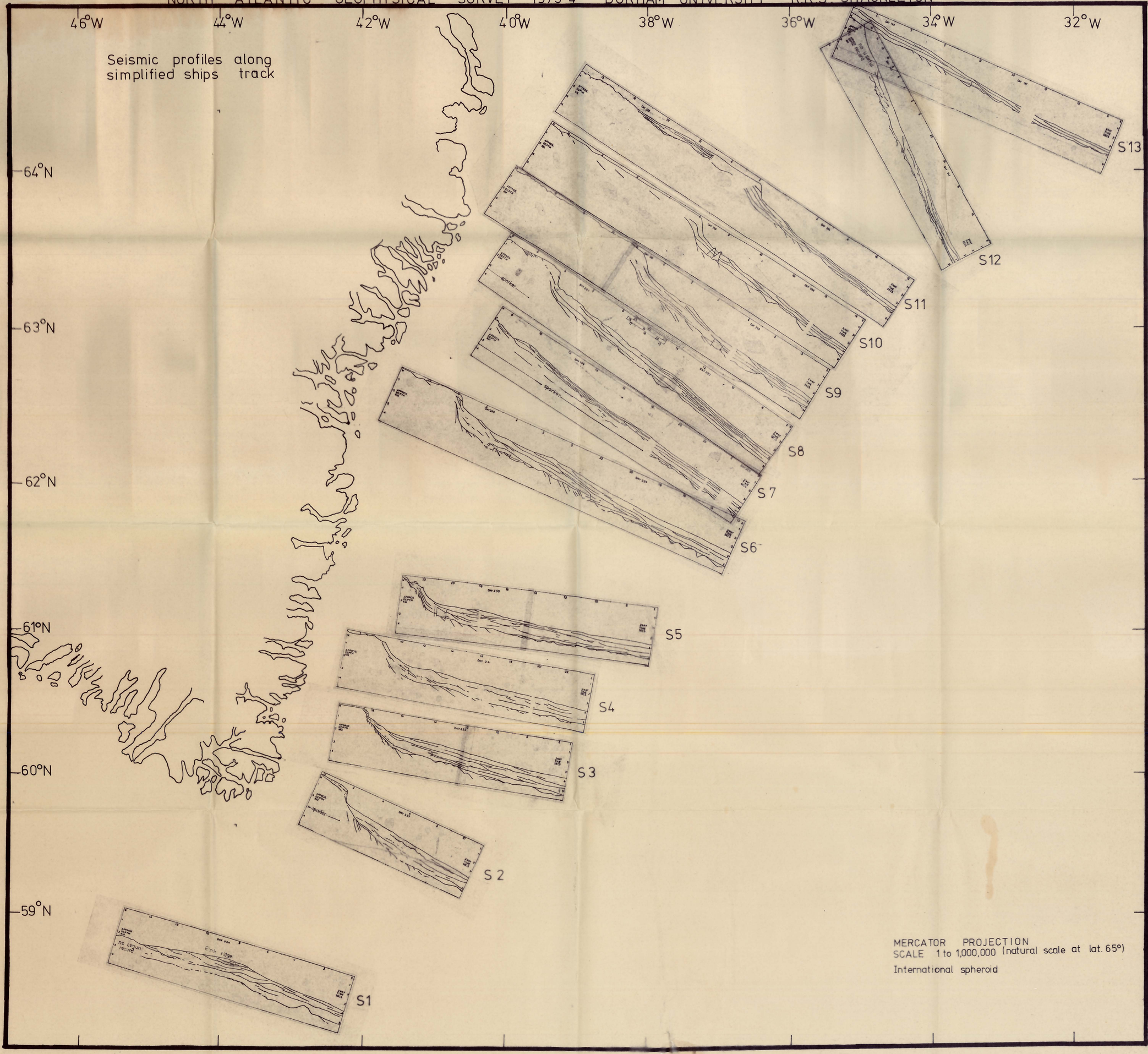

MERCATOR PROJECTION
SCALE 1 to 1,000,000 (natural scale at lat. 65°)
International spheroid